Groundwater Flow Modelling assisted by GIS and RS Techniques (Raya Valley - Ethiopia)

Mohammedsultan Abdella Hagos

March, 2010

Groundwater Flow Modelling assisted by GIS and RS Techniques (Raya Valley - Ethiopia)

by

Mohammedsultan Abdella Hagos

Thesis submitted to the International Institute for Geo-information Science and Earth Observation in partial fulfilment of the requirements for the degree of Master of Science in Geo-information Science and Earth Observation, Specialisation: Groundwater Assessment and Modelling.

Thesis Assessment Board

Chairman	Dr. Ir. M.W. Lubczynski	WRS, ITC, Enschede
External Examiner	Dr. W.W. Immerzeel	Future Water, Wageningen
First Supervisor	Dr. A.S.M.Gieske	WRS, ITC, Enschede
Second Supervisor	Dr. Ing.T.H.M.Rientjes	WRS, ITC, Enschede

INTERNATIONAL INSTITUTE FOR GEO-INFORMATION SCIENCE AND EARTH OBSERVATION
ENSCHEDE, THE NETHERLANDS

Disclaimer

Dedicated to
My family with Love and Gratitude

Abstract

The study focused on modelling of groundwater flow system in the Tigray Region of northern Ethiopia, assisted by GIS and RS techniques. The study area - Raya Valley- is a large fertile valley enclosed by high mountain ranges on the edge of the Afar Rift system. This part of the Tigray Region has abundant resources with respect to groundwater, fertile land, livestock potential and agro-climatic conditions. Ambitious project plans have been made to implement a pressurized irrigation project of about 18,000 hectare using the area's groundwater potential. The aquifer is characterized by unconsolidated material, which includes gravel and coarse sand with some pebbles and cobbles as colluvial deposits at the foot of the escarpment. The valley aquifer is replenished by direct recharge from rainfall and by runoff from the ephemeral river systems flowing from the western mountains. Several perennial springs are found in the western part of the valley.

The groundwater flow system in the unconsolidated deposits of the Raya Valley was modelled using PMWIN (Chiang et al., 1998) as pre- and post-processor for MODFLOW (McDonald and Harbaugh, 1988). The model was developed for steady-state conditions in an unconfined aquifer, represented by a single layer with a constant thickness of 100m. The grid cell size of the model was taken 250x250m and 17600 of active cells were used to represent the entire study area which is 1085 km^2. Model area and the elevations of top layer were delineated by the ASTER DEM optimisation and use of the topographic maps. Aquifer properties were assigned based on the analysis of pumping test data. The Chloride Mass Balance Method (CMB) was employed to estimate the recharge. Optimised parameters (hydraulic conductivity and recharge) were spatially distributed over the model area.

The model was calibrated using hydraulic head observations from more than 80 wells. A combination of trial and error and automatic methods were performed to calibrate the model using the observed hydraulic head until the root mean square error (RMSE) reached about 11m. The sensitivity of the calibrated model was tested by systematically changing the input parameters individually. The summary of the entire domain water budget showed that the model calculated inflow and outflow terms are in balance. The outflow was modelled through MODFLOW's drain and groundwater evapotranspiraton packages. The outflow components of the water budget of the Raya Valley were estimated as 92mmy^{-1} and 22mmy^{-1} for drainage and groundwater evapotranspiration respectively. While the model calibrated total recharge rate of the valley was 114mmy^{-1}. Beside this, annual groundwater recharge of the two sub-basins in the valley which are Mohoni and Alamata sub-basins using the inverse modeling were estimated as 66mmy^{-1} and 170mmy^{-1} respectively. All the available measured hydraulic heads were used for calibration. Therefore, the model was calibrated but not verified. Hence, the results obtained here should not be interpreted as a perfect simulation rather as system response within fairly realistic model input parameters. Finally, some recommendations were made for management and monitoring of the valley's aquifer.

Key Words: Raya Valley, Alamata, Mohoni, groundwater modelling, recharge, irrigation

Acknowledgements

I would like to express my sincere gratitude to the Government of Netherlands through the Netherlands Fellowship Programme (NFP) for granting me the opportunity to study for a Master of Science degree at ITC. I am grateful to my organization Tigray Region Water Resources Mines, and Energy Bureau for granting me leave of absence to pursue further studies and for all the help they have rendered this far.

Special thanks go to my first supervisor Dr. A.S.M. Gieske for his excellent guidance and encouragements throughout my study period and especially during the research work. I highly appreciate his continuous constructive criticism and invaluable advises in every aspect of my thesis which helped me to locate this research in the right direction.

I greatly thank my second supervisor Dr. Ing. T.H.M.Rientjes for his support, encouragement, invaluable suggestions and comments to improve my research work

I would like to thank Dr. Ir. M.W.Lubczynski for he taught me many of the aspects in groundwater modelling principles, which was highly useful for my research accomplishment. I would like also to extend my appreciation to all my lecturers for giving me all the basics of science.

I gratefully acknowledge all offices and persons who have given me data for my study. Ethiopian Ministry of Water Resources, National Meteorological Agency, Water Works Design and Supervision Enterprise and Tekeze Deep Water Wells Drilling Plc.

I am most thankful to Hiwot, Gebrehaweria, Gebrerufael, Daniel, Afework and drivers Assefa, and Wudneh, who helped me a lot in the primary and secondary data collection during my fieldwork.

I cannot end without acknowledging the support received from my fellow classmates. I really enjoy being with you. I will remember you for making my life more pleasant in The Netherlands.

Finally, my deep gratitude and appreciation goes to my family members for their unwavering support, and love throughout my life.

Last but not least to all Ethiopian friends with whom I had always a wonderful time full of fun and joy throughout this period.

For everything, the precious honour goes to Almighty Allah.

Table of contents

List of figures

List of tables

List of acronyms

ASTER	Advanced Space borne Thermal Emission and Reflection Radiometer
CMB	Chloride Mass Balance
DEM	Digital Elevation Model
DWL	Dynamic Water Level
EC	Electrical Conductivity
EIGS	Ethiopian Institute of Geological Survey
GIS	Geographic Information System
ITCZ	Inter-Tropical Convergence Zone
m.a.s.l	Meter above sea level
MAE	Mean absolute error
ME	Mean error
MCM	Million Cubic Meters
ET_o	Potential Evapotranspiration
REST	Relief Society of Tigray
RMS	Root mean square
RS	Remote Sensing
RVDP	Raya Valley Development Project
SAR	Sodium adsorption ratio
SRTM	Shuttle Radar Topographic Mission
SWL	Static Water Level
TDS	Total Dissolved Solids
TDWWD	Tekeze Deep Water Wells Drilling Plc
WWDSE	Water Works Design and Supervision Enterprise

1. Introduction

1.1. Background

Groundwater is one of the most valuable natural resources, which supports human health, economic development and ecological diversity. Because of its several inherent qualities (e.g., consistent temperature, widespread and continuous availability, excellent natural quality, limited vulnerability, low development cost, drought reliability), it has become an important and dependable source of water supplies in all climatic regions including both urban and rural areas of developed and developing countries (Todd, 2005). Of the 37 Mkm^3 of freshwater estimated to be present on the earth, about 22% exists as groundwater, which constitutes about 97% of all liquid freshwater potentially available for human use (Foster, 1998).

Groundwater is the subsurface water that occurs beneath the water table in the soils and geologic formations that are fully saturated (Freeze and Cherry, 1979). Quantification of the rate of natural groundwater recharge is a basic prerequisite for efficient groundwater resource management, and is particularly essential in arid and semi arid regions where such resources are often the key to economic development. Assessment of the groundwater resources of an aquifer system involves developing a quantitative understanding of the flow processes which operate within the aquifer. Three features must be considered: how water enters the aquifer system; how water passes through the aquifer system and how water leaves the aquifer system. Groundwater regime forecasting involves a study of modifications to the flow processes due to changes in any of these features; these changes may be natural or man-made.

The study area of this research is Raya Valley, which is found in Northern Ethiopia, in Tigray Region (Figure 3.1). It has an area of about 2500 km^2 with a semi arid climate. This study focused on the simulation of groundwater flow system in Raya Valley using Groundwater modelling with the help of GIS and RS techniques. The aquifer system was modelled using PMWIN (Chiang et al., 1998) as pre- and post-processor assuming steady state conditions.

Geographic Information System (GIS) was used to enter, store, retrieve, process and display spatial information in the form of maps or images including a database which is linked to the mapping. A digital elevation model (DEM) of 30 m resolution of the Advanced Space borne Thermal Emission and Reflection Radiometer (ASTER) on-board NASA's satellite Terra was downloaded and GIS was used to process the digital elevation model (DEM) of the study area which in turn helped to define the boundary of the valley, visualize the geomorphology of the area, delineate the sub-catchments, extract drainage patterns and obtain surface elevation.

Remote Sensing (RS) application to groundwater was helpful in identifying of lineaments that are thought to be faults and fracturing, to define boundary conditions such as streams, lake, wetlands, and seepage areas, recharge zones or evapotranspiration zones of the area.

Raya Valley is one of the resource-endowed parts of the Tigray Region with respect to groundwater, fertile land, livestock potential and agro-climatic conditions. It is located on the western edge of the Danakil basin that consists of a number of small closed basins separated by volcanic mountains. The basin fill is mainly composed of unconsolidated material, which includes gravel and coarse sand with some pebbles and cobbles as colluvial deposits at the foot of the escarpment and medium to coarse alluvial materials along the intermittent rivers and finer valley centre deposits (RVDP, 1997).

In the study area the need for groundwater use in the irrigation scheme exists, because rainfall and surface sources, due to their seasonal variability and scarcity, cannot meet the irrigation requirement of the study area. However, most of the previous studies have been concerned more with resource development to meet users' need with little attention to the groundwater resource management. Therefore, safe groundwater abstraction and proper groundwater management is crucial for sustainability of the resource. Quantification of the current rate of natural groundwater recharge is a basic prerequisite for efficient groundwater management and this is even more important in semi-arid regions where such resources are often the key economic development (Simmers, 1988). It will be especially critical where large and concentrated demands for groundwater both for irrigation and for domestic supply exist as in the case of Raya Valley. Thus, proper understanding of natural recharge and groundwater flow system is necessary and there is a need for means of quantifying and assessing the effect of continued extraction of the resource in the area. Groundwater modelling is an essential tool to evaluate the groundwater flow and quantifying its potential (Anderson and Woessner, 1992).

1.2. Problem statement

Although Raya Valley is rich in land resources for agricultural development, the lowland areas experience low rainfall which is insufficient for agricultural production. So people in the area have commonly used supplementary irrigation by flood diversion for many years. But due to erratic rainfall distribution in the area they often fail to satisfy the soil moisture condition for growing crops. As a result drought was affecting the area a number of times (REST, 1996). Now the need of agricultural development in the valley by using groundwater is growing continuously. Many wells were dug and groundwater is increasingly being used as source of water for irrigation. However, there is no control or management of the groundwater reserves. Hence, developing groundwater model simulation is essential not only to understand the natural groundwater flow but also the influence of extractions and irrigation schemes on the groundwater system.

Groundwater use is rapidly increasing in Raya Valley, bringing several benefits to small farmers by allowing them to grow more crops and minimizing the impact of water shortages that occur during dry season. But groundwater is not properly managed as an additional source. Government organisations as well as several private parties are engaged in construction of wells in the area. At the same time there is no well monitored and registered groundwater data. Because of that, clear records on this resource cannot be obtained.

Sustainable aquifer exploitation occurs when the rate of groundwater extraction is equal or less than the natural rate of groundwater replenishment for any level of aquifer storage. Thus to be able to exploit the aquifer in a sustainable manner with minimal impact on the environment there is a need to demarcate and evaluate the aquifer potential. In order to ensure a sensible management of

groundwater, proper evaluation is required, its present status should be studied and prediction of the future status of the water resource should be attempted. Then it is necessary to allocate areas with high groundwater potential to improve control of abstraction rates to ensure proper groundwater management.

1.3. Objectives

General objective

The main objective of this study is to assess the groundwater resources of the valley by studying the groundwater flow pattern in response to recharge and abstractions using a steady-state groundwater flow model together with the assistance of GIS and remote sensing techniques.

Specific objectives

The specific objectives are:-

- Examination of the physical and hydraulic boundaries of the valley.
- Development of a conceptual model representing the hydrogeological condition of the valley based on ground observations and data analysis.
- Estimation of the groundwater recharge using chloride mass balance method and through model calibration (with special attention to the different recharge mechanisms in the area).
- Analysis of the hydro-chemical data using AQUACHEM software, statistics and GIS.
- Setup and calibration of a steady-state groundwater flow model of the area.
- Development of scenarios illustrating effect of different irrigation stress conditions on the groundwater resource.

1.4. Research questions

To address the objectives mentioned above, the following research questions are posed:

- Can the conceptual model be transformed to a numeric model which is capable to simulate the observed conditions of the aquifer system?
- What are the main water sources and sinks of the valley?
- Can the groundwater recharge of the valley be estimated using chloride mass balance method and through model calibration?
- What is the natural flow pattern of groundwater in the study area?
- How accurate are the simulation results from the model developed?
- Can a steady state groundwater flow model of the area improve the understanding of flow patterns and predict the effect of future abstractions?

1.5. Methodology

The methodologies followed were based on the objectives of the study as stated in section 1.3. The key stages of the activities are presented as pre field, fieldwork and post field stages. Besides, the major sources of information and materials used are stated.

Pre field work

This stage included proposal writing, collection of necessary information about the area, collecting available secondary data from different sources, preparing base map and preparation for field work including acquisition of field equipments were conducted. Among the activities are, literature review, related to recharge estimation and principle of groundwater modelling, reviewing the feasibility reports of the previous works on the area to have good understanding about the problem and to define the approach to the research.

Field work

A field trip was conducted to collect secondary data from different sources and primary data from the study area. The primary data collection included, measuring groundwater levels, EC in situ measurements, taking readings of borehole locations and elevation using GPS and altimeter, collection of water samples from springs, boreholes, and surface water bodies for chemical analysis and field verification of the study area and identification of physical boundaries. The ground truth field observations were focused on the description of the geology, stratigraphy, geomorphologic setting, surface water divide, location of discharge, and recharge areas. The secondary data collection included collection of meteorological data (rainfall, T_{max}, T_{min}, relative humidity, wind speed and sunshine hours) from National Meteorological Service; well completion, pumping test data and reports of previous studies from Tigray Water Resources, Mines & Energy Bureau, Tekeze Deep Water Wells drilling Plc. and Water works Design and Supervision Enterprise.

Post field work (data processing and analysis)

Data processing was the main activity of this stage. The data collected during pre-fieldwork and during fieldwork were processed and analyzed. The main activities here are organizing the collected data and preparing the database for the input of the modelling process. Geographic Information System (GIS) was used to enter, store, retrieve, process and display spatial information in the form of maps or images including a database which is linked to the mapping. GIS was also used to download and process images of Landsat Enhanced Thematic Mapper (ETM), Advanced Space borne Thermal Emission and Reflection Radiometer (ASTER), Shuttle Radar Topographic Mission (SRTM) and the ASTER product of Global Digital Elevation Model (GDEM). The DEM was processed to define the boundary of the valley, visualize the geomorphology of the area, delineate the sub-catchments, extract drainage patterns, to produce topographic cross section lines and obtain surface elevations.

Remote Sensing (RS) application was used to define boundary conditions such as streams, lake, wetlands, seepage areas, recharge zones and evapotranspiration zones of the area. For this purpose Landsat Enhanced Thematic Mapper (ETM) image was downloaded and analysed. Landsat is preferred over other satellite data due to the availability of near to mid-infrared bands, which is useful for terrain and lineament analyses. Beside this, Landsat ETM provides eight spectral channels (one panchromatic with 15m spatial resolution, six bands ranging from visible to mid-infrared with 30m spatial resolution, and one thermal band with 60m spatial resolution), permitting a large spectrum of band combinations, useful in visual interpretation of different features.

Pumping test data were analysed to determine hydraulic parameters such as transmissivity and hydraulic conductivity. The laboratory analysis results of the water samples were processed and presented using AQUACHEM software. The determination of the chloride concentration in groundwater was also part of this analysis.

Groundwater recharge is an important variable in regional-scale hydrologic models and aquifer-system analysis (Yeh et al., 2007). The methodology selected for the estimation of recharge should be applicable in wide variety of climatic and hydrologic situations. In this study, Chloride Mass Balance (CMB) method and inverse groundwater modelling were applied to estimate the groundwater recharge. According to Simmers et al (1997), chloride is the most important environmental tracer and has been used to estimate rates of groundwater recharge under a wide range of climatic, geologic and soil conditions.

1.6. Outline of the thesis

The content of this thesis is briefly outlined as follows

Chapter one: Describes the introduction of the research that includes the problem statement, the objective of the research and research questions.

Chapter two: Discusses the review of previous studies in the area and literature review related to principle of groundwater modelling and recharge estimation methods

Chapter three: Describes the study area, in terms of location, climate, geology, geomorphology and land use types.

Chapter four: Data processing and analysis of primary and secondary data and translating the data to model input. Pumping test data, water chemistry data, and recharge estimations are parts of the analysis.

Chapter five: Explains the numerical groundwater flow model of Raya Valley, which includes, code selection, model design, model calibration and sensitivity analysis.

Chapter six: Deals with the pumping scenario analysis

Chapter seven: is dealing with the results and discussions.

Finally conclusions and recommendations of the study are presented in **Chapter eight.**

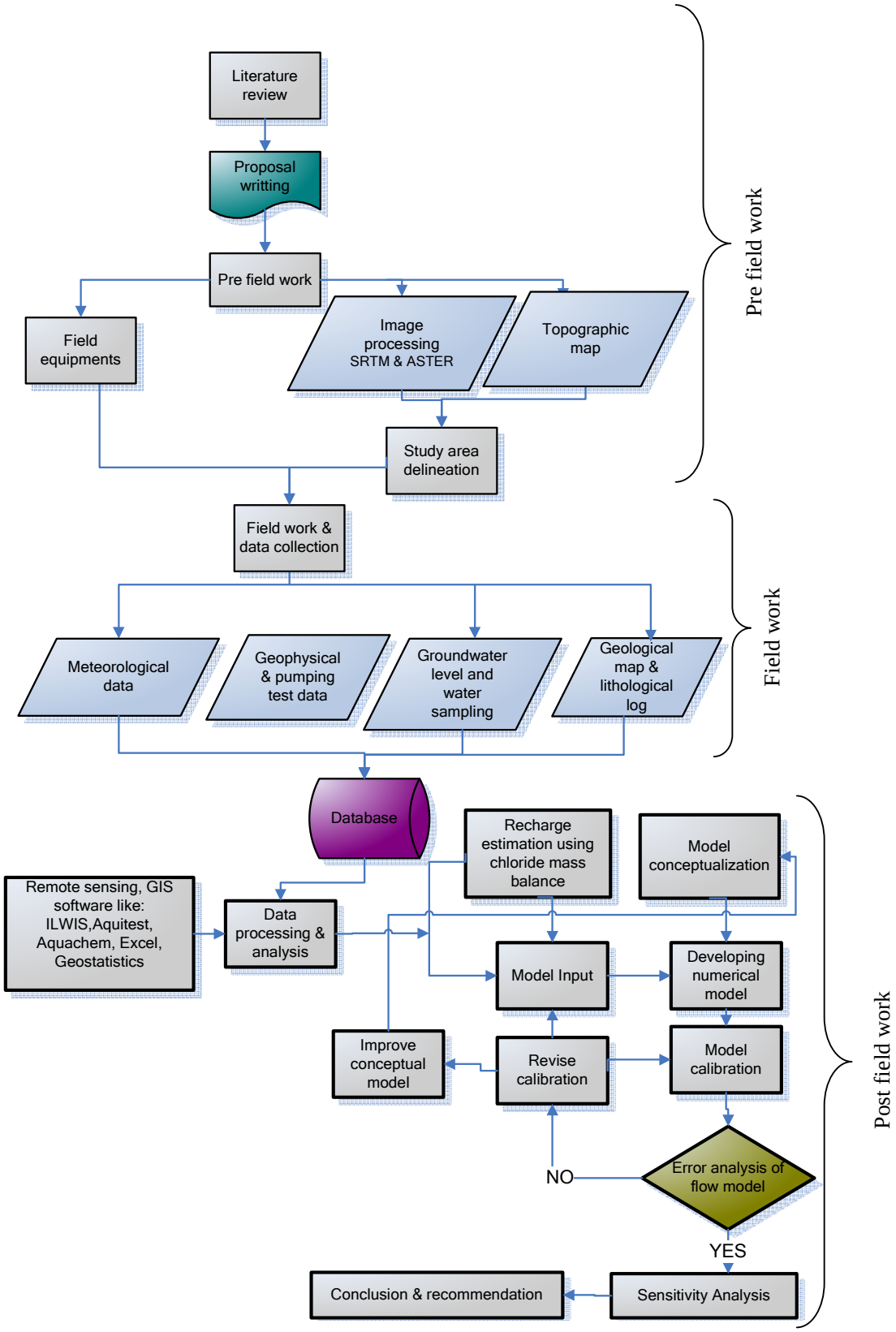

Figure 1.1 Flow chart of the methodology

2. Literature review

2.1. Review of previous studies

Several studies are available which were carried out to find a way of exploiting the available water resources in the Raya Valley area. REST (1996) made a preliminary study on the development of a project for the improvement of living conditions of the people in the project area in particular and the region in general. The study focuses on enhancing the agricultural production by using water resource of the area. In the study area a geophysical survey was conducted by German Consult in 1978, the Ethiopian Institute of Geological Survey (EIGS) in 1996 and the Tigray Water Mines and Energy Bureau at different levels. The surveys were aimed at determining the thickness of loose sediment, and depth to groundwater. A study with the objective to study a design of the Raya pressurized irrigation system which would enable to use the groundwater resources in the lower plain of Raya Valley was also made by (WWDSE, 2008b). According to Halefom (2006) the groundwater recharge from precipitation in the Alamata sub-basin was estimated to be about 80mmy^{-1} which accounts to approximately 10% of the annual precipitation. Most of the existing old wells found in the Raya Valley area have been constructed for community water supply purposes and are very shallow so that they have not penetrated the full thickness of the aquifer. However, recently, around 100 deep wells were drilled to implement modern pressurized irrigation activities by developing the groundwater resource of Raya Valley.

The annual amount of rainfall is relatively small and erratic as compared to other parts of the region. As a result the area is being affected by a recurrent drought. Due to this fact most of the rivers are intermittent. Hence, groundwater use is rapidly increasing in Raya Valley, bringing several benefits to small farmers by allowing them to grow more crops and minimizing the impact of water shortages that occur during the dry season.

Hydrological, geological and hydrogeological studies were carried out on the Raya Valley by a project known as Raya Valley Development Project (RVDP) to determine the groundwater resource potential, to give background information for dam studies, and to assess surface water resources for micro-dam constructions. In the hydrogeological work the groundwater flow directions were summarised to be West-East and North-South. Dessie (2003) carried out a study on the availability and usability of the water resources in the Raya Valley giving particular attention to the groundwater in the alluvial deposits, from geological, hydrological and chemical point of view.

In addition the following studies were conducted on the Raya Valley:

- German Agency for Technical Co-operation Ltd (1977) Pedology and water development, Kobo-Alamata Agricultural Development Program, Volume-II.
- REST, 1996. Raya Valley development study project, phase I (reconnaissance phase report), Relief Society of Tigray, Tigray National Regional Government.
- RVDP, 1997. Hydrogeology Feasibility Draft Report, Raya Valley Development Project Regional Government of Tigray.

- WWDSE, 2008. Raya Valley Pressurized Irrigation Project. Water Works Design and Supervision Enterprise in association with Concert Engineering and Consulting PLC executive Summary / Feasibility Final, Federal Democratic Republic of Ethiopia Ministry of Water Resources.

Most of the recent studies focused on the adaptation of the modern pressurized irrigation methods for the Raya Valley on a large scale.

2.2. Integration of RS, GIS and modelling techniques

Remote Sensing (RS) and Geographic Information System (GIS) based groundwater studies are recommended to be carried out in conjunction with field investigations to effectively exploit the expanding potential of RS and GIS technologies, which will perfect and standardize current applications as well as lead to development of new approaches and applications. It is concluded that both the RS and GIS technologies have great potential to revolutionize the monitoring and management of vital groundwater resources in the future. Several researchers have demonstrated that GIS, because of its sophisticated analysis and graphics capabilities, can provide a powerful platform for developing GIS-based groundwater model, calibrating and validating them, and presenting their results (Jha et al., 2007).

GIS can enter, store, retrieve, process and display spatial information in the form of maps or images (satellite, aerial photographs) including a database which is linked to the mapping. GIS provides an integrated platform to manage, analyze, and display spatial data. GIS has also been used to develop the digital elevation model (DEM) of the catchment which in turn helped to define the top of the aquifer. In this study to process the digital elevation model the DEM hydro-processing package in the ILWIS software was used.

Modern RS/GIS software enables digital RS data to be merged with other data. Digitised maps, e.g. road networks, or geological maps, can be combined with the images, making the interpretation easier. An existing thematic map can be visualised together with the information from a satellite image. In most studies the conceptual models essential as the backbone of the investigations, need to be quantified. Here again the techniques combining RS, GIS and simple models can be used to estimate fluxes. Mapping units can be based on geomorphology, geology, soils and vegetation. Some of the components of the hydrological cycle, such as actual evapotranspiration and groundwater recharge potential, may be estimated for different mapping. In this study the RS and GIS software like ILWIS, MapInfo, ArcGIS, and Global Mapper were used.

2.3. Groundwater recharge

Groundwater recharge can be defined in general sense as the downward flow of water reaching the water table, forming an addition to the groundwater reservoir (Lerner et al., 1990). In semi-arid regions, assessment of groundwater recharge is one of the key challenges in determining the sustainable yield of aquifers as recharge rates are generally low in comparison with average annual rainfall or evapotranspiration, and thus difficult to determine precisely (Yongxin and Beekman, 2003).

Among the groundwater recharge estimation methods are: the water table fluctuation method, chloride mass balance method, one dimensional soil water flow model, inverse modelling and groundwater balance method. The water table fluctuation method is an indirect method of deducing the recharge from the fluctuation of the water table (Sharda et al., 2006). The chloride mass balance method is based on the assumption of conservation of mass between the input of atmospheric chloride and the chloride flux in the subsurface (Yongxin and Beekman, 2003). The one dimensional soil water flow model in the unsaturated soils is mathematically formulated based on the Richard's equation that combines Darcy's law with the mass conservation equation. Inverse modelling is a technique by which model input is estimated from model output. Using inverse modelling, recharge and hydraulic conductivity values are usually estimated simultaneously. The problem of estimating aquifer parameters with the aid of a numerical model that uses limited observations and prior information is often referred to as inverse modelling. The fundamental benefit of inverse modelling is its ability to auto calibrate optimal parameter values for an aquifer region that produce the best fit between observed and simulated hydraulic heads and flows (Lakshmi Prasad and Rastogi, 2001).The groundwater balance method is based on the general hydrological principle in which the amount of water entering a control volume during a defined time period (inflow), minus the amount of water leaving the volume during the time period (outflow), equal the change in the amount of water stored (ΔS) in the volume during that period. As discussed by Simmers et al. (1997), quantifying the current rate of groundwater recharge is a basic prerequisite for efficient groundwater resource management and is practically vital in arid regions where such resources are often the key to economic development. Groundwater recharge quantification is fraught with problems of varying magnitude and hence substantial uncertainties. It is therefore desirable to always apply and compare a number of independent approaches.

2.4. Groundwater modeling

There are two areas of hydrogeology where we need rely on models of real hydrological system: to understand why a flow system is behaving in a particular observed manner and to predict how a flow system is behaving (Fetter, 2001). There are several ways to classify groundwater flow models, models can be either transient or steady state and one, two or three spatial dimension. Steady state flow occurs when at any point in a flow field the magnitude and direction of the flow are constant with time (Anderson and Woessner, 1992).

Selecting the appropriate conceptual model for a given problem is one of the most important steps in the modelling process. The key data requirements in the process of conceptualization include data about hydro-stratigraphic units, surface water bodies, physical and hydraulic boundaries, recharge and discharge zones. The most common numerical methods to solve flow problems are finite differences and finite elements. Finite-difference grids are easy to understand and require less input data than finite-element grids (Anderson and Woessner, 1992). The finite difference method, as applied in the computer code MODFLOW, was used in this study. The code is based on the physical theory of groundwater movement Darcy's law and the continuity equation. PMWIN was used as a pre- and post-processing. This program supports seven additional packages which are integrated with the original MODFLOW (Chiang and Kinzelbach, 2001).

Once the conceptual model is translated into a numerical model in the form of governing equations, with associated boundary and initial conditions, a solution can be obtained by transforming it into a numerical model and writing a computer program (code) for solving it. This includes, design of grid, setting boundary and initial conditions and preliminary selection of values for aquifer parameters. The input parameters include model grid size, layer elevations, boundary conditions, hydraulic conductivity/transmissivity, recharge, and additional model input for steady state modelling. Model calibration consists of changing values of model input parameters in an attempt to match field conditions within some acceptable criteria (Anderson and Woessner, 1992). Sensitivity analysis is useful in determining which parameters most influence model results. These parameters will be emphasized in future data collection attempting to improve model accuracy.

3. Description of the study area

3.1. Location

Raya Valley is located in Northern part of Ethiopia, Tigray Regional State at about 170 km south of the province capital Mekelle (Figure 3.1). It is situated between 12^0 05' and $12^0$55' latitude and $39^0$21' and $39^0$55' longitude. The valley consists two sub-basins, namely, the Alamata and the Mohoni sub-basins (Figure 3.4). It is bounded by the Korem Mountains in the west, the Chercher Mountains in the east and in the south by low E-W surface divide near Kobo town separating the Alamata sub-basin from the Golina sub-basin to the south. The valley opens to the north and narrows to the south. The transition to the Afar depression is marked by a low range of volcanic hills which form the eastern boundary.

The Raya Valley is considered as part of interconnected valleys of the Ethiopian rift system. It has an area of about 2500 km^2. Raya Valley is among the sub-basins on the western edge of the Danakil basin that consists of a number of small closed basins separated by volcanic mountains. The basin fill is mainly composed of unconsolidated material, which includes gravel and coarse sand with some pebbles and cobbles as colluvial deposits which are developed from recent alluvial and colluvial sediments that originated from mountain ranges that bounded the sub-basins on the eastern and western peripheries. The average altitude of the valley floor ranges from 1370 m a.m.s.l. to 1600 m a.m.s.l. while the mountain ridges range from 1600 m a.m.s.l. to 3600 m a.m.s.l. The Sulula River is the longest river running from north to south in the eastern part of the area. It drains the surface water and the groundwater around the outlet where the groundwater level rises during the rainy season. The high gradient from west to east is approximately 1000m within about 30km which favours the emergence of springs at different elevations.

3.2. Geomorphology and drainage

3.2.1. Geomorphology

The local and regional relief setting gives an idea about the general direction of groundwater flow and its influence on groundwater recharge and discharge. The field observation indicated that the Raya Valley is characterized by a graben-like structure bounded by north-south aligned ridges on the western and eastern sides of the valley. The width of the Raya Valley ranges from about 23 km in the northern and central parts to about 5 km in the southern end of the valley. The valley is divided into Alamata and Mohoni sub-basins by undulating surfaces and volcanic hills outcropping in the east-west direction (Figure 3.4).

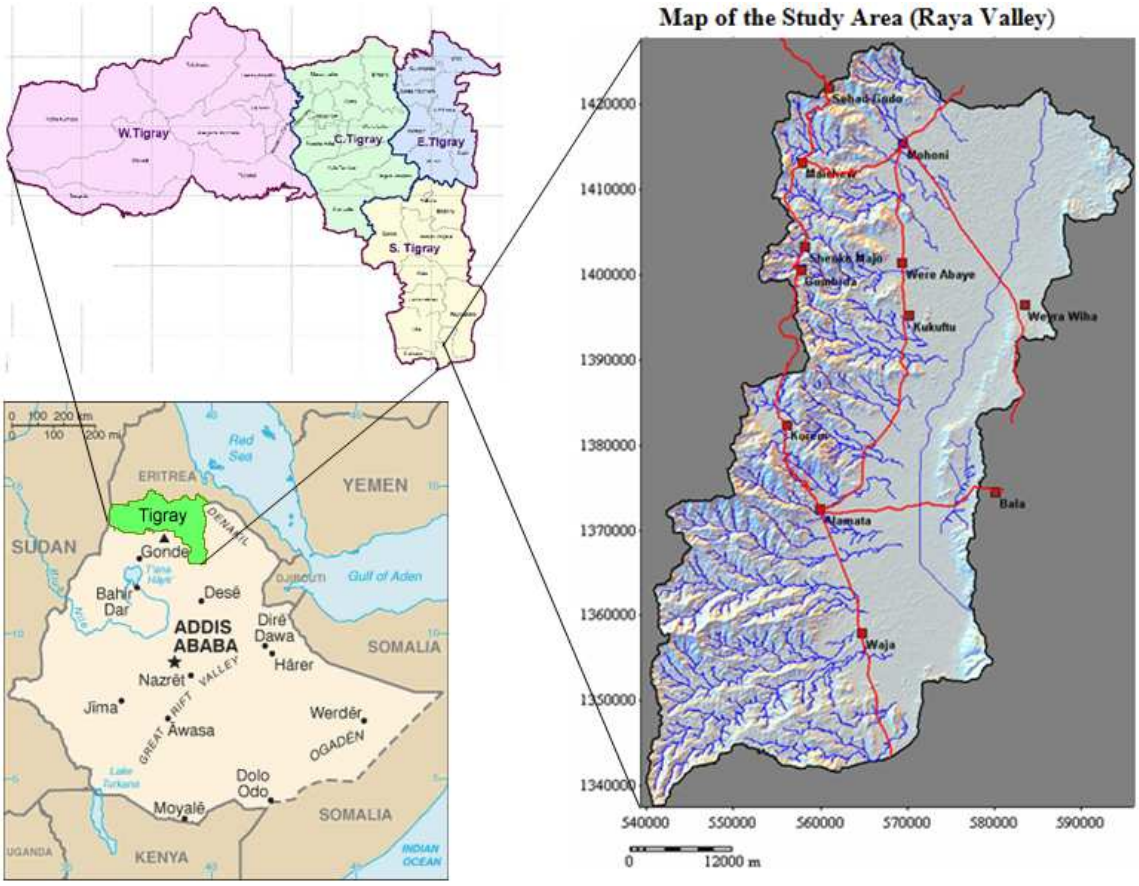

Figure 3.1 Location map of the study area

The chain of mountains bordering the valley area on the western and eastern sides, are characterized by steep slopes covered with vegetation of low density. These generate a large amount of runoff. Though the area receives highly variable rainfall, runoff generated from the western escarpments of the valley causes intermittent flooding of the valley floor adjacent to the rivers during the rainy season. Many of the rivers that enter the valley area terminate on the eastern periphery of the sub-basins where they form occasional flash floods and temporary wetlands in some parts mostly in the Alamata sub-basin. In order to visualize the physiography of the study area, a digital elevation model (DEM) of ASTER image 30m resolution was processed and compared with a topographic map of scale 1:50,000 using GIS software. This enabled to see the different landform units. The minimum height in the study area is about 1370 m a.m.s.l whereas the maximum height is found to be 3600m a.m.s.l. The western escarpment is more pronounced than the eastern margin as it can be seen from DEM. The latter margin is also the western rift escarpment of the Afar depression.

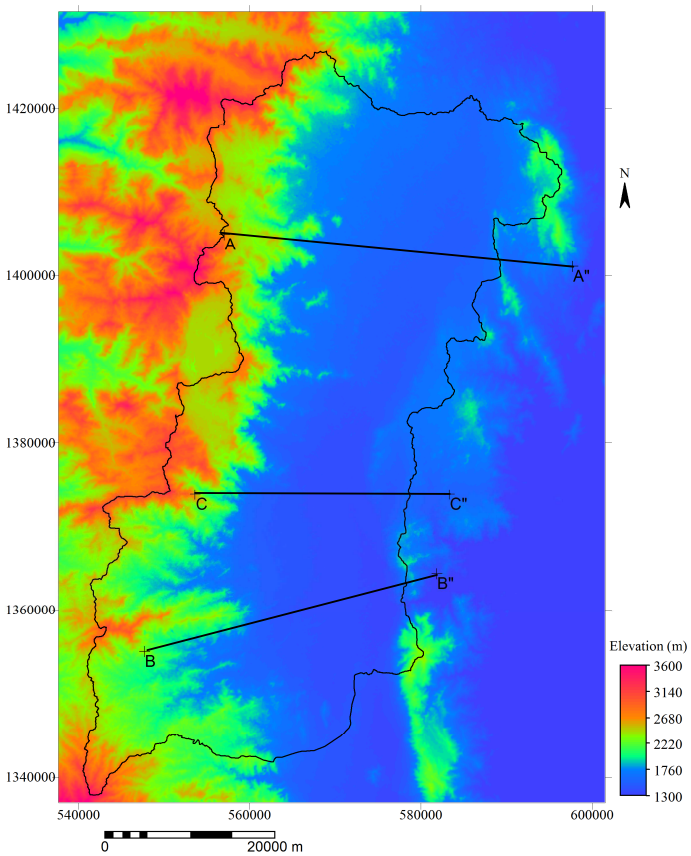

Figure 3.2 DEM of the study area and cross-section lines

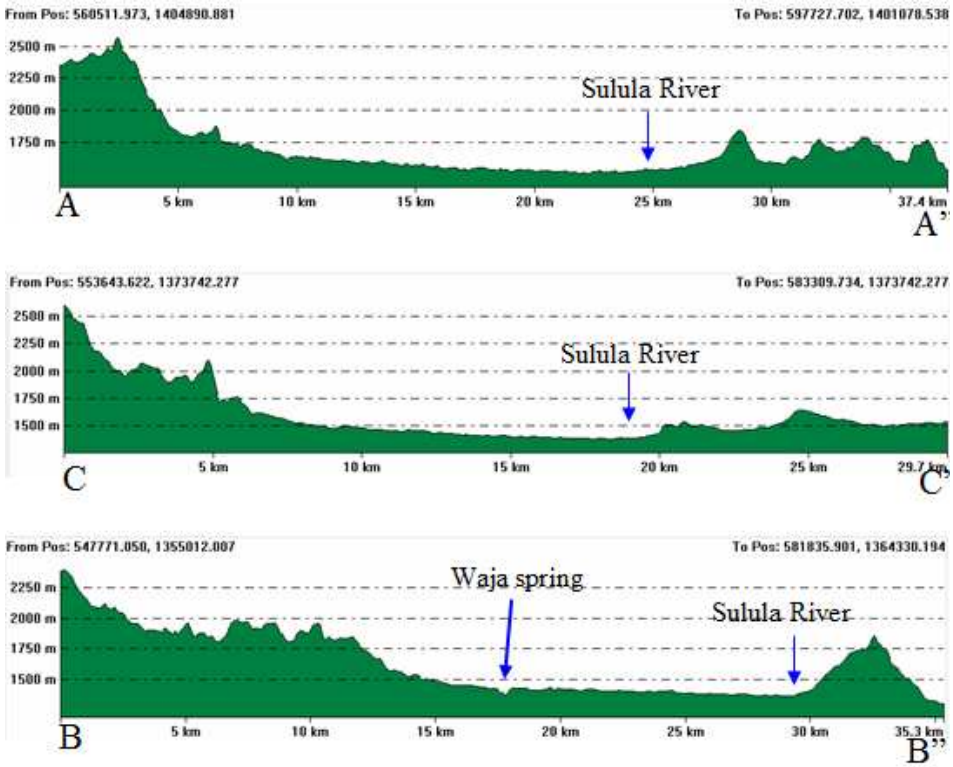

Figure 3.3 Cross-section lines of the digital elevation model of the area

From the cross-section lines it is clear that the valley floor dips towards the east while the western hills are higher in elevation than the eastern ones. The sections also show that the valley is wider in the northern part than the southern part. The cross-section line B-B'' indicates that Waja spring emerges where the surface topography intersects to the groundwater head.

3.2.2. Drainage

The Raya Valley consists of several separate drainage units emerging from the western highlands and partly from eastern highlands, which have a sub-parallel flow path in east-west directions. The western margin of the valley is a source of most of the rivers in the study area (Figure 3.4). Most of the streams that originate in the Mohoni highlands flow south-easterly following the dip direction and join the major river system of the Sulula River. In the Raya Valley plain there are no perennial rivers and streams except some springs at the western edge (at the transition point from escarpment to plain) and runoff from these springs disappears in the central part of the valley. This situation has made groundwater the primary source for water supply in the valley i.e. for water supply of the towns and rural population and for irrigation purposes. The central and eastern part of the valley is characterized by a sparse drainage system. During the field visit in September none of the rivers in these parts of the valley was flowing. The longest river in the study area is the Sulula River which is running north-south adjacent to the eastern periphery of the valley. It is connected on the surface with streams flowing from the eastern margin and it also acts as drainage for the groundwater system. The Sulula River cuts through the eastern range of hills at Selembir. From there the river flows down into the Afar depression. The gap at Selembir is the only possible surface water outlet from the valley.

3.3. Climate

The position of the Inter-Tropical Convergence Zone (ITCZ), seasonal variations in pressure systems and air circulation, results in the seasonal distribution of rainfall over the study area. This low pressure area of convergence between tropical easterlies and equatorial westerlies causes equatorial disturbances (Gamachu, 1977). The area has a semi-arid climate with mean annual rainfall of 724 mm. The distribution of rainfall over the highland areas is influenced by orographic effects and is significantly correlated with altitude. The area is characterized by a bimodal rainfall pattern with a short rainy season "Belg" from March to April and a long rainy season "Kiremt" from July to September with a peak in August. The other months of the year are generally dry.

The study area varies in altitudes ranging from 1370 to 3600m a.m.s.l. The area comprises of lowland plain areas with altitudes of 1370 to 1600 m a.s.l, while the mountain areas and the plateaus are situated with in the altitude ranges of 1600 to 3600m a.m.s.l. This variability in altitude brings variability in rainfall and temperature. The quantitative description of the climatic variability was discussed in chapter four.

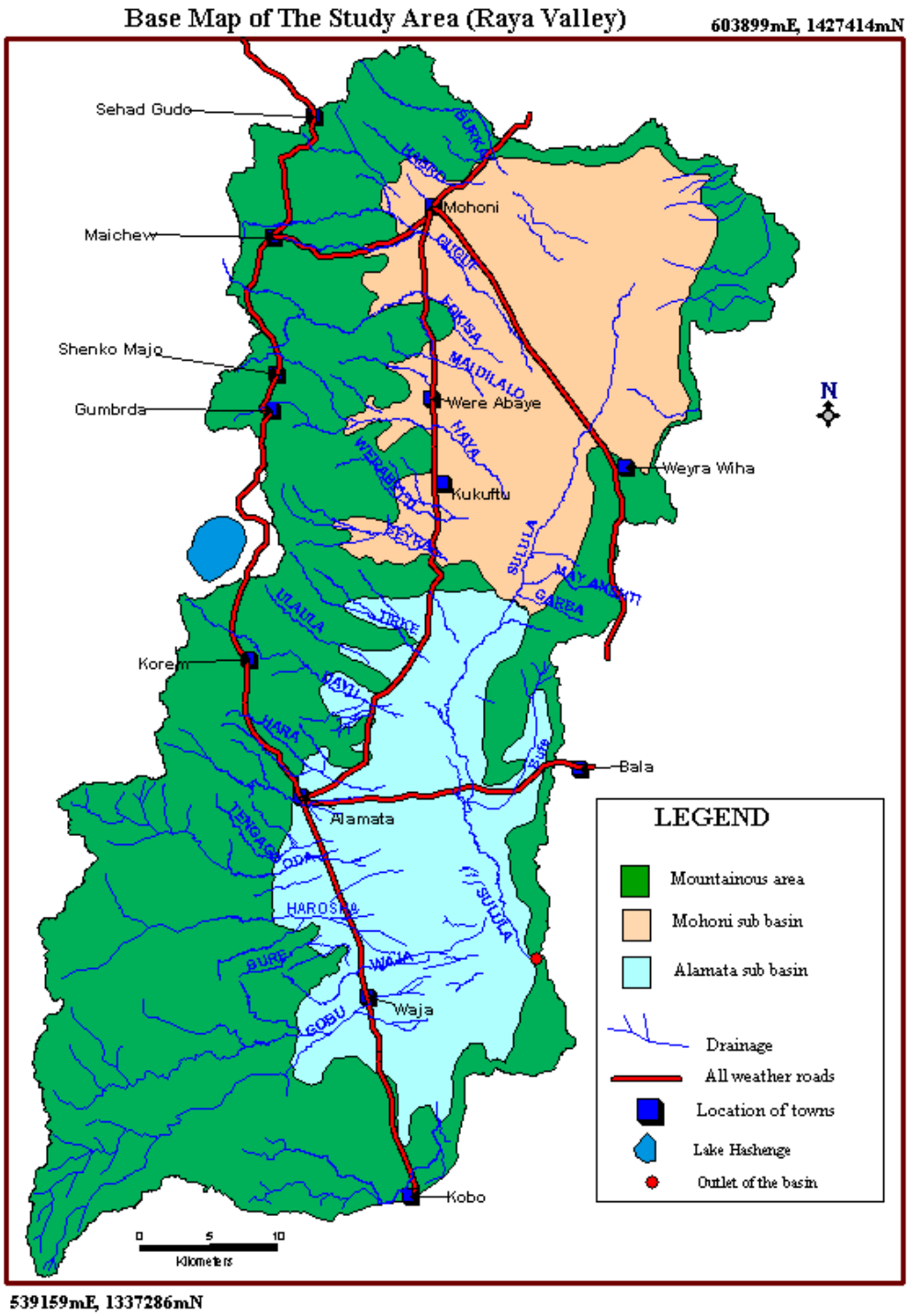

Figure 3.4 Base map of the study area

3.4. Land use and land cover types

Land use is important in groundwater studies, because it is a prominent factor affecting the recharge. According to Dessie (2003) five land cover types are identified in the area. These are forest, agricultural area, water, woodland, and bare-land. Woodland and agricultural area are the dominant

land use classes in the area. The land use map of the Raya sub -scene is shown in Figure 3.5 with the summary in Table 3.1.

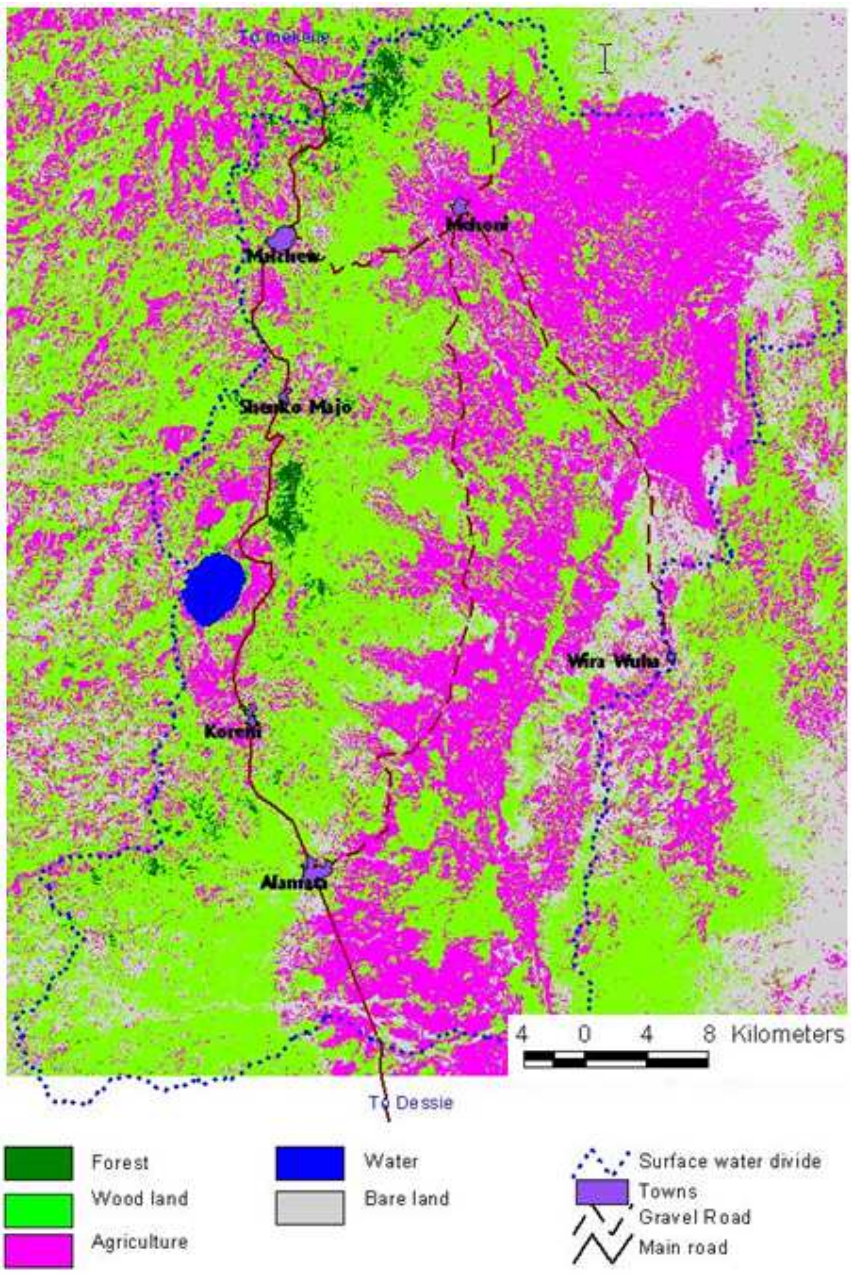

Figure 3.5 Supervised land cover and use classification of the sub-scene consisting the Raya Valley (Dessie, 2003)

Table 3.1 Land use and land cover proportion in the a sub - scene of Raya Valley

Land cover type	Wood land	Bare land	Agriculture	Forest	Water
Raya sub -scene	48.80%	19%	31.10%	0.80%	0.30%

3.5. Geology and hydrogeology

3.5.1. Geology

Regional geology

The geological units in Ethiopia fall into one of the following three major categories, the precambrian basement, late palaeozoic to early tertiary sediments and the cenozoic volcanics and associated sediments (Mengesha et al., 1996). According to Kazmin (1975) major transgression-regression cycles took place during the Mesozoic. It is believed that the cyclic uplift, transgression-regression and intensive volcanism and rifting through geologic times has resulted in a complex geology and strange relief in Ethiopia. The starting of the subsidence of the Afar depression and the subsequent volcanism was restricted at first to the evolving rifts and then to axial zones which later became a focus of quaternary and recent volcanic activity. Meanwhile the sedimentary process has continued in this era forming a valley fill and lacustrine deposits within the developing rifts.

Local geology

The Raya valley is a sub-basin at the western edge of the Danakil basin. The major lithological units in the study area are basaltic rocks on the plateau and escarpments and alluvial deposits derived from these basalts on the valley floor. According to Mengesha et al. (1996) the valley of the study area is dominated by thick undifferentiated alluvial and lacustrine sediments bounded on the east and west by Hashange formation, which is a series of volcanic rocks characterized by alkaline (olivine) and transitional basalt flows with tuff intercalations, rare rhyolites from fissures and dissected by dikes and sills. Based on the lithological log of the boreholes drilled in the area, the valley plain sediments thickness ranges from few meters to more than 250 meters. The minimum thickness occurs near the western and eastern flanks of the valley whereas the maximum thickness is obtained towards the central part of the valley. The floor of the valley plain is a flat plain with decreasing slope from north toward south and from west to east. As observed from the lithological log of the boreholes drilled in the valley, the alluvial deposits are composed of intercalating layers of gravel, gravely sands, silty sands, clay, and silty clay. According to previous study conducted on the study area RVDP (1996) and Dessie (2003) the rock units in the area has been classified as follows:

Volcanic rocks

The volcanic rocks that are found in the study area are: amygdoloidal basalt, alkali olivine basalt, aphanitic basalt and agglomerates. The amygdoloidal basalt is composed of porophyroblasts of pyroxene and olivine. It is found in the lower zones of the successions. Alkali olivine basalt is one of the major volcanic covers in the study area. Aphanitic basalt forms swarms of highly jointed dykes with variable trends. The agglomerates commonly form block and volcanic bombs in some cases forming small hills in different parts of the study areas.

Sedimentary Rocks

The sandstone rock sub-units that are found in the study area are: Sandstone, limestone and quaternary alluvial deposits. The sandstone rock unit outcrops near the Bala town. Its area coverage is small as compared to other formations in the study area. The limestone unit is found in the north eastern part of the study area near to Adi Bedera. The quaternary alluvial deposits are found as valley fill. More than 40 % of the study area consists of alluvial deposits derived from the weathering and erosion of the surrounding basaltic rocks. The thickness of this deposits increases as one move from the foot of the escarpment to the centre. At the foot of the mountains the major types of unconsolidated materials are colluvial deposits derived from the surrounding escarpments. The sediments are coarser on the periphery of the valley and get finer towards the centre. The maximum thickness drilled in the alluvial deposit from the collected data is 288m. This is a well in Alamata sub-basin with borehole name RPW-093-08.

3.5.2. Hydrogeology

Raya and Kobo are the prominent alluvial grabens running N–S parallel to the escarpment. As the previous studies and drilling in different parts of the valley plain show, the valley is mainly composed of sedimentary basin fill deposits of high groundwater potential. But due to the variation of thickness, grain size and sorting of the alluvial deposit, the groundwater potential is not uniform throughout the valley. Areas with very fine alluvial deposit and massive basaltic domes have low groundwater potential and this is indicated by low yielding boreholes. According to the drilled well data the main aquifer in Raya Valley consists mainly of alluvial deposits having a thickness in the valley plain ranging from about 40 to more than 250 meters. The minimum thickness is the western and eastern flanks of the valley whereas the maximum thickness is obtained towards the central part of the valley. The floor of the valley plain has a decreasing slope from north toward south. In the central part of the Alamata sub-basin clay lenses act as confining layers. The depth of the groundwater varies from 0 to about 50m in Alamta sub-basin and from 20 to about 60m below ground level in Mohoni sub-basin. As Alamata sub-basin has more recharge area and thick alluvial deposit, it has more groundwater potential than Mohoni sub-basin. Currently, in both sub-basins there are more deep well drilling activities for the implementation of modern pressurized irrigation systems. The western part of the aquifer has generally unconfined groundwater condition, whereas the south-eastern part is characterized mostly by semi-confined to confined conditions. In latter part of the area some artesian wells were also observed. According to the pumping test data analysis, the hydraulic conductivity values of the aquifer ranges from about 1 to 39md^{-1}. The main source of groundwater recharge of Raya Valley is mainly through seasonal floods from adjacent highlands of the western, northern and eastern sides of the valley. In addition to the alluvial deposits the volcanic rocks are acting as an aquifer when fractured. But the volcanic aquifer does not have such a high potential as the alluvial deposits.

4. Analysis and model input data preparation

4.1. Meteorological data analysis

4.1.1. Rainfall

Rainfall data from nine rain gauge stations which have been considered to describe the rainfall regime of the Raya Valley were collected and analysed (Figure 4.1). Missing data is a common case for the stations. However, the selected stations for ten years (1996 to 2005) have relatively consistent data that can be used for the purpose of this study. The average monthly meteorological data of these 10 years was taken for analyses. The mean annual precipitation has a bimodal distribution with most of the rainfall occurring during the months July to September while there is a short rainy season from March to April. The other months are generally dry (Figure 4.3). Korem gauging station in the western highland reported a maximum annual rainfall depth of 1356mm and minimum annual rainfall depth, i.e. 465mm, was reported at Waja gauging station, located within the valley floor. The moving average interpolation technique with inverse distance method was applied to study the spatial distribution of the rainfall within the catchment (Figure 4.1). For the tables of these climatic variables (see Appendix 1). Thiessen polygon method was applied to see the mean annual rainfall for the entire valley. In the Thiessen polygon method, the study area is divided into polygons with the rain gauge in the middle of each polygon assumed to be representative for the rainfall on the area of land included in its polygon. These polygons are made by drawing lines between gauges, and then making perpendicular bisectors of those lines form the polygons. The weighted mean of the precipitation was calculated using equation 4.1 which resulted in 724mm of mean annual rainfall for the entire Raya Valley (Table 4.1).

$$P = \frac{A_1P_1 + A_2P_2 + A_3P_3 + ... + A_iP_i ... A_nP_n}{A_t} \qquad (4.1)$$

Where:

P	=	Mean annual rainfall for the entire valley	[mm]
A_i	=	Area enclosed between the i^{th} and the i+1 isohyets	[km^2]
P_i	=	Mean annual rainfall of the i^{th} and the i+1 isohyets	[mm]
A_t	=	Total area of the valley	[km^2]

Table 4.1 Mean annual rainfall using Thiessen polygon method

Station	Easting (m)	Northing (m)	Elevation (m)	P_i (mm)	A_i (km^2) (km^2)	P_iA_i/A_t (mm)
Alamata	560502	1372456	1547	821	419	134
Waja	565315	1357995	1446	656	481	122
Kobo	568641	1343604	1524	734	155	44
Korem	556673	1382295	2466	1022	288	114
Maichew	558432	1412871	2438	778	224	68
Mohoni	570019	1415122	1767	521	541	109
Chercher	583783	1386254	1786	723	363	102
Zoble	581470	1354118	2139	777	67	20
Muja	531341	1326927	2749	705	39	11
Total					2577	724

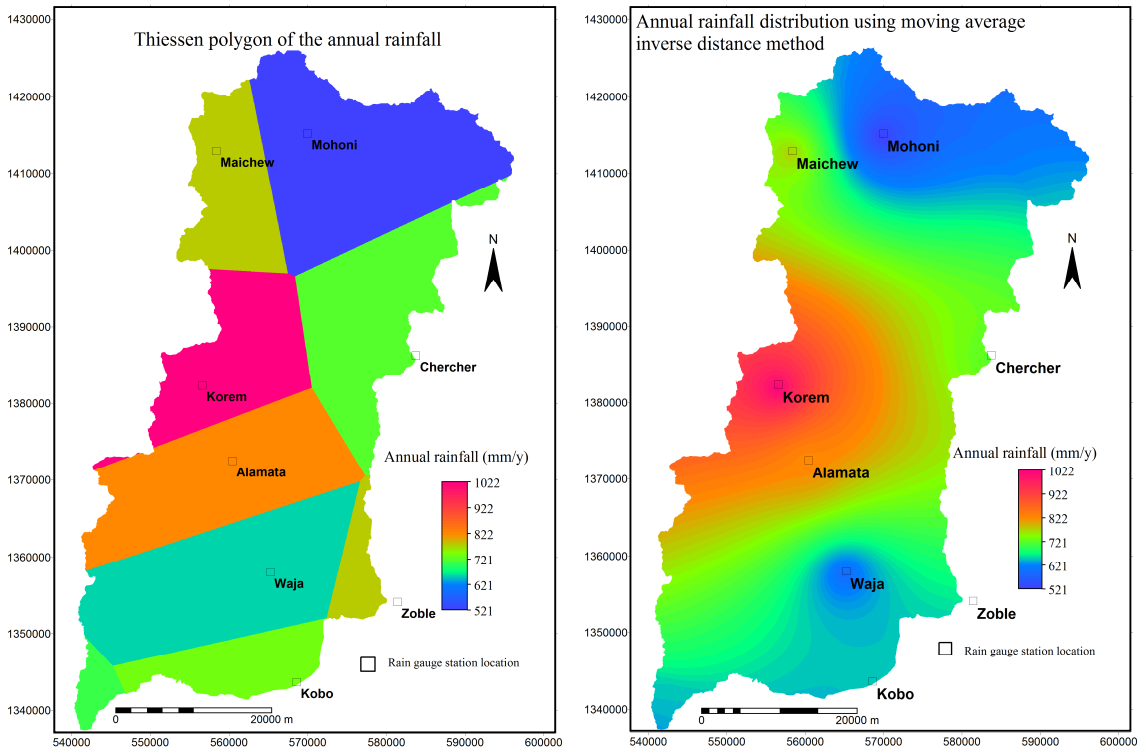

Figure 4.1 Spatial distribution of rainfall over the Raya Valley and station locations

The stations, Korem, Maichew and Zoble are found in the highlands of the Raya Valley area, whereas the others are in the lowland area. Generally, the lowland areas get lower rainfall than the highlands. However, all the stations have similar rainfall pattern with bi-modal rainfall type having maximum rainfall in July to August. For the record lists of all the stations see Appendix 1.1.

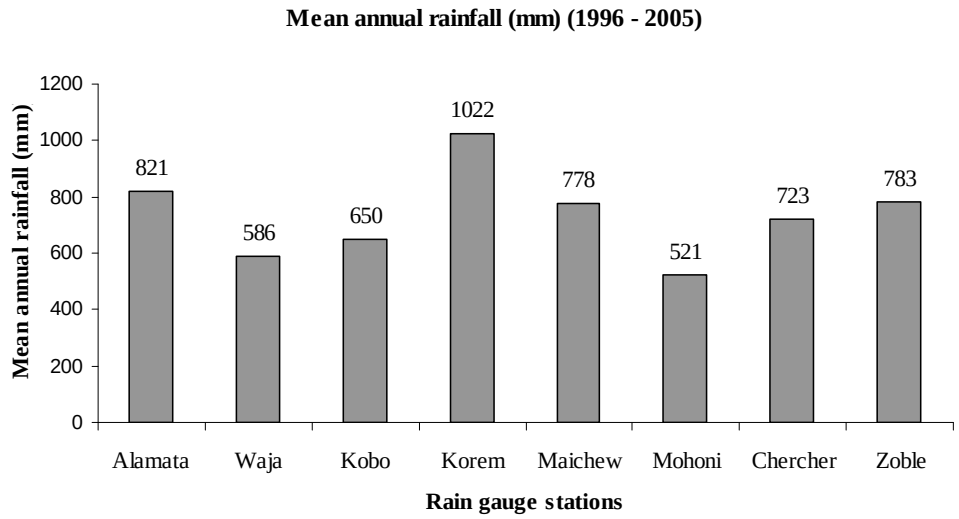

Figure 4.2 Mean annual rainfall of the stations

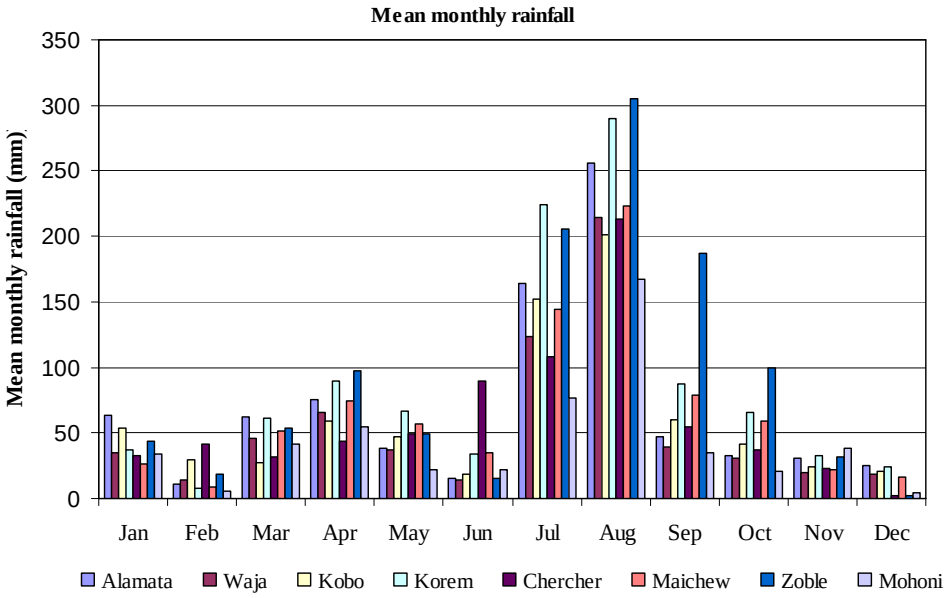

Figure 4.3 Mean monthly rainfall of the stations

4.1.2. Temperature

Alamata and Korem stations were selected to see the climatic variation in the lowland and highland areas of the Raya Valley respectively. The average monthly maximum temperature of both stations in Figure 4.4 show highest record in June and lowest value in January. They have about 9 ^{o}C difference in their maximum temperature. The maximum temperature in Korem station ranges from 19 to 25 ^{o}C and in Alamata station from 27 to 34 ^{o}C. The record for all the station is presented in Appendix 1.2.

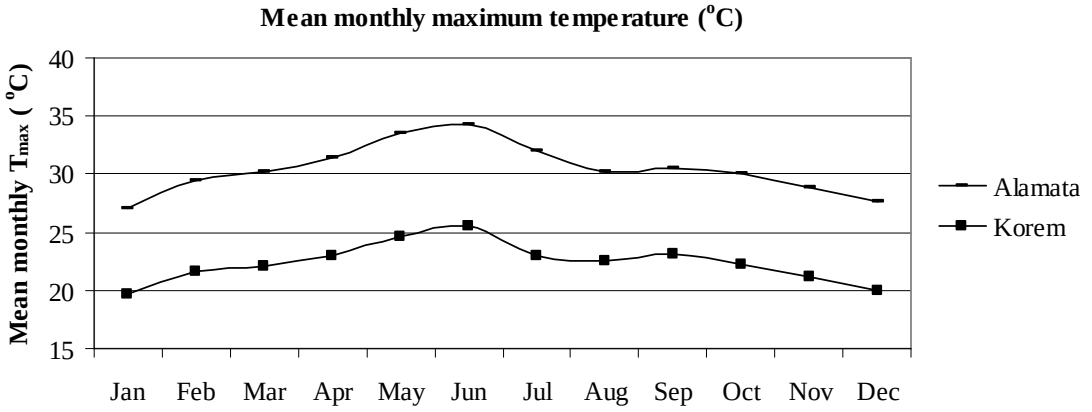

Figure 4.4 Mean monthly maximum temperature of Alamata and Korem stations

The average monthly minimum temperature of Alamata and Korem stations in Figure 4.5 showed lowest value of 12 °C and 4°C in the month of December and highest values of 17 and 10°C in the month of June respectively. The stations have generally significant difference in their average monthly temperature. However, the trend of the temporal variation is similar in both areas. The record for all the stations is shown in Appendix 1.3.

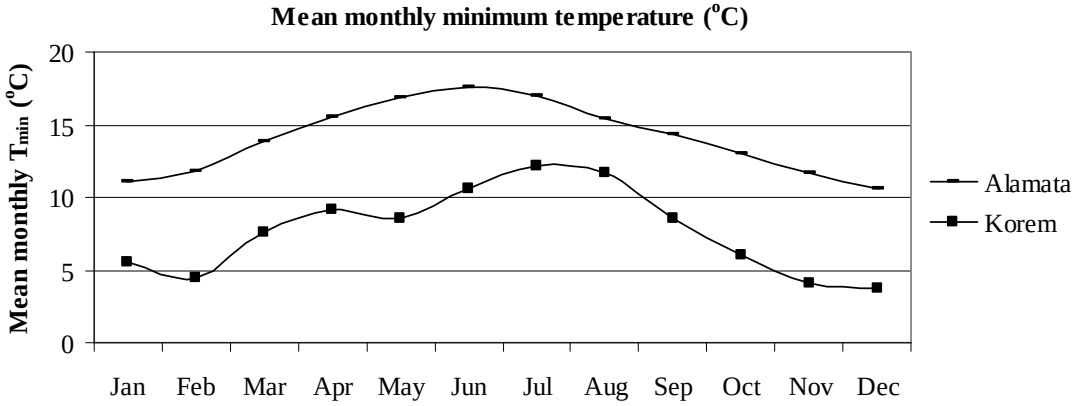

Figure 4.5 Mean monthly minimum temperature of Alamata and Korem stations

4.1.3. Relative humidity (RH)

The relative humidity data is available for stations of Kobo, Maichew and Mohoni. The RH data of Kobo station were recorded at 1200, 1800 and 0600 local times (Figure 4.6). The mean monthly relative humidity ranges from 30% in June to about 57% in January. For Maichew it ranges from 41.5 to 70% and for Mohoni station from 52 to 70%. The average monthly relative humidity of these three stations can be taken with in the range of 47% to 55%. For the record list see Appendix 1.4.

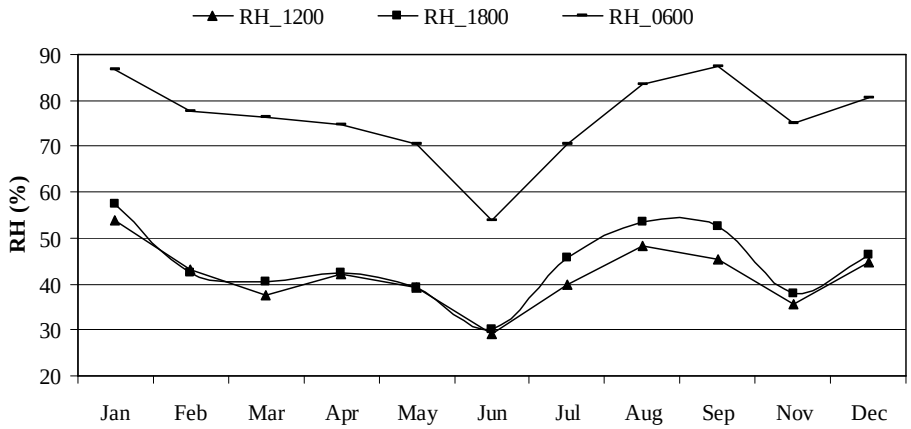

Figure 4.6 Mean monthly relative humidity of Kobo station at 1200, 1800 and 0600 local time

4.1.4. Wind speed

Wind is characterized by its direction and velocity. Wind direction refers to the direction from which the wind is blowing. For the computation of evapotranspiration, wind speed is the relevant variable. Mean wind speed values of Kobo vary between 1 ms^{-1} in September and 2.04 ms^{-1} in March. For Maichew station it varies between 1.1 ms^{-1} in January and 3.25 ms^{-1} in July (Figure 4.7) (See Appendix 1.6).

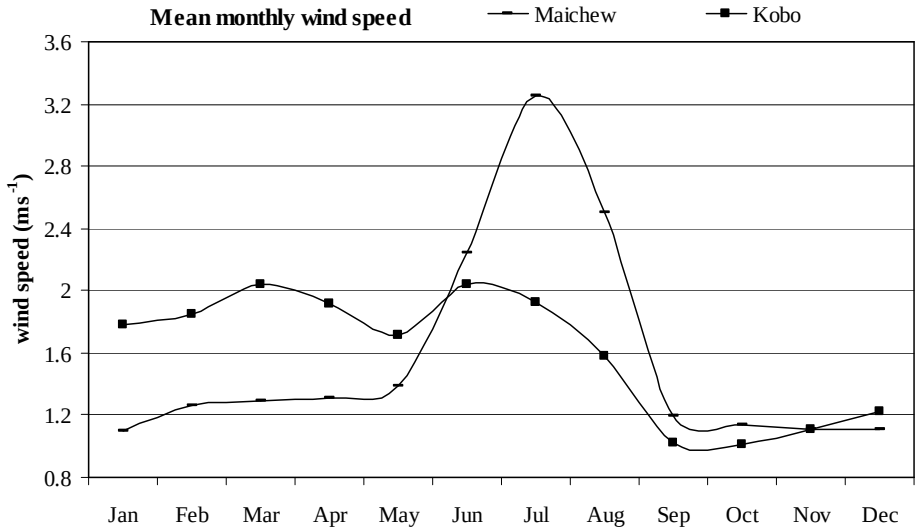

Figure 4.7 Mean monthly wind speed of Maichew and Kobo stations

4.1.5. Solar radiation

Solar radiation governs the rate of evaporation changing large quantities of liquid water into water vapour. Hence the evapotranspiration process is determined by the amount of energy available to vaporize water. Sunshine hour duration data are available for Kobo and Maichew stations. Mean sunshine hours determined for the Kobo station is above 8.0 hours in the months of October to December and March to May. In the other months it decreases up to 5.3. For Maichew station it rises

above 8 for April and May and for the remaining period it decreases to a minimum of 5.0 which is in July. (See Appendix 1.5).The mean monthly sunshine durations of the Kobo and maichew stations are 7.6 and 7.2 hours respectively.

4.1.6. Evapotranspiration

Evapotranspiration is the process in which water is returned to the atmosphere by a combination of evaporation and transpiration. Potential evapotranspiration is the water loss that will occur under given climatic condition without deficiency of water supply while actual evapotranspiration is the amount of water that actually returns to the atmosphere depending on the availability of water. The evapotranspiration can be estimated from weather data. Different methods have been developed to estimate the potential evapotranspiration, from point measured data (Allen et al., 1998). In this study the Penman-Monteith and Hargreaves methods were used to estimate the potential evapotranspiration. The Penman-Monteith method incorporates the effect of factors such as altitude, aerodynamics, geographic location and solar radiation for the evaluation. The ET_o values were determined for a 10 years period, from year 1996 to 2005. The FAO CROPWAT version 8.0 was used to estimate the potential evapotranspiration, which uses the (FAO56) Penman-Monteith equation. This method was applied for Kobo and Maichew stations which have relatively better meteorological data, whereas for the other stations, since they have no wind speed and sunshine hour duration data, Hargreaves equation was used, because this method needs only temperature and extraterrestrial radiation (R_a) data. The mean air temperature in the Hargreaves equation is calculated as an average of T_{max} and T_{min} and R_a is computed from information on location of the site and time of the year. Therefore air temperature is the only parameter that needs to be measured.

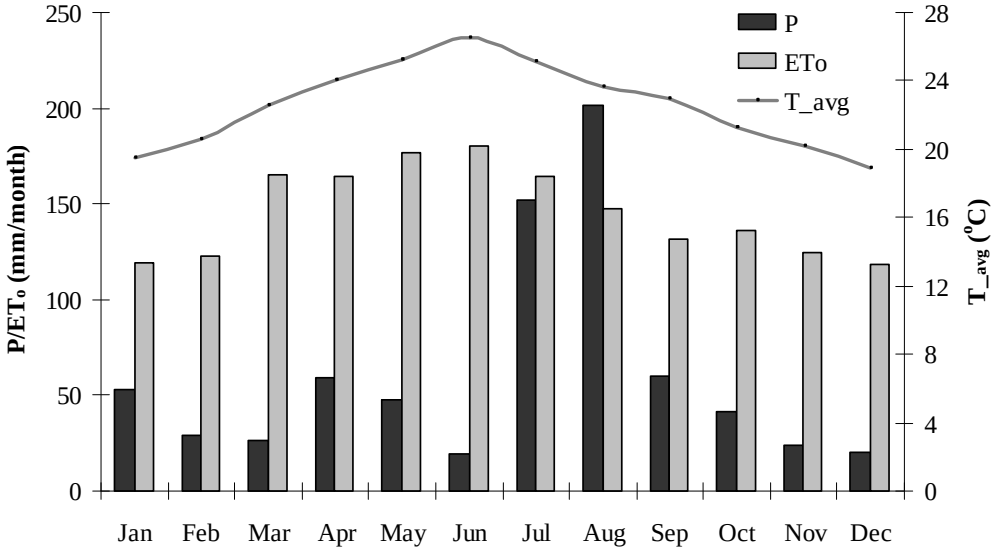

Figure 4.8 Kobo station mean monthly (P), (ET_o) and ($T_{\_avg}$) from 1996 to 2005

Kobo station is found in the lowland of the Raya Valley. As is shown in figure 4.8 the monthly precipitation ranges from 19mm in June to 201mm in August with annual precipitation of 734mm. The ET_O was calculated using Penman-Monteith method. The station has high annual ET_O (1752mm)

ranging from 118mm in December to 180mm in June. The average temperature also ranges from 19 ^{o}C in December to 26.5 ^{o}C in June (Table 4.3).

.

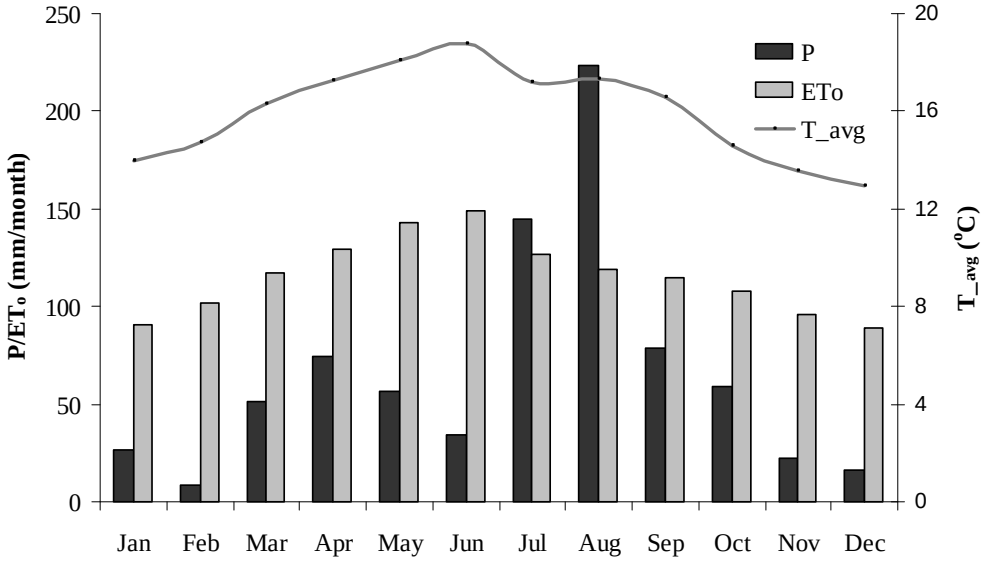

Figure 4.9 Maichew station mean monthly P, ET_o and $T_{\_avg}$ from 1996 to 2005

Maichew station is found in the highlands of the Raya Valley. As compared to Kobo station this station has higher precipitation and lower ET_o and temperature. This variation is related to the elevation difference of the stations. As is shown in Figure 4.9 the monthly precipitation ranges from 223mm in August to 8mm in February with annual precipitation of 796mm. The ET_o and the average temperature have their minimum values in June and their maximum values in December. The annual ET_o of this station is 1387mm (Table 4.4).

The result of the Penman-Monteith showed that the mean annual evapotranspiration for Kobo and Maichew are 1752 and 1387 mmy^{-1} respectively. Also ET_o was calculated using Hargreaves equation and shown in Table 4.2. The result of the ET_o values from Hargreaves equation are about 8% greater than the Penman-Monteith results (Table 4.2).

Table 4.2 Annual ET_o (mmy^{-1}) results of Penman-Monteith and Hargreaves methods

	Kobo	Maichew	Alamata	Korem	Waja	Chercher	Zoble	Mohoni
Annual ET_o Hargreaves	1896	1410	1960	1511	1939	1502	1729	1770
Annual ET_o Penman-Monteith	1752	1387						

Table 4.3 Kobo station ET_o calculation using Penman-Monteith equation

Month	T_{max} (^oC)	T_{min} (^oC)	Humidity (%)	Wind Speed (Kmd^{-1})	Sun Shine (Hours)	R_n ($MJm^{-2}d^{-1}$)	ET_o (mmd^{-1})	ET_o monthly
Jan	26.2	12.8	60.2	153.8	7.8	18.2	3.8	119.0
Feb	28.7	12.4	56.2	159.8	7.4	19.2	4.4	122.6
Mar	29.8	15.3	46.4	176.3	8.4	22.0	5.3	165.5
Apr	31.2	16.9	49.7	165.9	8.2	22.1	5.5	164.1
May	33.2	17.2	41.4	147.7	8.6	22.4	5.7	176.4
Jun	34.5	18.5	31.7	176.3	6.6	19.2	6.0	180.3
Jul	32.1	18.1	39.3	166.8	5.3	17.4	5.3	164.6
Aug	30.6	16.8	51.8	136.5	6.0	18.6	4.8	147.6
Sept	30.8	15.2	52.9	88.1	6.7	19.3	4.4	131.7
Oct	29.6	13.0	42.2	87.3	8.5	21.0	4.4	136.4
Nov	28.5	11.9	40.8	95.9	9.3	20.6	4.2	124.8
Dec	27.0	10.9	40.4	105.4	8.5	18.8	3.8	118.7
Average	30.2	14.9	46.1	138.3	7.6	19.9	4.8	1752.0

Penman-Montheith equation was used in Eto Calculations with the values for Angstrom's Coefficients: a = 0.25 and b = 0.5

Table 4.4 Maichew station ET_o calculation using Penman-Monteith equation

Month	T_{max} (^oC)	T_{min} (^oC)	Humidity (%)	Wind Speed (Kmd^{-1})	Sun Shine (Hours)	R_n ($MJm^{-2}d^{-1}$)	ET_o (mmd^{-1})	ET_o monthly
Jan	20.2	7.7	66.3	95.0	7.0	17.1	2.9	90.5
Feb	21.8	7.7	56.3	108.9	8.3	20.3	3.7	102.2
Mar	22.5	10.0	61.0	111.5	7.0	19.8	3.8	117.2
Apr	23.4	11.1	57.0	113.2	8.2	22.2	4.3	129.0
May	24.2	11.9	49.9	120.1	8.8	22.9	4.6	142.6
Jun	24.8	12.8	41.5	193.5	7.2	20.1	5.0	149.4
Jul	22.2	12.3	62.6	280.8	5.0	16.9	4.1	127.1
Aug	22.0	12.7	66.6	216.0	5.3	17.5	3.8	119.0
Sept	22.5	10.7	61.8	102.8	6.8	19.5	3.8	114.6
October	20.8	8.5	61.8	98.5	7.5	19.5	3.5	108.2
Nov	20.2	7.0	59.1	95.9	7.8	18.5	3.2	96.0
Dec	19.3	6.7	65.7	95.9	7.7	17.6	2.9	89.0
Average	22.0	9.9	59.1	136.0	7.2	19.3	3.8	1387.0

4.2. Hydrochemical analysis

The natural and geochemical environment adds mineral content and biological elements to water, but many also give rise to undesirable or toxic properties, either through deficiency or excess of various elements. Water quality is a consequence of the natural physical and chemical state of the water as well as any alterations that may have occurred as a consequence of human activities. Water chemistry data can be used to infer flow directions, identify sources and estimate amount of recharge (Anderson and Woessner, 1992). Dissolved constituents in the water can provide indications on its geologic history, through which it has passed and its mode of origin within the hydrologic cycle (Freeze and

Cherry, 1979). Water naturally contains several different dissolved inorganic constituents. The major cations are calcium, magnesium, sodium and potassium; the major anions are chloride, sulphate, carbonate, and bicarbonate (Fetter, 2001).

4.2.1. Water sampling and accuracy of chemical analysis

Groundwater samples were collected from boreholes during the field visit in September 2009. Beside this, existing groundwater samples analysis results of 2008 were collected and used in this study. A total of 6 new samples which were collected and analysed during field work and 27 existing chemical analysis results of 2008 were acquired from Water Works Design and Supervision Enterprise. The location of the water samples are indicated in Figure 4.12. The chemical analysis of the samples collected during the field visit was conducted by Water Works Design and Supervision Enterprise Laboratory service at Addis Ababa on October 1, 2009. Electrical Conductivity was measured with portable devices during the field investigation. The field measured conductivity which is also influenced by the high temperature, ranges from 600μScm^{-1} to 2800μScm^{-1} (the latter value is from a hot spring). In general, most samples from the boreholes fall within the range of 412μScm^{-1} to 1740μScm^{-1}. Samples taken from very shallow hand dug well in the outlet and from the hot spring showed EC values greater than 2500μScm^{-1}. The cold spring of Waja has shown a conductivity of 780μScm^{-1}.

As is shown in figure 4.12 most of the samples were taken from the central part of the Alamata sub-basin and only six samples were takes from Mohoni sub-basin. This is because of the borehole distribution of the sub-basins. The details of the water samples are presented in table form in Appendix 2.1.

4.2.2. Reliability check

In all electrically neutral solutions, the sum of the cations should be equal to the sum of anions in $meql^{-1}$ (Hounslow, 1995). Based on the electro-neutrality, analysis of water samples with a percent balance error <5% is regarded as acceptable (Fetter, 2001). To evaluate the accuracy of the chemical analysis, a reliability check was conducted using AquaChem software. The analyzed data were checked using the following methods and the numbers of samples that pass the attention value in each test are presented in Table 4.5.

Table 4.5 Reliability check of the water sample results

Check	Unit	Attention Value	No. of Passed samples
Balance ((C-A)/(C+A))*100	$meql^{-1}$	<5%	31
TDS Entered/Conductivity	$meql^{-1}$	55< ## <75%	33
$K^+/(Na^+ + K^+)$	$meql^{-1}$	<20%	32
$Mg^{2+}/(Ca^{2+} + Mg^{2+})$	$meql^{-1}$	<40%	12
$Ca^{2+}/(Ca^{2+} + SO_4^{2-})$	$meql^{-1}$	>50%	32
$Na^+/(Na^+ + Cl^-)$	$meql^{-1}$	>50%	31

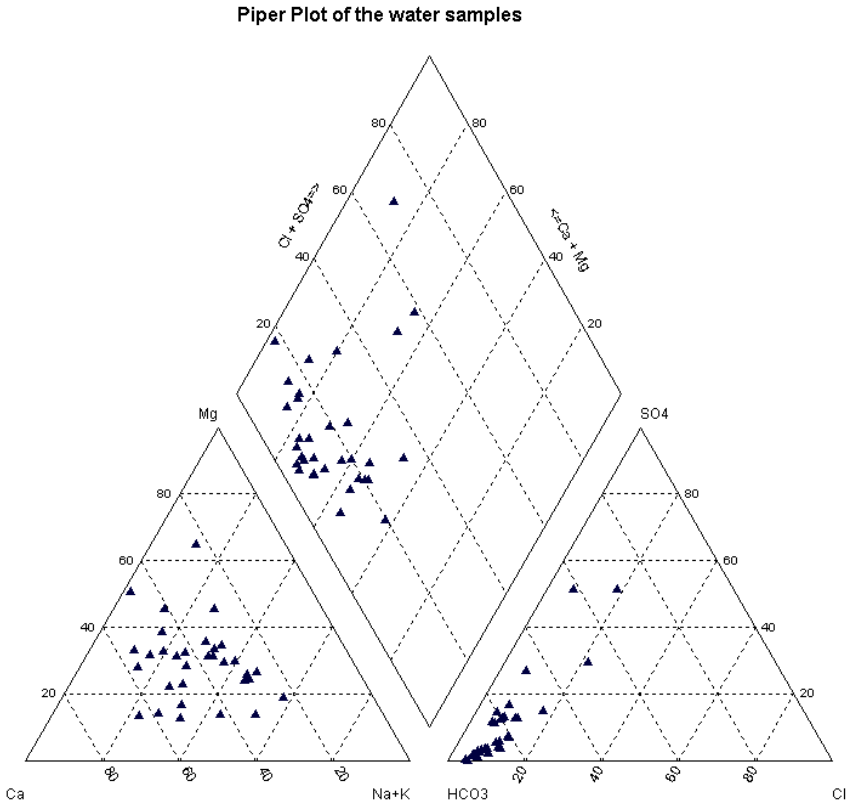

Figure 4.10 Piper diagram of 33 water samples from boreholes in the study area

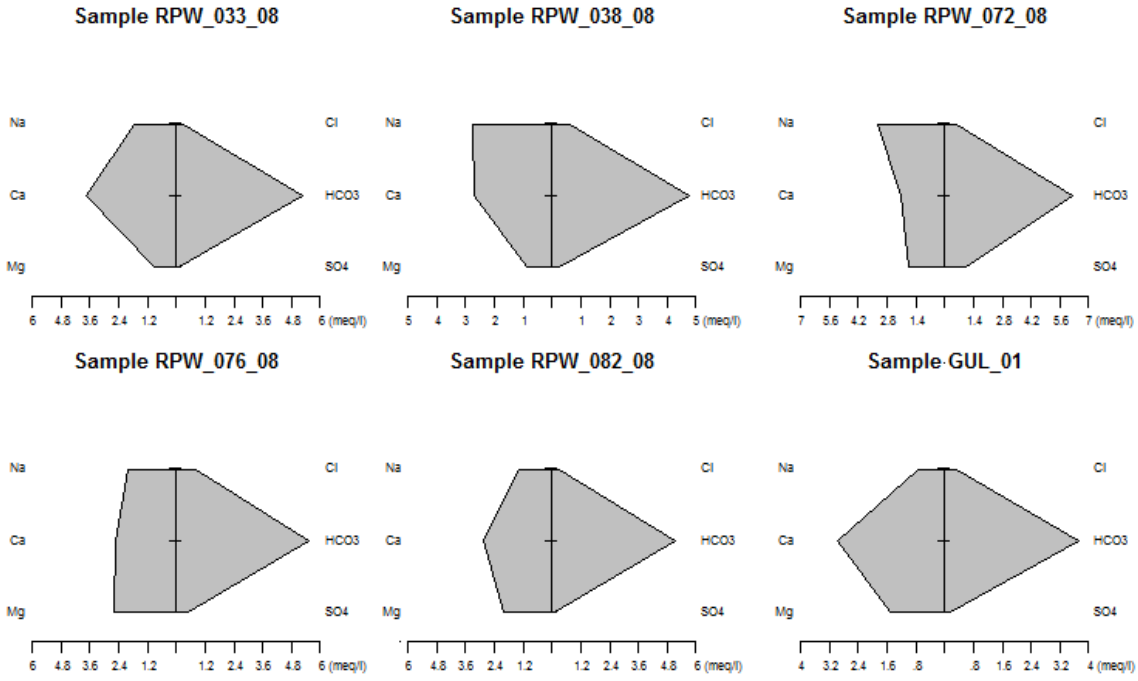

Figure 4.11 Stiff diagrams of water samples from boreholes and Golina River

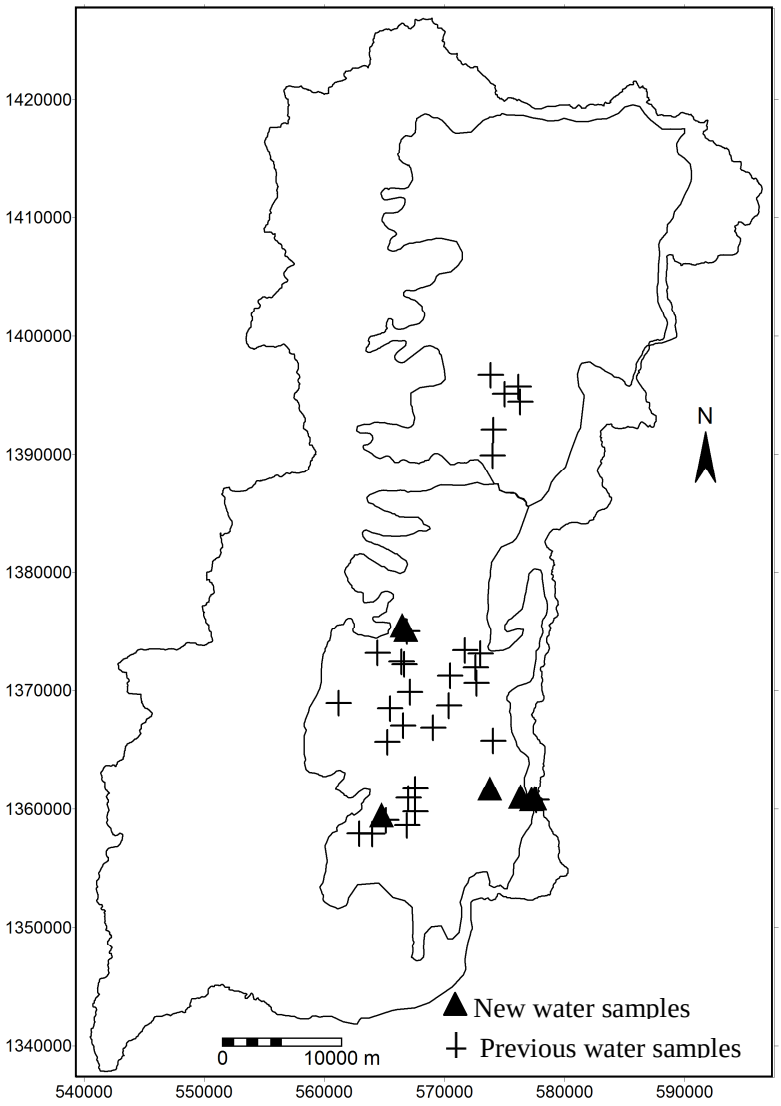

Figure 4.12 Location map of new and previous water samples

4.2.3. Chemical characteristics of the water type in the study area

The water in the study area is either, Ca- Mg, Mg-Ca, Mg - Na, Na - Ca/Mg or Ca - Na Bicarbonate types. The chemical properties of the groundwater could be associated with the geology of the area. The electrical conductivity in the area ranges from 412µScm^{-1} in RPW-076-08 to 2800 µScm^{-1} in a hand dug well. Considering only the boreholes, the conductivity ranges from 412µScm^{-1} to 1740 µScm^{-1}. The conductivity increases from the western escarpment towards the valley floor. This could be associated with the geology, the groundwater flow direction and possible evaporation.

Higher concentration of nitrates is a result of infiltrating sewage discharges in the groundwater. Higher concentration of nitrate was found in boreholes and hand dug wells, where the groundwater depth is shallow. Borehole (BH_31) with sample ID BHA08 showed 75mgl^{-1} nitrate concentration. This well is fitted with hand pump and found on the way to Bala village. The water sample from Golina River shows a water type of Ca- Mg- HCO_3. Samples taken from two artesian wells, one near

Kobo at Abare and one in Gerjele area, showed a water type of Na-Ca-HCO_3 and Ca-Na-HCO_3 respectively. The water type of all the samples are shown in Appendix 2.1 The concentration of bicarbonate in the samples ranges from 227 to 589mgl^{-1}. The highest bicarbonate concentration were detected in borehole RPW-088-08 which is 589mgl^{-1}, this borehole has also high $NO3^-$, SO_4^{2-} and Cl^- which are 43, 281, 151 mgl^{-1} respectively (see Appendix 2.1).

The Piper diagram and Stiff pattern analysis of the AquaChem 5.1 computer program was applied to plot the cation and anion concentration of all tested samples in $meql^{-1}$. Both the diagram and the pattern for all analysed water samples in Raya Valley showed that most of the groundwater is calcium-magnesium-sodium bicarbonate type (Figures 4.10 and 4.11). Stiff patterns for all the water samples are presented in Appendix 2.2.

Table 4.6 Summary statistics of the groundwater sample results

Constituent	Unit	Minimum	Maximum	Mean
EC	(μScm^{-1})	412.00	1740.00	738.00
TDS	(mgl^{-1})	268.00	1134.00	485.00
PH		6.75	8.45	7.38
Ca^{2+}	(mgl^{-1})	24.00	151.20	68.26
Mg^{2+}	(mgl^{-1})	9.76	170.80	34.93
Na^+	(mgl^{-1})	0.51	164.00	58.58
K^+	(mgl^{-1})	0.20	8.40	2.30
HCO_3^-	(mgl^{-1})	227.40	589.30	378.46
NO_3^-	(mgl^{-1})	0.20	75.70	10.03
Cl^-	(mgl^{-1})	8.24	150.96	29.71
SO_4^{2-}	(mgl^{-1})	0.29	429.83	59.55
SAR		0.01	2.90	1.52

Sodium adsorption ratio (SAR)

Sodium concentration is important in classifying irrigation water, because if water used for irrigation is high in sodium and low in calcium, the cation-exchange complex may become saturated with sodium. This can destroy the soil structure owing to dispersion of the clay particles. A low SAR (2 to 10) indicates little danger from sodium (Fetter, 2001). As Table 4.6 shows the SAR of the total samples analysed in the area varies from 0.01 to 2.9 therefore, the tested samples are safe from sodium danger.

Figure 4.13 Borehole (BH_31) with sample ID BHA08 with NO_3^- concentration of 75mgl^{-1}

Figure 4.14 Outlet of the basin, water sample SPO_01 (NO_3^-=44 mgl^{-1} and Cl^-=113mgl^{-1})

4.3. Groundwater recharge estimation

Estimating the rate of aquifer recharge is the most difficult of all measures in the evaluation of groundwater resources. Estimation of groundwater recharge requires modelling of the interaction between all of the important processes in the hydrological cycle such as infiltration, surface runoff, evapotranspiration and groundwater level variations (Jyrkama and Sykes, 2007).

Groundwater recharge in the Raya Valley is controlled by various factors like: climate, geomorphology and geology. In the study area, recharge takes place in the hills located on the west and east part of the study area. On the hills much runoff is created which infiltrates along the hill slope areas. Due to the presence of alluvial fans with coarsely grained sands, enhanced high infiltration rate occurs. Beside this, due to the orographic effect occurring around the hills, the highland areas receive comparatively high rainfall as compared to the flat part of the basin.

There are many methods available for quantifying recharge depending on different processes and sources of recharge. Each method has its own limitations in terms of applicability and reliability. The reliability of the recharge estimation method will be determined by the objective of the study.

Estimation of the groundwater recharge in the study area is difficult due to lack of data especially on the surface hydrology. The runoff from the hills and the discharge of the outlet of the basin are not known. Therefore to make an initial estimate of the groundwater recharge for the input of the model, the Chloride Mass Balance (CMB) method was used.

Rain water

The chloride concentration of the rain water in the Raya Valley was adapted from the results of Bahrdar and Mekelle rain water results, because they all have the same rain source origin (ITCZ). According to Gebrerufael (2008) the water samples from Bahrdar in combination with the rainfall water sample from Mekele were analysed and the result was found to be 0.8 mgl^{-1} $\pm$0.2 mgl^{-1}.

Groundwater

Thirty one groundwater samples were analysed for their chloride content. The chloride content of the collected groundwater samples ranges from 8.24 to 151mgl^{-1} with a standard deviation 30. The high standard deviation can indicate that the groundwater chloride concentrations may originate from various flow components in the unsaturated zone. The recharge calculation by chloride mass balance method gives an average long-term estimate of recharge. According to Eriksson (1985), the average groundwater chloride content should be calculated as the harmonic mean, given by equation 4.2.

$$Cl_{gw,avg} = \frac{N}{\sum_{i=1}^{N} \frac{1}{Cl_{gw}}} \qquad (4.2)$$

Where:

Cl_{gw} = individual chloride concentration of samples
$Cl_{gw,avg}$ = harmonic mean of the chloride content in the groundwater
N = total number of observations

Based on the collected groundwater samples, the harmonic mean of the chloride content in the groundwater of Raya Valley area was calculated as 19mgl^{-1} (Appendix 2.1).

Inflow water from the hills

The chloride content of the inflow water from the hills was estimated from the water samples of the springs emerging from the highlands and water sample from the Gulina River. Accordingly the harmonic mean of the chloride content of the inflow resulted as 16 mgl^{-1}.

Amount of runoff from the hills

To estimate the amount of runoff from the surrounding hills to the valley floor is very difficult because there is no hydrometric measuring station in the area. The study of Raya Valley Development Project (1998) has tried to approximate the runoff of proposed dam sites by using the historic discharge measurement of Golina River which lies outside the study area near Kobo town using the SCS model and regionalisation approach. The other approach chosen was to approximate the runoff from the western escarpment through the use of the annual flow generated using SCS model for each proposed dam on RVDP project. Accordingly the runoff coefficient of the mountainous area was approximated to range from 0.22 to 0.13.

Based on the previous study, the initial runoff coefficient value for this study was taken as 0.1. The drainage areas of the western and eastern highlands were subdivided into sub-catchments (Figure 4.15) to spatially distribute the annual rainfall amount and to estimate the runoff amount from each specific catchment area, and latter to distributed the recharge accordingly on the model area.

Table 4.7 Sub-catchments of the Alamata sub-basin

Catchment	Area (km^2)	Rainfall (mmy^{-1})	Rainfall (Mm^3y^{-1})	10% of the rainfall (Mm^3y^{-1})
Tirke	43	1007	43.3	4.3
Ula Ula	28	1022	28.6	2.9
Dayu	74	982	72.7	7.3
Hara	66	922	60.9	6.1
Itu	42	861	36.2	3.6
Tengago	30	821	24.6	2.5
Oda	79	821	64.9	6.5
Harosha	154	755	116.3	11.6
Mersa	151	656	99.1	9.9
Gobu	165	671	110.7	11.1
Warsu	17	734	12.5	1.2
Dikala	61	734	44.8	4.5
Bufe	54	723	39.0	3.9
Total	964			75.3

Table 4.8 Sub-catchments of the Mohoni sub-basin

Catchment	Area (km^2)	Rainfall (mmy^{-1})	Rainfall (Mm^3y^{-1})	10% of the rainfall (Mm^3y^{-1})
Burka	50	521	26.1	2.6
Habro	32	521	16.7	1.7
Guguf	124	675	83.7	8.4
Fokisa	99	675	66.8	6.7
Haya	89	752	66.9	6.7
Werabeyti	20	992	19.8	2.0
Beyra	70	962	67.3	6.7
Total	484			34.7

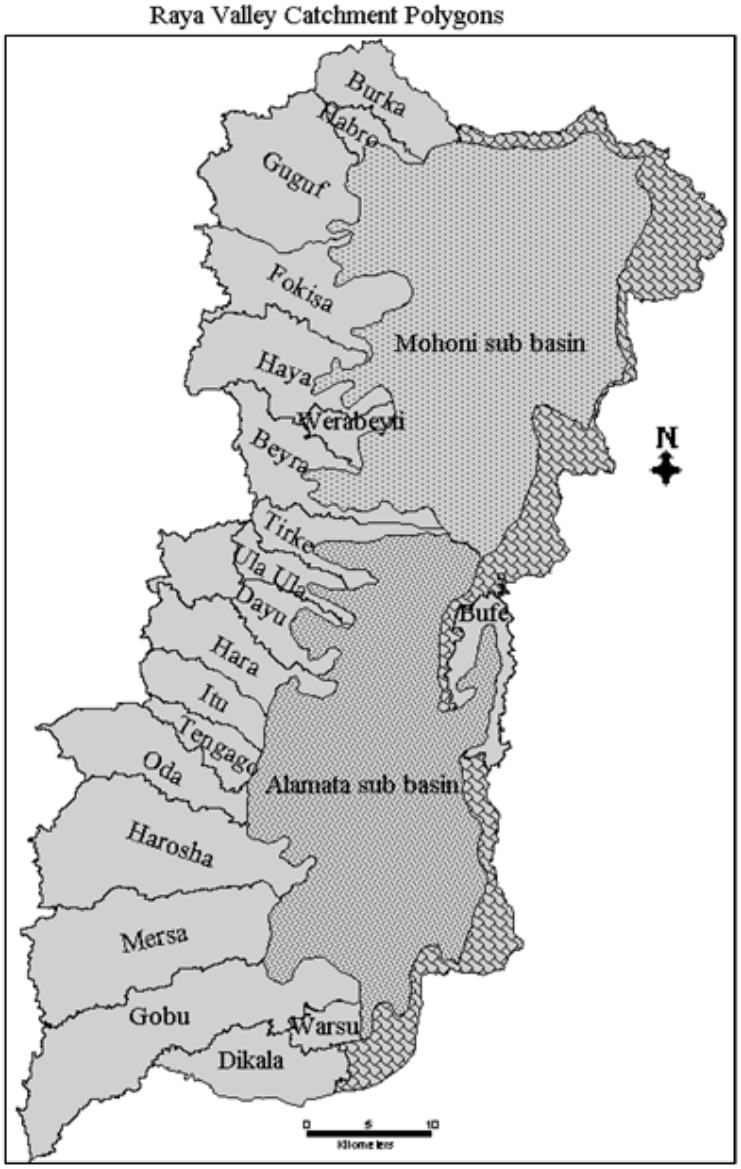

Figure 4.15 Sub-catchments of the Raya Valley and the two sub-basins

Table 4.9 The annual rainfall and the inflow from surrounding hills

	Rainfall (mmy^{-1})	Area valley (km^2)	Rainfall (Mm^3y^{-1})	Area source (km^2)	Inflow as 10% (Mm^3y^{-1})
Mohoni	697	579	404	484	35
Alamata	772	506	391	964	75
Raya Valley	724	1085	786	1448	110

The sub-catchments in the sub-basins were delineated through the DEM hydro-processing package in ILWIS software using the ASTER DEM of 30m resolution. The annual rainfall for each sub-catchment was estimated according to their area coverage on the Thiessen polygone map of the Raya Valley area.

Mohoni sub-basin has a total source area of $484km^2$ from seven sub-catchments (Table 4.8), whereas the Alamata sub-basin has a total source area of $964km^2$ from thirteen sub-catchments (Table 4.7). Hence, Alamata sub-basin has an inflow of almost twice of the Mohoni sub-basin. The locations of the sub-catchments were shown in Figure 4.15.

4.3.1. Chloride mass balance method

Chloride Mass Balance (CMB) method is based on the assumption of conservation of mass between the input of the atmospheric chloride and the chloride flux in the subsurface (Gieske, 1992) and (Yongxin and Beekman, 2003). Since chloride is a conservative tracer, water evaporation and plant uptake by transpiration concentrate rainwater derived chloride in the soil. Groundwater recharge estimated from the mass balance of chloride assumes steady-state conditions. However, this will be valid only when there are no additions from external sources like fertilizers or weathering products which might be associated with a significant amount of chloride. The chloride concentration in groundwater may originate from different flow components in the unsaturated zone. Hence, the calculation of groundwater recharge rate using chloride concentrations of groundwater results in total recharge rate. In this study area, the main sources of recharge to the groundwater are the inflow from the hills and the direct rainfall. Therefore, the source of chloride is not only from the direct rainfall but also from the inflow. Accordingly the formula for calculating the total recharge is;

$$R_{gw} = \frac{P\,Cl_p + I\,Cl_i + D}{Cl_{gw}} \qquad (4.3)$$

Where

R_{gw}	=	Groundwater recharge	$[Mm^3y^{-1}]$
P	=	Average annual precipitation	$[Mm^3y^{-1}]$
$Cl_{p.}$	=	Chloride content in precipitation	$[mgl^{-1}]$
D	=	Dry deposition of chloride measured during the dry season	$[mgl^{-1}]$
Cl_{gw}	=	Harmonic mean of chloride concentrations in groundwater	$[mgl^{-1}]$
I	=	Inflow from the highlands	$[Mm^3y^{-1}]$
Cl_i	=	Harmonic mean of chloride content in the inflow	$[mgl^{-1}]$

Chloride of rain water (Cl_p) = 0.8 mgl^{-1}

Chloride of groundwater (Cl_{gw}) = 19 mgl^{-1}

Chloride of the inflow from the highlands (Cl_i) = 16 mgl^{-1}

However, in this study there is no record in relation to dry chloride deposition (D) on the study area. Therefore it is assumed to be zero. Hence the equation 4.3 was reduced to:

$$R_{gw} = \frac{P\,Cl_p}{Cl_{gw}} + \frac{I\,Cl_i}{Cl_{gw}} \qquad (4.4)$$

Table 4.10 Recharge estimation using CMB method

		Mohoni sub basin	Alamata sub basin	Raya Valley
P	(Mm^3y^{-1})	404	391	786
I	(Mm^3y^{-1})	35	75	110
R_{gw}	(Mm^3y^{-1})	46	80	126
R_{gw}	(mmy^{-1})	80	160	116

The groundwater recharge for Raya Valley, Mohoni and Alamata sub-basins considering 10% of the rainfall on the source area as inflow to the valley were estimated as 126, 46 and 80Mm^3y^{-1} respectively. These groundwater recharge estimations can not be taken as reliable estimation because, the inflow from the hills need to be estimated using hydrometric stations. However, these estimations were used as initial estimation values for the groundwater flow modelling and hence, all the groundwater recharge estimations were compared with the model calibrated recharge estimation values and discussed in chapter seven.

4.4. Pumping test data analysis

Pumping test is a critical task where very important information and data are collected regarding the overall groundwater condition of the given area. In this study, the analysis of the pumping test data was carried out to determine the aquifer hydraulic parameters like transmissivity and hydraulic conductivity. The aquifer parameters are important as they give an understanding of groundwater flow in the system. The analysis was done by using AquiferTest V.4.2 program. Generally all the analytical methods assumed the aquifer is homogeneous and isotropic, groundwater flow is horizontal and Darcy's law is valid, discharged at constant rate, fully penetrating well of very small diameter and geologic formations are horizontal and have infinite horizontal extent (Kruseman and de Ridder, 1992). A pumping test analysis of the area was previously carried out by Dessie (2003) and (WWDSE, 2008a).

The aquifers in the study area are mainly Quaternary alluvial and colluvial deposits with fractured and weathered basalt in places, particularly in the highlands. The total number of wells inventoried in the study area is more than 170. But most of the older wells have incomplete data. In this study 31 wells were selected for analysis (Figure 4.16), which have relatively complete pumping test data, deeper in depth and well distributed in the valley area. But to represent the area, pumping test analysis results of

previous studies and from the reports of Water Works Design and Supervision Enterprise and Tekeze Deep Water Wells Drilling Plc. were compiled and used. Pumping tests were conducted on a productive well except in four wells where observation wells were used. Most of the tested wells have continuous and recovery pumping test data. The duration of pumping test in each well is variable, ranging from 32 to 72 hours. According to WWDSE (2008a) aquifer tests carried out on four well fields (WF4, WF6, WF9 and WF 13) (Figure 4.16) and calculated the average transmissivity of the different well fields. The aquifer tests were selected and conducted on the central wells with five observation wells for each pumping wells (Table 4.11).

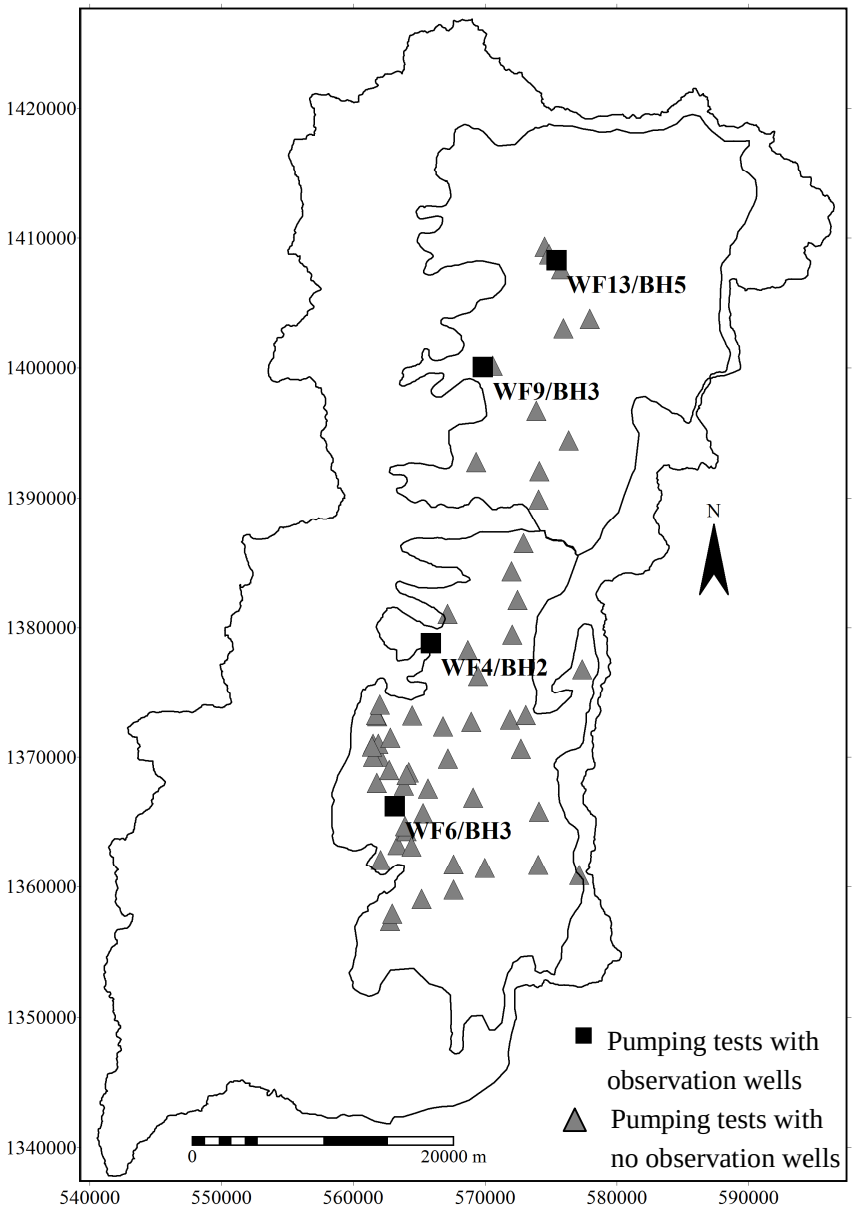

Figure 4.16 Location of the wells with analysed pumping tests

Table 4.11 Central wells used for aquifer tests with 5 observation wells for each

Well field	Central well	Q ls^{-1}	T (m^2d^{-1})	Storage coeff. (10^{-4})
WF-13	WF-13/BH5	49.7	2143	4.6
WF-9	WF-9/BH3	30.0	2804	7.0
WF-4	WF-4/BH2	49.7	1185	4.8
WF-6	WF-6/BH3	30.0	652	3.2

Source: WWDSE Addis Ababa, Ethiopia

Storage coefficient (storativity) is the volume of water released from storage of an aquifer per unit horizontal area of an aquifer and per unit drop of the water-table or potentiometric surface. It is a dimensionless ratio and always less than unity. The size of the storage coefficient is dependent whether the aquifer is unconfined or confined. In regards to a confined aquifer, water derived from storage is relative to the expansion of water as the aquifer is depressurized (pumped) and, compression of the aquifer. In a confined aquifer setting, the load on top of an aquifer is supported by the solid rock skeleton and the hydraulic pressure exerted by water. Because of these variables, the storage coefficient of most confined aquifers range from 10^{-5} to 10^{-3}. On the other hand, in an unconfined aquifer setting, the predominant source of water is from gravity drainage and the expansion of water and compaction of the rock skeleton is negligible. Thus, the storage coefficient is approximate to value of specific yield and ranges from 0.1 to about 0.3 (Kruseman and de Ridder, 1992).

The storage coefficients calculated from aquifer tests for the four wells in the Raya Valley; ranges from of 3.2×10^{-4} to 7×10^{-4} (Table 4.11). Hence, this storativity value range can indicate that the aquifer is more of semi-confined aquifer type than unconfined. However, as they are only from four wells they cannot represent the valley. Beside this, drawdown curves of most constant rate test indicate semi-confined to unconfined conditions.

Single-well aquifer tests frequently are analyzed with the Cooper-Jacob (1946) method. Transmissivity is estimated by fitting a straight line to drawdown on an arithmetic axis versus time on a logarithmic axis in a semi-log plot. Drawdown in confined and unconfined aquifers have been analyzed by many practitioners using the Cooper-Jacob method, regardless of differences between field conditions and theory (Halford et al., 2006). The Cooper-Jacob straight line method is most commonly used method of analysis, mainly due to its relative simplicity. The original Cooper-Jacob method was based on horizontal flow to fully penetrating wells in confined aquifers, but can also be used in unconfined aquifers where the drawdown is a small portion (<20%) of the original aquifer saturated thickness (Cashman and Preene, 2001).

In the study area as is observed from the pumping test data the duration of pumping was more than a day and the drawdown observed for all the wells were very small as compared to the aquifer thickness (Table 4.12). The area is characterized by unconfined aquifer around the recharge area and semi-confined to confined aquifer towards the south-east part i.e. near to the discharge area. Therefore, for this study interpretation of single-well tests with the Cooper-Jacob method remains more reasonable than most alternatives.

4.4.1. Cooper-Jacob straight-line time-drawdown method

Constant rate tests

The constant rate test is performed by pumping the well with a constant rate for periods usually longer than one day. This type of test helps to determine the aquifer parameters like transmissivity, hydraulic conductivity and storage coefficients. Beside this, it provides information on the physical limitations of an aquifer i.e. recharge and discharge boundaries.

The Cooper-Jacob straight-line time-drawdown method was used here. In this method a semi-log plot of the field drawdown data (linear scale) versus time (normal log scale) was made (Figure 4.17). A straight line is then drawn through the field-data points. The value of the drawdown per log cycle of time, (h_o- h), is obtained from the slope of the graph. The values of transmissivity were calculated using the following equations:

$$T = \frac{2.3xQ}{4\pi(h_0 - h)} \qquad (4.5)$$

Where:

T	=	Transmissivity	$[L^2T^{-1}]$
Q	=	Pumping rate	$[L^3T^{-1}]$
(h_o - h)	=	Drawdown per log cycle of time	[L]

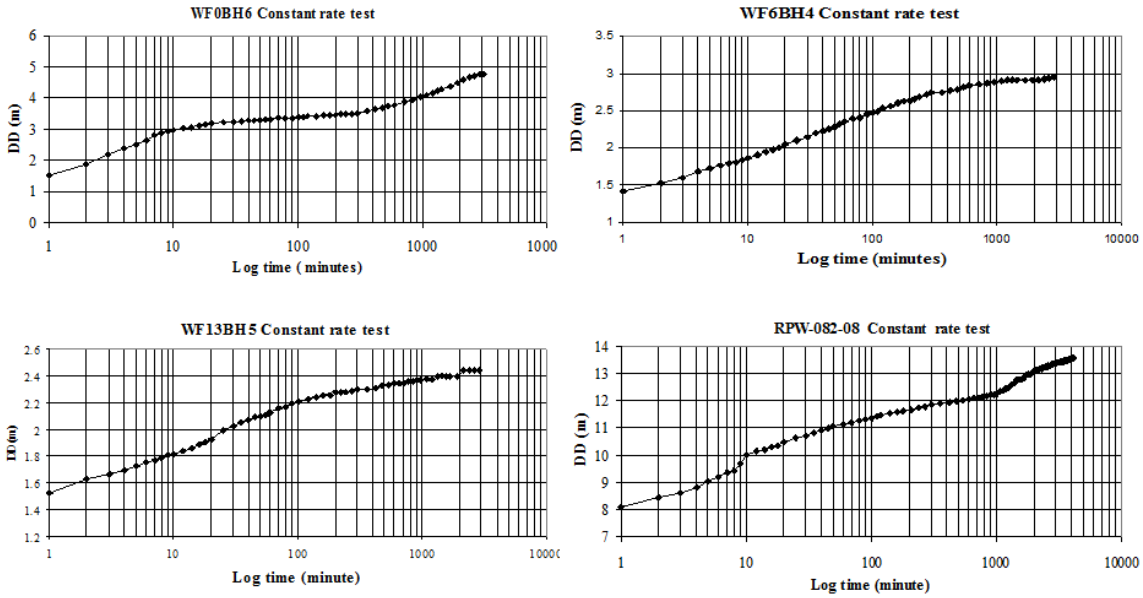

Figure 4.17 Constant rate tests with the Cooper-Jacob Straight-Line Time-Drawdown

Table 4.12 Summary of the Constant rate test

Well	Discharge (ls^{-1})	Duration (hr)	Drawdown (m)
WF0BH6	40	52	4.8
WF6BH4	40	48	2.9
WF13BH5	44	48	2.4
RPW-082-08	41	72	13.6

Figure 4.17 shows the constant rate test of wells: WF0BH6, WF6BH4, WF13BH5 and RPW-082-08. The calculated transmissivity values of these wells are presented in Table 4.14. Under ideal case the data plot is along a straight line rather than along a curve. As it is shown in Figure 4.17, wells WF6BH4 WF13BH5 are most likely represent leaky to unconfined type of aquifer whereas, wells WF0BH6 and RPW-082-08 resembles to unconfined condition. Beside this, the transmissivity values found from the constant rate test were compared with recovery test to check the accuracy of the constant rate test. The graphs of the other wells are presented in Appendix 4.1.

4.4.2. Theis recovery method

At the end of the constant rate test usually recovery measurements are taken. Recovery test help to verify the accuracy of the pumping data and assist to confirm the results of the aquifer parameters determined by the constant rate test. Recovery data are more reliable than pumping data for the reason that no pumping is involved during this test and hence no water level reading problems associated with the pumping action is encountered. Theis recovery method is applicable to data from single well recovery tests conducted in confined, leaky or unconfined aquifers (Kruseman and de Ridder, 1992). This method was used in this study to calculate the transmissivity and to compare the values with those obtained from the constant rate test. Residual drawdown versus time graphs were produced, where time was on the logarithmic scale and the drawdown on the linear scale then slope of the line per one log cycle was taken and the transmissivity was calculated using the following Theis recovery equation:

$$T = \frac{2.3xQ}{4\pi\Delta S} \qquad (4.6)$$

Where:

T	=	Transmissivity	$[L^2T^{-1}]$
Q	=	Pumping rate	$[L^3T^{-1}]$
ΔS	=	Change in residual drawdown per log cycle of time	[L]

In this study the recovery test data was analysed and the transmissivty was calculated for each wells and shown in Table 4.14 and the corresponding curves for the other wells are presented in Appendix 4.2.

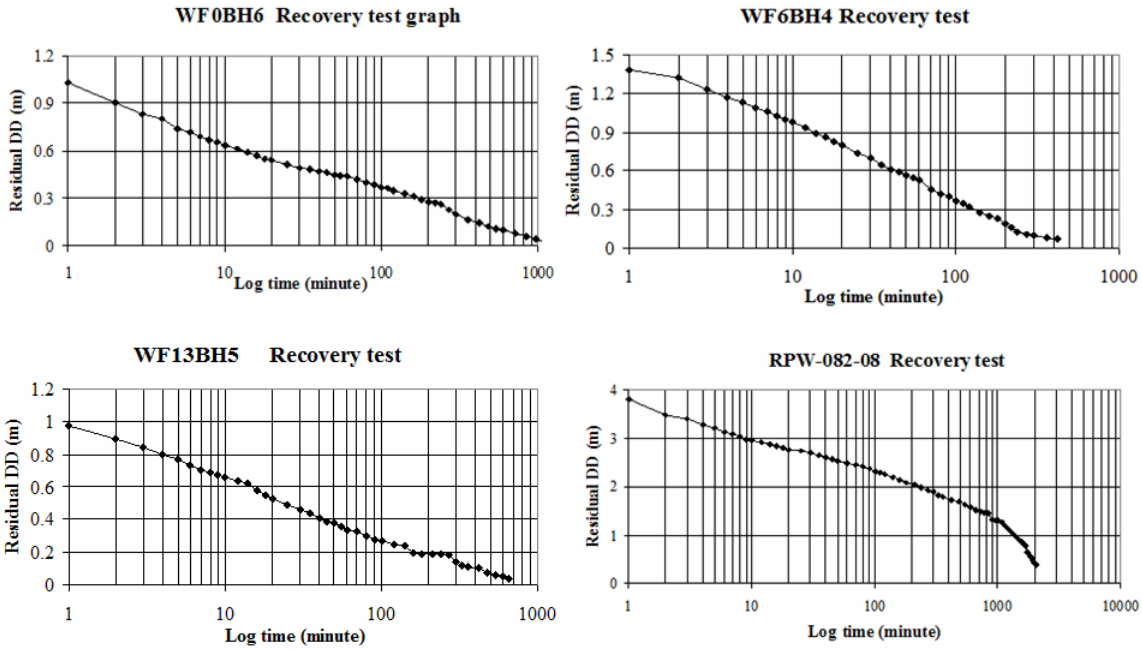

Figure 4.18 Graphs of the Theis recovery method

From the pumping test analysis together with the field observations and previous work, it seems that the aquifer in most part of the valley especially in the recharge areas is unconfined type and leaky to confined around the south-eastern part of the valley, where during the field visit artesian wells were observed. This might be due to the presence of clay layer around the discharge areas which is confining the aquifer below. According to the pumping test analysis result, the area is characterized by a wide range of transmissivities and hydraulic conductivities. The hydraulic conductivity ranges from 1 to 39mday^{-1}. In some of the wells the hydraulic conductivity is high and in others it is low which is indicative of the heterogeneous condition of the subsurface lithology. The variability in the hydraulic properties mainly results from the type of the alluvial deposit which ranges from coarse gravel to silt and clay. Summarized results of the analysis are given in Table 4.14. All graphs of the analysis are provided in Appendix 4.

4.4.3. Well abstraction

Groundwater has been abstracted for water supply of the towns and villages in the valley. Beside this there are some wells which are in use for irrigation. However, the abstraction rate from the wells used for domestic water supply and for irrigation is unknown. The only data collected was from Alamata water supply office, which is the yearly total water abstracted from five wells, supplying water to Alamata town (Table 4.13). The abstraction rate is increasing each year and new wells were equipped recently.

Table 4.13 Annual water abstraction data from Alamata town water supply office

Year	1996	1997	1998	1999	2000
Abstracted water (m^3)	298264	264040	340802	397390	459237

Table 4.14 Summary of the pumping test data analysis

Well index	Easting (m)	Northing (m)	Depth (m)	Aquifer thickness (m)	SWL (m)	Q (ls^{-1})	Duration (minute)	DD (m)	T (CRT) (m^2d^{-1})	T (Recov.) (m^2d^{-1})	Specific capacity (md^{-1})	K (md^{-1})
WF13/BH5	575406	1408290	132	84.2	36.2	44.0	2880	2.4	2566	2038		24.2
WF9/BH3	569798	1400023	128	107.3	20.7	30.0	3120	13.7	474	396	243	3.7
WF9/BH4	570553	1400160	150	118.0	25.8	44.0	2880	3.4	2784	2400		20.3
WF4/BH1	567110	1381023	172	127.0	40.7	39.5	2880	7.1	525	543	800	4.3
WF0/BH4	562697	1368978	106	80.0	10.3	40.0	3120	14.5	226	228	233	2.9
WF0/BH6	561399	1370777	93	54.0	30.2	40.0	3120	4.8	904	2109	664	39.1
WF6/BH3	563156	1366192	96	71.5	24.5	30.0	3120	7.6	938	675	467	9.4
WF6/BH4	563912	1364685	122	86.0	27.5	40.0	3120	3.0	1304	1122	2320	13.0
WF7/BH1	564378	1363098	137	109.0	27.8	44.0	2880	1.7	3164	2320	9550	21.3
RPW-030-08	573856	1396696	174	116.6	47.5	25.0	4320	5.3	299	345	348	3.0
RPW-034-08	576332	1394432	226	173.0	47.0	25.0	4320	12.0	204	239	238	1.4
RPW-036-08	574094	1392035	160	94.4	39.6	30.0	4320	3.4	1178	1302	1520	13.8
RPW-038-08	574039	1389891	182	139.0	39.0	25.0	4320	20.0	87	77	126	0.6
RPW-045-08	572436	1382113	178	140.7	29.3	30.0	4320	28.1	139	92	162	0.7
RPW-057-08	569431	1376222	201	186.6	8.8	31.0	4320	19.9	185	220	199	1.2
RPW-064-08	564467	1373141	112	66.3	21.7	35.0	4320	8.4	1259	1178	379	17.8
RPW-072-08	572671	1370616	262	236.7	17.3	32.3	4320	15.6	200	177	186	0.7
RPW-076-08	567162	1369865	232	211.6	14.5	38.8	4320	7.9	409	361	535	1.7
RPW-078-08	569076	1366877	96	60.0	30.1	30.0	4320	15.1	168	314	152	5.2
RPW-082-08	574045	1365777	276	260.5	9.5	41.8	4320	13.6	462	688	332	2.6
RPW-083-08	565271	1365661	170	152.6	11.4	50.0	4320	8.7	608	659	417	4.3
RPW-087-08	567591	1361714	170	155.6	6.4	41.0	4320	6.3	658	658	1010	4.2
RPW-092-08	571968	1384297	194	147.1	42.9	33.6	4320	4.9	1063	409	734	2.8
RPW-093-08	567588	1359766	288	276.1	5.9	46.0	4320	15.7	251	316	468	1.1
RPW-095-08	565153	1359042	196	182.4	5.6	53.0	4320	17.3	177	144	346	0.8
RPW-098-08	562933	1357904	154	140.4	5.6	48.3	4320	8.5	914	1135	672	8.1
WF13/BH1	574502	1409298	137.5	76.0	51.9	34.0		2.6	1495	1417		18.6
WF13/BH2	575754	1407602	168	132.0	31.2	37.5		4.3	914	734		5.4
WF13/BH4	574836	1408721	144	92.0	43.9	32.0		3.8	1935			21.0
Dejena/BH3	575918	1403062	169		43.4	31.8		21.9	150	144		

Table 4.15 Statistics of the transmissivity values in m^2d^{-1} from recovery and constant rate tests

	Min	1^{st}Qu	Median	Mean	3^{rd}Qu	Max
Constant rate test	87.0	215.0	525.0	815.2	1000.0	3164.0
Recovery test	77.0	276.5	409.0	759.0	1128.0	2400.0

4.5. Digital elevation model (DEM)

In order to determine more accurate surface elevation, digital elevation model product of the Advanced Space borne Thermal Emission and Reflection Radiometer (ASTER) on-board NASA's Satellite Terra with 30m resolution was used. To assess the vertical accuracy of the DEM, ground control points are prepared from the topographic maps of the study area and from field measurements. The vertical accuracy of the DEM is assessed by comparing the extracted elevation value at a number of check points with those prepared from the topographic maps as ground control elevation points. The relationship between the ground elevation and the elevation from ASTER DEM is shown in Figure 4.19. The elevations from ASTER DEM and those from the topographic map show high correlation with $R^2 = 0.99$ and the comparison at the check points for the study area results in a root

mean square error of 19 meters. The elevation extracted from the DEM was corrected by the regression equation obtained from the comparison, which is y = 0.95x + 67.80, where Y is the elevation from ASTER and X is the elevation from topographic map of the area. Then using the map value function in ILWIS, the required elevations at the well locations were extracted. This corrected ASTER DEM was applied to define the boundary of the valley, to visualize the geomorphology of the area, delineate the sub-catchments, to extract drainage patterns, to produce topographic cross section lines and to obtain the elevation of top and bottom of the aquifer.

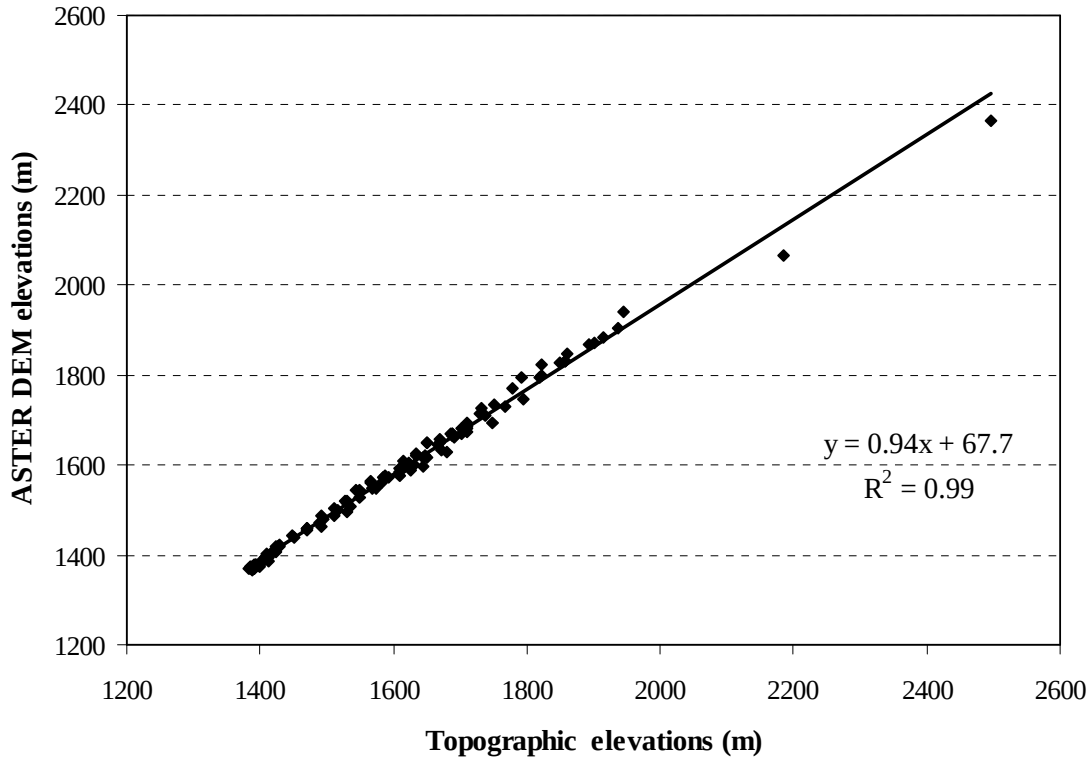

Figure 4.19 Comparison between topographic map and ASTER DEM elevations

5. Groundwater flow modeling of Raya Valley

5.1. Introduction

There are two areas of hydrogeology where we need to rely on models of real hydrological system: to understand why a flow system is behaving in a particular observed manner and to predict how a flow system is behaving (Fetter, 2001). There are several ways to classify groundwater flow models, models can be either transient or steady state and one, two or three spatial dimension. Steady state flow occurs when at any point in a flow field the magnitude and direction of the flow are constant with time (Anderson and Woessner, 1992).

This chapter focused on the simulation of groundwater flow system in the Raya Valley using groundwater flow modelling. The main recharge zones are the Korem Mountains in the west and the Chercher Mountains in the east. The valley opens to the north and narrower to the south. The transition to the Afar depression is marked by a low range of volcanic hills which form the eastern boundary. The aquifer system was modelled using PMWIN (Chiang et al., 1998) as pre- and post-processor for MODFLOW (McDonald and Harbaugh, 1988) assuming steady-state conditions. The aquifer was modelled under unconfined condition represented by a single layer with a constant thickness of 100m. The grid cell size of the model was taken 250x250m and 17600 of active cells were used to represent the entire study area which is 1085 km^2. Model area and the elevations of top layer were delineated by the ASTER DEM optimisation and use of the topographic maps. Aquifer properties were assigned based on the analysis of pumping test data. Recharge to the major component of the system was considered to take place as direct infiltration of precipitation and as inflow from surrounding hills. The Chloride Mass Balance Method (CMB) was employed to estimate the recharge. Optimised parameters (hydraulic conductivity and recharge) are spatially distributed over the model area. A combination of trial and error and automatic methods were used to calibrate the models using the observed hydraulic head.

5.1.1. The modelling process

To ensure that the modelling study is performed correctly, it is important to use a proper modelling methodology. This will also increase confidence in the results of the model (Anderson and Woessner, 1992). Figure 5.1 shows a modelling protocol suggested by Anderson and Woessner (1992) which was applied in this study.

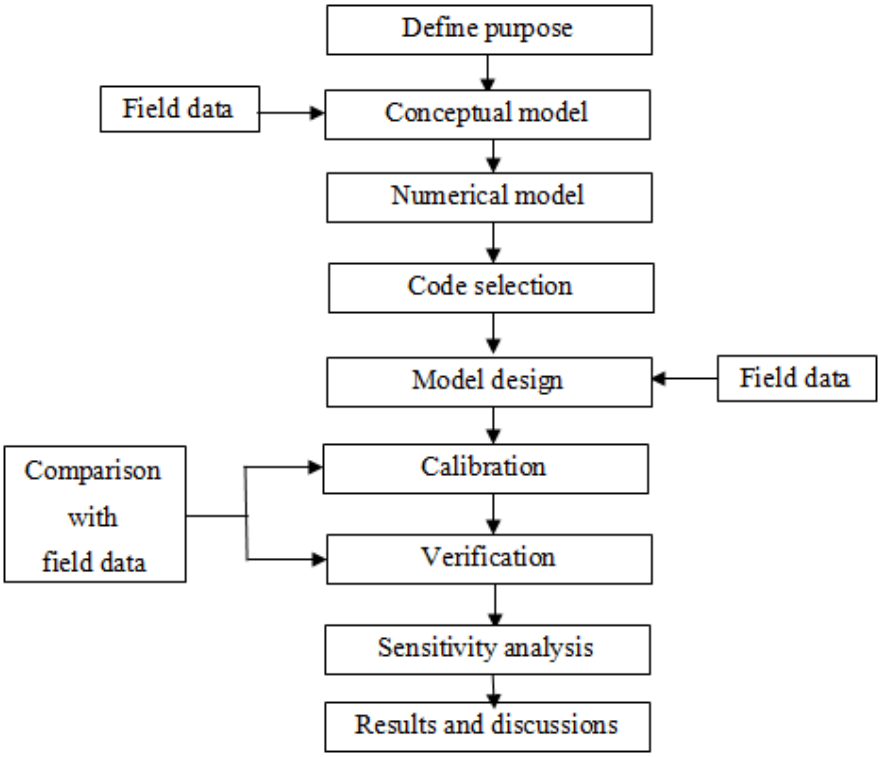

Figure 5.1 Steps in a modelling protocol adopted from Anderson and Woessner (1992)

5.2. Conceptual model

Selecting the appropriate conceptual model for a given problem is one of the most important steps in the modelling process. Over simplification may lead to a model that lacks the required information, while under simplification may result in the lack of data required for model calibration and parameter estimation. A conceptual model describes how water enters an aquifer system, flows through the aquifer system and leaves the aquifer system. Briefly it describes the hydrologic system with respect to aquifer properties, flow characteristics and boundary conditions. According to Anderson and Woessner (1992) there are three steps in building a conceptual model: defining hydrostratigraphic units, preparing a water budget and defining the flow system.

Based on the limited data available, a simple conceptual model was developed for the groundwater flow in the Raya Valley. In developing this model, a number of simplifying assumptions were made. The assumptions made in this study are: the model consists of a single layer, the model is two dimensional, and the aquifer is unconfined with constant thickness. The groundwater flow is also assumed to be horizontal. In principle, ground-water flow and contaminant transport in a porous medium domain are three-dimensional. However, when considering regional problems, one should note that because of the ratio of aquifer thickness to horizontal length, the flow in the aquifer is practically horizontal. The horizontal dimension may be from tens to hundreds of kilometres with a thickness of tens to hundreds of meters (Bear, 1979).

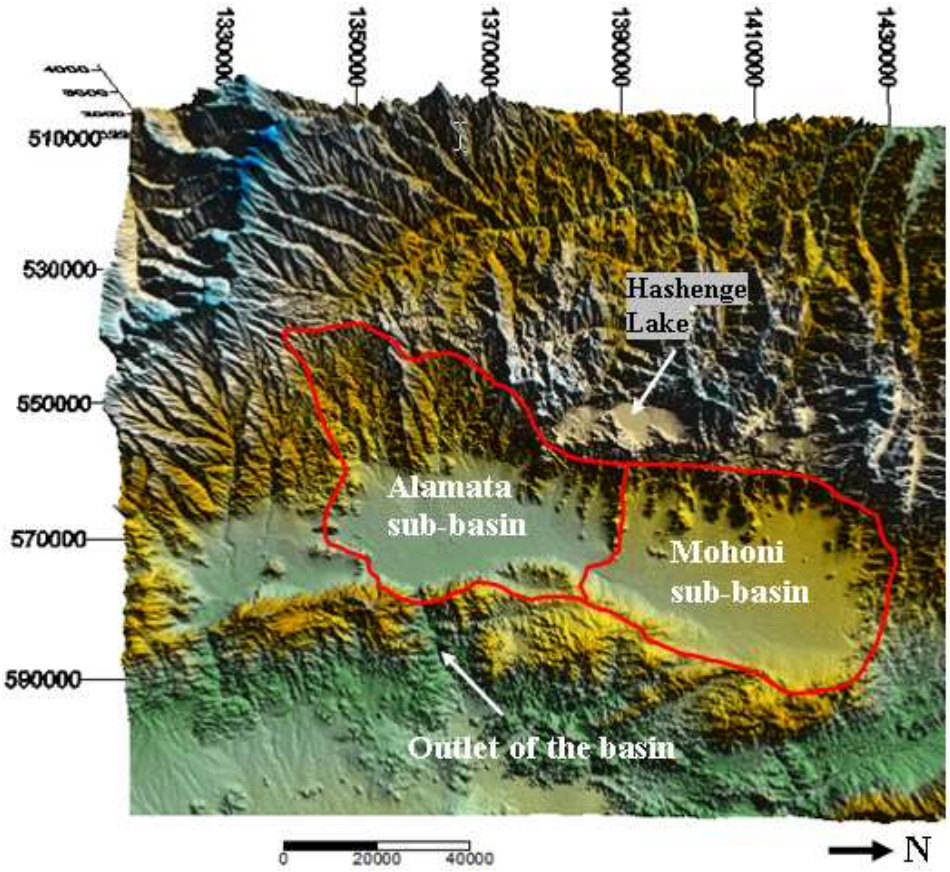

Figure 5.2 Overview of the Raya Valley area

Simplification is necessary because complete reconstruction of the field system is not feasible. The conceptual model should be simplified as much as possible while it is still remains complex enough to represent the system behaviour (Anderson and Woessner, 1992). To simplify the complex nature of the area, a simplified conceptual hydrogeological model of the groundwater system of the Raya Valley was developed on the basis of information about geology, hydrogeology and hydrology. For the modelling purpose, the system is considered in a steady-state throughout the year. Based on the borehole data 100 meters of average aquifer thickness is considered. The conceptual system of the valley is shown in Fig 5.3 below.

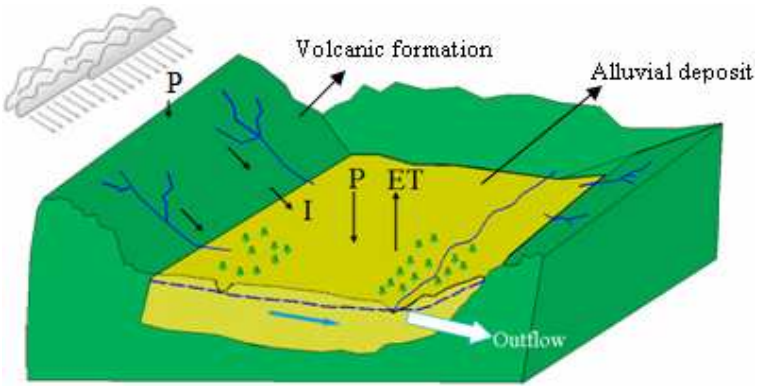

Figure 5.3 Conceptualization of the study area

5.2.1. Boundary conditions

Boundary conditions are constraints imposed on the model grid that express the nature of the physical boundaries of the aquifer being modelled. Boundary conditions have great influence on the computation of heads within the model area. As defined by Anderson and Woessner (1992) there are three types of mathematical conditions used to represent hydrogeologic boundaries:

- Specified head boundaries (Dirichlet conditions)
- Specified flow boundaries (Neuman conditions)
- Head-dependent flow boundaries (Cauchy or mixed conditions)

Boundary conditions are mathematical statements specifying the dependent variable (head) or the derivative of the dependent variable (flux) at the boundaries of the problem domain. In steady-state simulation, the boundaries largely determine the flow pattern. Therefore correct selection of boundary conditions is a critical step in model design (Anderson and Woessner, 1992).

The model area is bounded by Korem and Maichew Mountains in the north-west, the Chercher Mountains in the east and in the south by lower E-W surface divide near Kobo town separating the Alamata sub-basin from the Golina sub-basin to the south. The valley opens to the north and narrows to the south. The transition to the Afar depression is marked by a low range of volcanic hills which form the eastern boundary. The valley has only one outlet through the south-eastern part of the area. The topographic divides primarily define the lateral model boundaries. These natural features act as no-flow (Q = 0) boundaries as they are considered coincident with ground-water divides. Therefore, the entire outer model boundary was simulated as a no-flow boundary, with the exception of the outlet of the valley at the south-east of the area. The groundwater exits the system at this location as groundwater outflow. At the bottom of the layer, the no-flow boundary was assigned assuming that the boundary coincides with the massive impermeable basalt rock. The drain package was applied along the lower reach of the Sulula River, which cuts through the eastern range of hills at Selembir, to simulate the groundwater discharge through the outlet. The out let has a width of about 30m and cuts through the basaltic rock.

5.2.2. Stratigraphic units

Defining hydrostratigraphic units is crucial in determining the number of layers controlling groundwater flow within the system. A hydrostratigraphic unit is comprised of geological units of similar hydrogeological properties. Numerous geological units may be grouped together or a single formation may be subdivided into different aquifers and aquitards (Anderson and Woessner, 1992)**.** Based on the borehole logs obtained during drilling the basin fill is mainly composed of unconsolidated material, which includes gravel, coarse sand, some pebbles and cobbles as colluvial deposits on the foot of the escarpment and medium to coarse alluvial materials along the intermittent rivers and silty-clay to clay in the valley centre deposits. In most of the borehole logs the different grain sizes of alluvial deposits are found representing intercalating layers of sand, silt and clay. The alluvial deposit in the sub-basin is underlain by massive basalt rock (Table 5.1). Therefore in the model design the aquifer is simulated as a single layer (Figure 5.4).

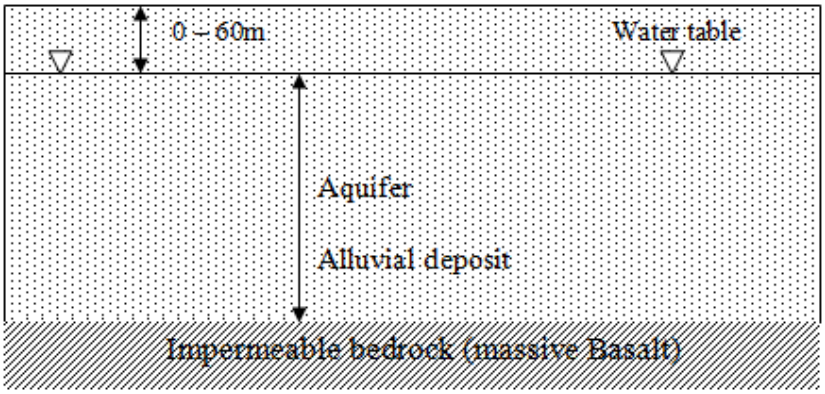

Figure 5.4 Schematic profile of the geological formations of the model area

The lithologic log in Table 5.1 belongs to a borehole which is located in the south-western part of the area. As is shown in the table the alluvial deposit is composed of boulders, coarse gravels, sands, and silt-clay to clay. Beside this, the log shows that the alluvial deposit is an intercalation of these different grain sizes and is underlain by massive basalt at a depth of 172m.

Table 5.1 The lithologic units of borehole RPW-030-08 in the south-western part of the area

	Depth (m)	
Lithology Description	**Form**	**To**
Top soil	0	6
Fine sand	6	10
Coarse sand	10	16
Gravel	16	42
Coarse sand with boulder	42	46
Clay	46	48
Coarse sand with boulder	48	52
Sticky clay	52	70
Coarse sand with boulder	70	74
Clay	74	86
Medium sand	86	90
Clay	90	96
Medium sand	96	100
Clay	100	106
Medium to coarse sand	106	116
Clay	116	120
Gravel with clay	120	126
Coarse sand with clay	126	144
Clay	144	150
Coarse sand	150	156
Boulder	156	164
Highly weathered &fractured basalt	164	170
Weathered basalt	170	172
Massive basalt (fresh)	172	174

Source: (WWDSE, 2008b) drilled by Al-Nile Business Group

5.2.3. Sinks and sources of the model area

In the Raya Valley the primary groundwater sources are direct recharge from precipitation and inflow from runoff from surrounding mountains or higher elevation locations. The primary output or sinks are groundwater outflow and groundwater evapotranspiration (ET_g) (Figure 5.3).

Recharge

Recharge in the model area originates from the direct precipitation and from runoff from surrounding mountains or higher elevation locations. This runoff was conceptualized as diffuse which is the process of surface runoff as occurring all along the boundary edge of the modeled ground-water system and the recharge was simulated as a specified-flow boundary along the top grid layer of the model. Different recharge zones were used depending on the source area (Figure 5.7). As was discussed in chapter 4 the recharge was estimated using the CMB method which represents the long term average recharge.

Groundwater evapotranspiration (ET_g)

ET_g occurs either as evaporation when the water level is close to the land surface or as transpiration through phreatophytes characterized by deep roots tapping groundwater. It is assumed that the nearer the water table is to the land surface, the greater the plant roots will be in direct contact with the water table and the greater will be the amount of water withdrawn from the saturated zone. In MODFLOW, evapotranspiration is approximated as a linearly varying rate that ranges from a maximum at elevations at or above land surface and decreases to zero below some depth, referred to as an extinction depth (Figure 5.5). The ET_g was simulated in the model by evapotranspiration package in MODFLOW. Three evapotranspiration zones (Figure 5.7) were identified in the model area based on the field visit and satellite image interpretations. The elevation of the ET surface in the MODFLOW was assumed as the topographical surface and the extinction depth was set at 5.0m considering the estimated maximum rooting depth of the area.

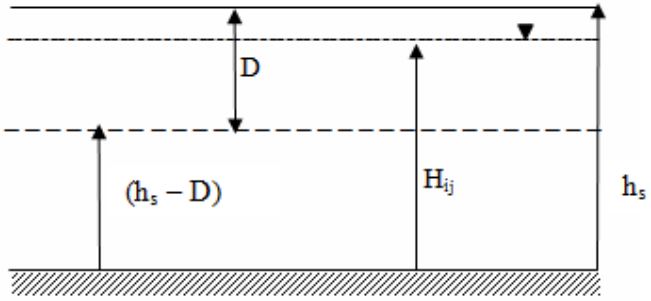

Figure 5.5 Representation of evapotranspiration in MODFLOW (Anderson and Woessner, 1992)

The evapotranspiration package removes water from the saturated groundwater regime based on the following assumptions:
When water table is at or above the elevation of the ET surface (h_s), evapotranspiration loss from the water table is at the maximum ET rate (ET_{max}); no evapotranspiration occurs when the depth of the water table below the elevation of the ET surface exceeds the ET extinction depth (D) and in between

these two extremes evapotranspiration varies linearly with the water table elevation. These assumptions can be expressed as in equation 5.1:

$$Q_{ET} = ET_{max} \frac{\left(H_{ij} - \left(h_s - D\right)\right)}{D} \qquad \text{For } (h_s\text{-}D) <= H_{ij} <= h_s \qquad (5.1)$$

Where:

Q_{ET}	=	Evapotranspiration flow rate	$[L^3T^{-1}]$
ET_{max}	=	Evapotranspiration loss from the water table at the maximum ET Rate	$[LT^{-1}]$
H_{ij}	=	Hydraulic head at the cells	[L]
h_s	=	Elevation of the ET surface	[L]
D	=	ET extinction depth	[L]

Groundwater outflow

The means of groundwater discharge from the aquifer system is mainly by discharge to streams. The Sulula River is in hydraulic contact with the aquifer system, where in the lower reaches of the river groundwater is drained to the river. The groundwater discharge from the aquifer is expressed as springs and seepages along the river bed mainly in the lower reaches of the river and marshy areas in the flat lying parts of the valley. The flow of water between an aquifer and overlying river is commonly simulated using river package as follows:

$$QRIV = CRIV\left(HRIV - h\right) \qquad \text{For h>RBOT} \qquad (5.2)$$

$$QRIV = CRIV\left(HRIV - RBOT\right) \qquad \text{For h<=RBOT} \qquad (5.3)$$

$$CRIV = \frac{KLW}{M} \qquad (5.4)$$

Where:

QRIV	=	rate of leakage between the river and the aquifer	$[L^3\ T^{-1}]$
CRIV	=	hydraulic conductance of the river bed	$[L^2T^{-1}]$
HRIV	=	head in the river	[L]
h	=	hydraulic head in cell	[L]
RBOT	=	elevation of the bottom of the riverbed	[L]
K	=	hydraulic conductivity of the riverbed material	$[LT^{-1}]$
L	=	length of the river within a cell	[L]
W	=	width of the river	[L]
M	=	thickness of the riverbed	[L]

The groundwater drained to the river can be simulated by setting RBOT equal to HRV in the river package, for this case the river package acts the same as the drain package. The drain package works in a much the same way as the river package, except that leakage from the drain to the aquifer is not allowed (Anderson and Woessner, 1992). Due to the absence of river level measurement data, a drain package is applied to simulate the groundwater discharge to the gaining reaches of the river. The recharge to the aquifer from the loosing reaches of the river was assumed to be take place by the vertical aerial recharge which was integrated in the chloride mass balance method. Therefore, the

groundwater outflow from the aquifer in the model was simulated by a drain package representing the main Sulula River.

Drain package

Drain package is different from river package in that the flow is directed only from the aquifer towards the drain and it stops when the head in the aquifer drops below the elevation of the drain. The rate of flow entering the drain (QD) is calculated from the following equation 5.5 (McDonald and Harbaugh, 1988):

$$QD = C_d (h - d) \qquad \text{For } h > d \qquad (5.5)$$

$$CD = \frac{KLW}{M} \qquad (5.6)$$

Where:

K	=	equivalent to hydraulic conductivity of the drain material	[LT^{-1}]
L	=	length of the drain within the cell	[L]
W	=	the width of the stream within the cell	[L]
M	=	the thickness of stream bed material	[L]
h	=	aquifer hydraulic head	[L]
d	=	elevation of the drain	[L]

The value of CD was adjusted during calibration process, L is approximated to the length of the cell, W is estimated to 20m and M is estimated to 3m. Since no measurements of theses value were available, it was impossible to be accurate on a detailed level.

5.2.4. The model area

The ASTER DEM was processed to define the boundary of the model area, visualize the geomorphology of the area, delineate the sub-catchments, and extract drainage patterns. The grid size of the model was taken as 250m x 250m with 137 columns and 297 rows. A total of 17600 active cells were used to represent the entire model area which is 1085 km^2 (Figure 5.6). Model area and the elevations of top layer were delineated by the ASTER DEM optimisation and use of the topographic maps.

5.2.5. Aquifer geometry

The aquifer extent was made based on the available details of the boreholes. Top of aquifer elevation was assigned based on the datum level of the area, which was obtained from the DEM processing. The bottom elevation of the aquifer was obtained by deducting the aquifer thickness from the top elevation. The aquifer thickness was obtained from the drilled borehole log data and found to have an average value of 100m. The aquifer has a length of about 68 km along N-S and about 12 km in width along E-W direction. However, the irregularly shaped model area has a total area of about 1100 km^2 (see Table 4.9).

5.3. Numerical model

Development of a numerical model allows for a detailed analysis of the movement of water through the hydrogeologic units that constitute the groundwater flow system. Groundwater flow in the unconsolidated deposits of the Raya Valley was simulated using the U.S. Geological Survey modular three-dimensional finite-difference groundwater flow model, MODFLOW (McDonald and Harbaugh, 1988). This numerical modelling was performed using the interface of PMWIN processing MODFLOW, Version 5.3 (Chiang and Kinzelbach, 2001) as code environments for data input and output management. It is founded on the physical theory of groundwater movement: Darcy's law and the continuity equation. The steady-state groundwater flow is simulated based on the following governing differential equation under two-dimensional aerial view (Anderson and Woessner, 1992).

$$\frac{\partial}{\partial x}(K_x \frac{\partial h}{\partial x}) + \frac{\partial}{\partial y}(K_y \frac{\partial h}{\partial y}) + R = 0 \qquad (5.7)$$

Where:

K_x and K_y	=	Components of the hydraulic conductivity along x, and y axes	$[LT^{-1}]$
R	=	Flux per unit volume representing sources/sinks term	$[T^{-1}]$
h	=	Hydraulic head	[L]

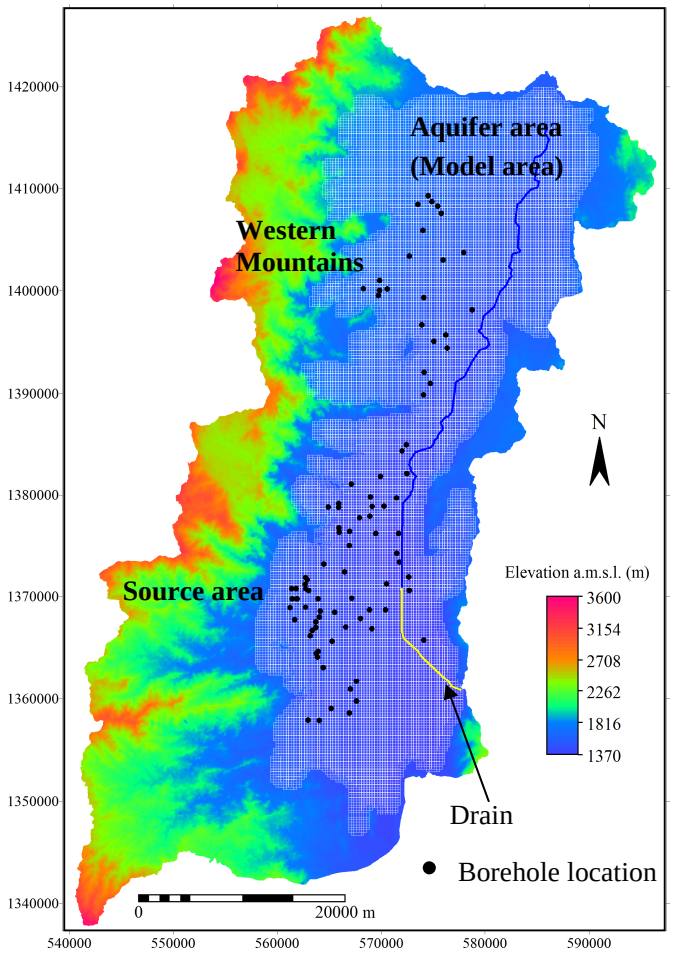

Figure 5.6 Discretization of the model area

5.3.1. Data input for the model

The model input data were processed and analysed in chapter four. The DEM was processed to define the boundary of the model area and to obtain the ground surface elevation. More than 80 borehole coordinates and observed water levels were saved in a text-file and then imported into the model, where the elevation of each cell was interpolated. Boundary conditions were chosen so that the model domain would be as limited to the aquifer area of the basin as possible. Model cells outside chosen boundary conditions were inactivated. The hydraulic conductivity values from the pumping test analyses were used as initial values in the model input by making different zones according to the pumping test data distribution. Sixteen zones were assigned to represent the hydraulic conductivity distribution in the sub-basin. The estimated recharge values were distributed as initial values in the model area after making ten recharge zones according to the source area. Beside this, three groundwater evapotranspiration (ET_g) zones were delineated where the groundwater level is close to the surface and forms a swampy area. These are the Gerjele, Tumuga and the swampy area near the outlet (Figure 5.7).

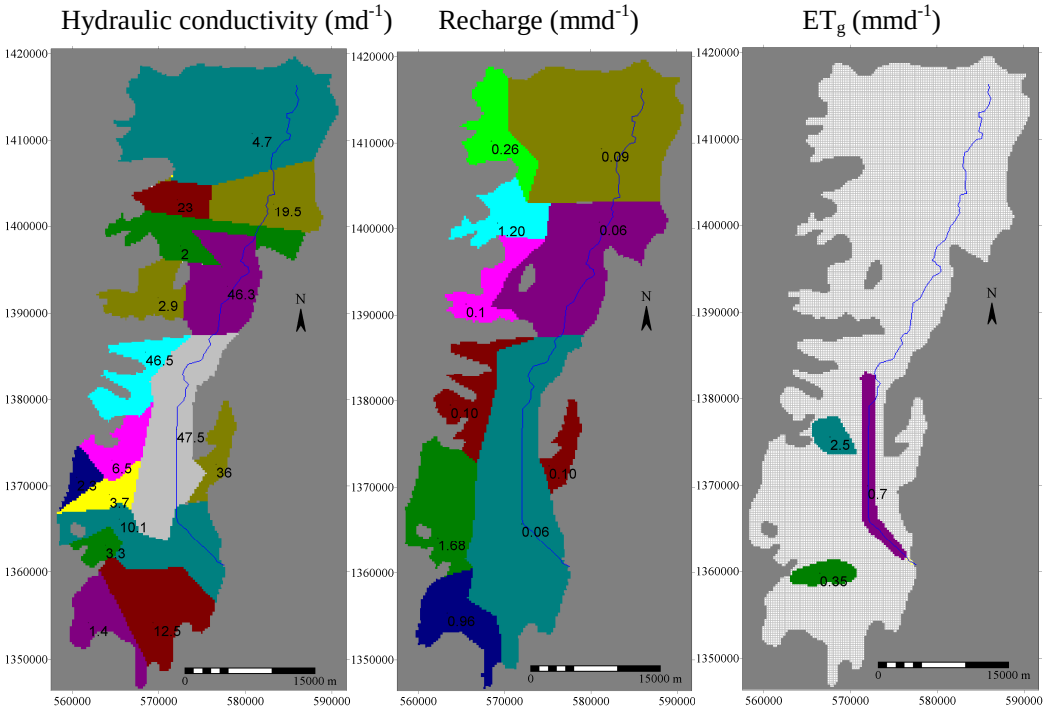

Figure 5.7 Zone maps of hydraulic conductivity, recharge and groundwater evapotranspiration

5.3.2. Model execution and calibration

Model execution includes the entry of prepared input data into the selected computer code, and interpretation of the model results. Model results were compared with the calibration target and if the error in the simulated results is acceptable, the model is considered calibrated; if the level of error is unacceptable, parameter values are adjusted and the model is run again until acceptable results are achieved. The model was run with the interactive method.

5.3.3. Calibration target and uncertainty

In trial-and-error calibration, parameter values are initially assigned to each node in the grid. During calibration, parameter values are adjusted in sequential model runs to fit simulated heads to the calibrated targets. Calibration target is a calibration value and its associated errors. In this study the hydraulic heads obtained from groundwater level measurement data were used as calibration values. The calibration target was to match hydraulic heads simulated by the model with the measured heads. Hydraulic heads were obtained from static water level records measured during drilling. It should be noted that most of the measured head data and the uncertainty of the model are associated with errors due to the following reasons:

- The water level measurements were taken from the pumping wells, without monitoring well
- The water level measurements are one time measurement i.e. during well completion.
- Measurement errors are related to measuring instrument and operator errors.
- Digital elevation models (DEMs) have difficulties in replicating hydrological patterns in flat landscapes. Errors are due to averaging ground surface elevations.
- The lineaments in the surrounding basaltic hills can be of tectonic origin. Hence, there may be fault systems that extend up to great depth. This may enhance water withdrawal from the aquifer which was not considered in the conceptualization of the model and might contribute to the model uncertainty.

Moreover, the groundwater level data are not well distributed in the entire model area. All the mentioned uncertainties made the calibration not only uncertain in some part of the model but also constitute a challenging and arduous task. Hence, the measured head values may not represent the actual water level of the field condition. The standard deviation of the groundwater level below ground level showed a value of about 13m. Therefore, considering the standard deviation of the water level together with the cumulative effect of the mentioned uncertainties in the input data; it was reasonable to assume a RMS error of 13m as predefined calibration target. More than 80 wells were selected for calibration of the steady-state model. Figure 5.6 shows the location of the wells. At the beginning, the model was calibrated for the condition without abstraction, which helps to check the model reliability in generating field condition when it is subjected only to the natural stresses. Then estimated abstraction amount of water was used in order to see the effect of abstraction on the model calibrated hydraulic head and on the overall water budget of the area. Here, estimated abstraction value was used because during this study no data was obtained about the actual total abstraction for irrigation and for water supply, except for Alamata town water supply which is reported as about $0.5 Mm^3 y^{-1}$.

5.3.4. Trial-and-error calibration

Trial-and-error calibration was the first technique to be used and is still the technique preferred by most users (Anderson and Woessner, 1992). It is the process of manual adjustment of input parameters until the model simulates the measured heads within range of the error criteria. The model was calibrated for steady-state conditions, assuming constant recharge and steady discharge neglecting seasonal fluctuations. Calibration was conducted through trial and error by varying aquifer hydraulic conductivity, recharge and evapotranspiration values. During the calibration the parameter values and their zones were modified manually and trial runs were carried out until the model output

was within the range of the pre-defined error criterion. The best fit results were achieved after the model area was divided into 16 zones of hydraulic conductivity, 10 zones of recharge and 3 zones of groundwater evapotranspiration (Figure 5.7). The hydraulic conductivity values applied during the calibration ranges from 1 to 47md^{-1}. The procedure followed for the trial-and-error calibration is presented in Figure 5.8.

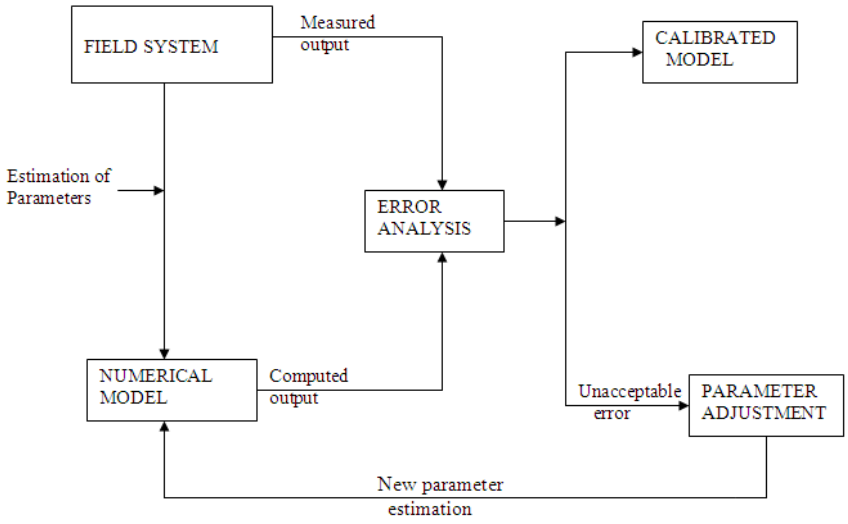

Figure 5.8 Trial and error calibration procedures (adapted from Anderson and Woessner, 1992)

5.3.5. Evaluation of calibration

The results of the calibration should be evaluated both qualitatively and quantitatively (Anderson and Woessner, 1992). The measured and simulated heads together with their differences are listed in Appendix 5. The average of the differences was then used to quantify the average error in the calibration. The three ways of expressing the average difference between simulated heads (h_s) and measured heads (h_m) are: the mean error (ME), the mean absolute error (MAE) and the root mean square error (RMS). The objective of the calibration is to minimize these error values.

$$ME = \frac{1}{n}\sum_{i=1}^{n}\left(h_{m,i} - h_{s,.i}\right) \quad (5.8)$$

The mean difference between measured heads and simulated heads

$$MAE = \frac{1}{n}\sum_{i=1}^{n}\left|\left(h_{m,i} - h_{s,i}\right)\right| \quad (5.9)$$

The mean of the absolute value of the differences in measured and simulated heads

$$RMSE = \sqrt{\left[\frac{1}{n}\sum_{i=1}^{n}\left(h_{m,i} - h_{s,i}\right)^2\right]} \quad (5.10)$$

The average of the squared differences in measured and simulated heads

These measures of errors can only be used to evaluate the average error in the calibrated model. The RMSE is usually thought to be the best measure of error if errors are normally distributed. The

maximum acceptable value of the calibration criterion depends on the magnitude of the change in heads over the problem domain (Anderson and Woessner, 1992).

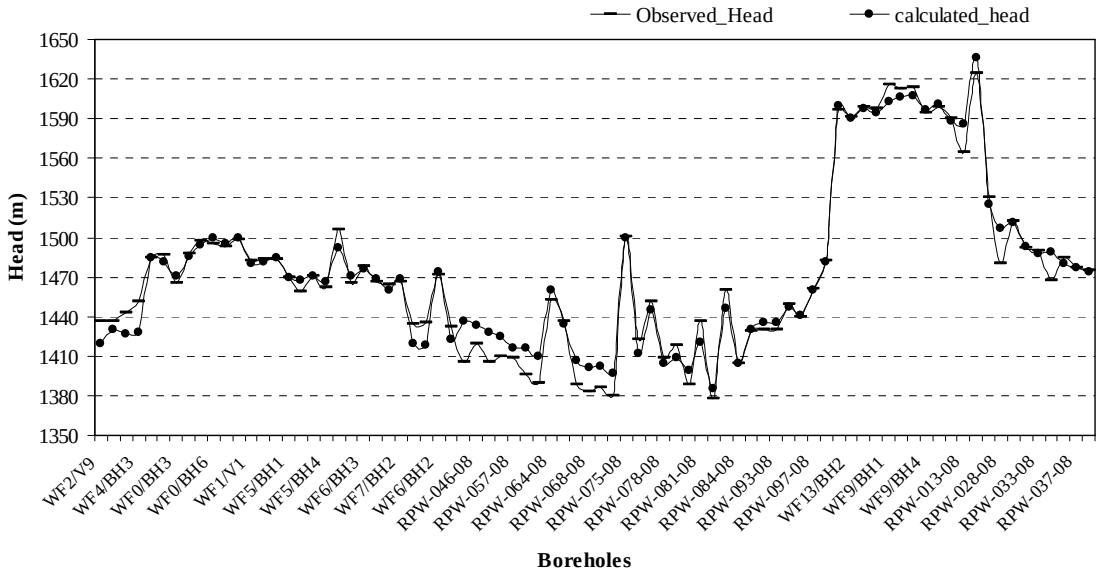

Figure 5.9 Comparison between the observed and the model simulated heads

A scatter plot of measured against simulated heads is another way of showing the calibrated fit (Fig.5.10). The scatter plots are visually examined whether points in a plot show deviation from the straight line in a random distribution or have systematic deviation, where systematic deviation of the plots can indicate systematic error in adjusting the parameter values with in a zone. The scatter plot shows a correlation coefficient of 0.97 and a RMSE of 10.7m.

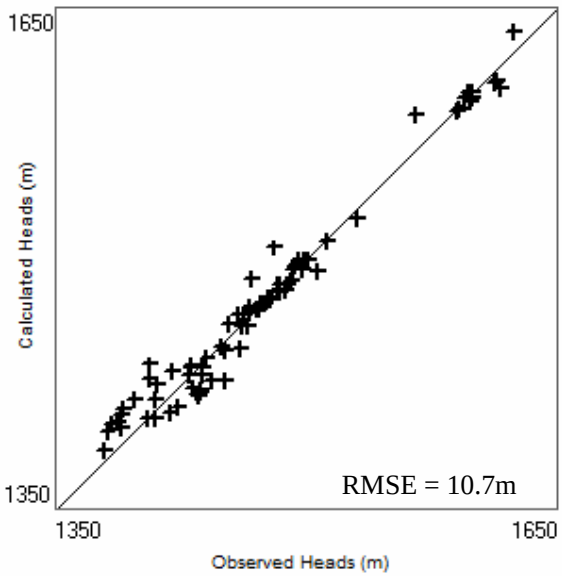

Figure 5.10 Graphical representation of measured versus simulated heads

Automatic calibration was introduced to improve the fit obtained by the manual calibration. The method facilitated by nonlinear least squares regression and associated statistics, known as Parameter Estimation Program, PEST, which is linked to PMWIN was employed to calibrate the model. PEST was supplied with initial values of the parameters together with their reasonable lower and upper boundary values to be optimized and the set of observations, which PEST can compare with the model outputs. Initially, PEST executes MODFLOW with the given initial parameter values and outputs of MODFLOW are compared with the given set of observed data and estimate the objective function (RMSE). Then the PEST starts minimizing the objective function by adjusting parameters. The manual best adjusted parameter values were assigned as initial values to the PEST automatic calibration and finally with small improvement the model was calibrated with a RMSE of 10.7m. The differences in simulated and observed heads are tabulated in Appendix 5. The summary of the error analysis for the calibrated model is shown in Table 5.2.

Table 5.2 Error summary of the calibrated model

ME	-1.4 m
MAE	7.8 m
RMSE	10.7 m

Since, the above three measures of error only quantify the average error not about the distribution of the errors in the model area; comparison of contour maps of simulated and measured heads, scatter plots of the residual error and map of the residual heads were used to make qualitative analysis of the spatial distribution of errors.

As is shown in Figure 5.11 about 70% of the simulated water levels are within ten metres of measured levels and 82% of the total is with in 15 meters. The residual water level which is the difference between simulated and measured is distributed for values over the whole ranges of water levels, higher to lower. This suggests that there is little bias in model simulation for the entire model area.

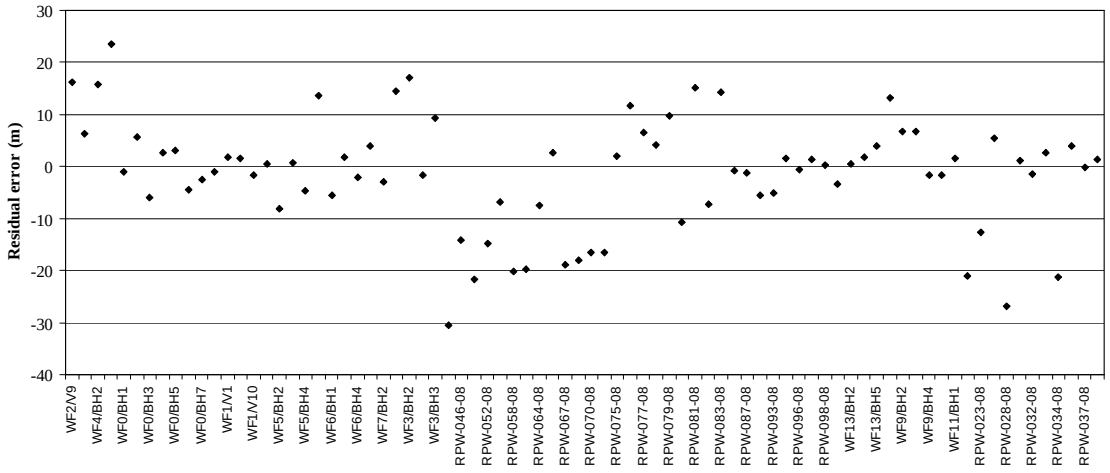

Figure 5.11 Model residual compared to field measured water levels

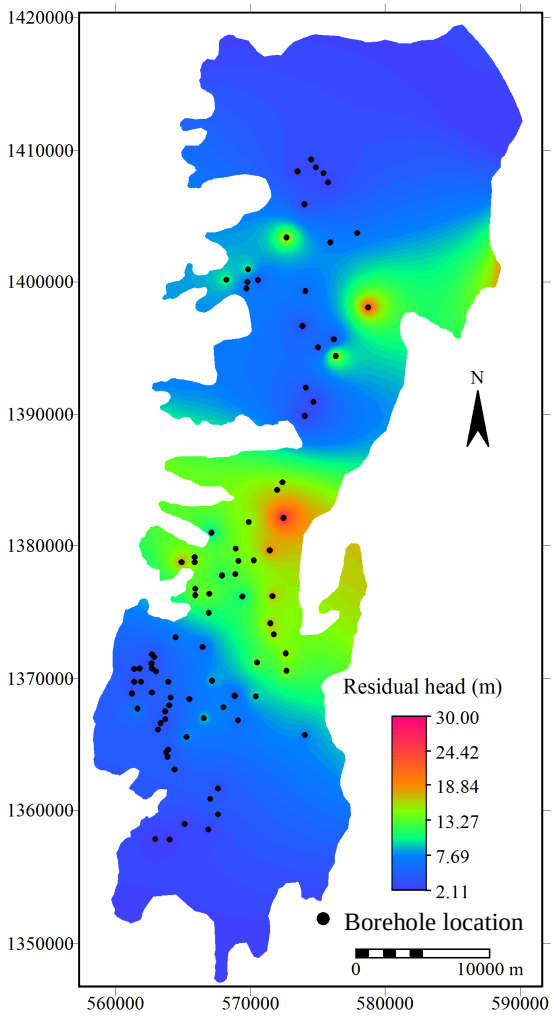

Figure 5.12 Residual head map of the model area

The residual head map which is the absolute head difference between the observed and model simulated in Figure 5.12 shows that the model has some uncertainties in simulating the observed heads in the northern part of the Alamata sub-basin and in some places in the Mohoni sub-basin. However the majority of the area was simulated well.

The contour map of the hydraulic head represents the top of the ground water surface in an aquifer. It provides an indication of the directions of groundwater flow in the aquifer system and groundwater recharge and discharge areas. The contour maps of the simulated heads (Figure 5.13) were analyzed to see whether the results are comparable with the actual field condition. The flow direction determined in the conceptual model was compared with the simulated flow. The groundwater flow direction in Mohoni sub-basin shows a general trend of north-south, whereas in Alamata sub-basin the flow direction is towards south-east of the sub-basin from north, south and west part of the sub-basin.

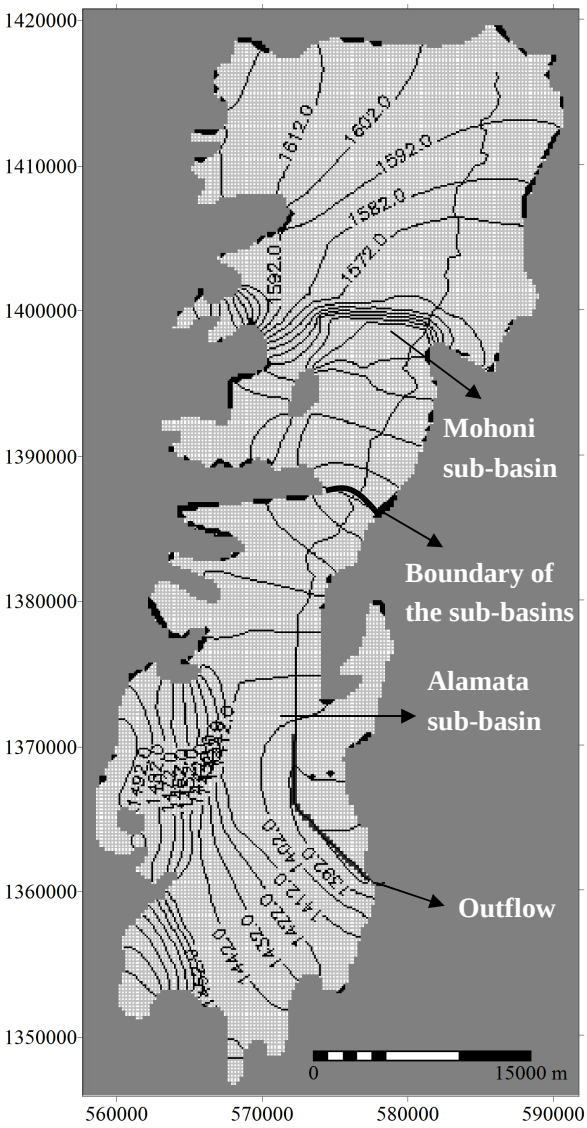

Figure 5.13 Contour map of model simulated hydraulic head

5.4. Water budget of the model domain

Another way of checking the amount of residual error in the solution is to compare the total simulated inflows and outflows as computed by the water budget of the entire domain (Table 5.3). Preparation of a water budget involves the identification and quantification of all flows in and out of the groundwater system. The water budget of the model area is one of the ways to quantitatively evaluate the movement of groundwater through an aquifer system. The basic equation for a water budget (or water balance) under a steady state condition is that sum of inputs to the aquifer equals the sum of outputs from the aquifer.

$$\sum \text{Inputs} = \sum \text{Outputs} \qquad (5.11)$$

In this study the water balance is established based on the modelling water budget tool in MODFLOW. In the model area the inflow term is the recharge and the outflow terms are drain, groundwater evapotranspiration and well abstraction for the pumping scenario. The inflows and outflows of the total water budget over the entire aquifer are in balance which is consistent with the steady-state modelling hypothesis. The summary of the entire domain water budget was shown in Table 5.3.

Table 5.3 Water budget of the whole domain in Mm^3y^{-1}

Flow term	In	Out	In - Out
Drains	0	100	-100
ET_g	0	24	-24
Recharge	124	0	124
Total	124	124	0
Discrepancy [%]	0.00		

Table 5.4 Water budget of the whole domain in mmy^{-1}

Flow term	In	Out	In - Out
Drain	0	92	-92
ETg	0	22	-22
Recharge	114	0	114
Total	114	114	0
Discrepancy [%]	0.00		

The drain and the groundwater evapotranspiration which are the outflow components of the water budget were estimated by the steady state model as $92mmy^{-1}$ and $22mmy^{-1}$ respectively (Table 5.4). The model calibrated recharge rate of the valley is $114mmy^{-1}$, while the chloride mass balance method showed that a recharge of $116mmy^{-1}$. Hence, the recharge estimated by chloride mass balance method agrees well with the recharge estimated by the model calibration.

Zone budget in MODFLOW which is a computer program that computes sub-regional water budgets using results from the MODFLOW groundwater flow model was used after the sub-regions of the Alamata and Mohoni sub-basins were designated by specifying zone numbers. Then separate budget was computed for each zone. The budget for a zone includes a component of flow between each adjacent zone. Accordingly, the water budget of the sub-basins is presented in Table 5.5 and 5.6.

Table 5.5 Water budget of the Alamata sub-basin in Mm^3y^{-1}

Flow term	In	Out	In - Out
Horizontal exchange	38	0	38
Drains	0	100	-100
ET_g	0	24	-24
Recharge	86	0	86
Total	124	124	0

Table 5.6 Water budget of the Mohoni sub-basin in Mm^3y^{-1}

Flow term	In	Out	In - Out
Horizontal exchange	0.0	38.0	-38.0
Recharge	38.0	0.0	38.0
Total	38.0	38.0	0.0

As is shown in Tables 5.5 and 5.6 the model calibrated groundwater recharge of Mohoni sub-basin is about $38Mm^3y^{-1}$ and recharge to the Alamata sub-basin is about $86Mm^3y^{-1}$. As was described in chapter four the recharge to the sub-basins were estimated using CMB method as 46 and $80Mm^3y^{-1}$ for Mohoni and Alamta sub-basins respectively. The estimated recharge by the CMB method for Mohoni sub-basin was most likely overestimated as compared to the model calibrated recharge value. This can indicate that considering the inflow amount as 10% of the rainfall in the source area is high for this sub-basin.

5.5. Calibration results

The evaluation of the calibrated model result showed that most of the simulated heads were within the pre-established calibration target and the water budget of the entire domain also confirmed that the inflow and the outflow components are in balance (Table 5.3). The overall results of the model simulated heads are comparable with the measured heads and the model simulated flow directions are also in agreement with the conceptual model flow directions. The measure of errors evaluated by ME, MAE and RMSE are in the acceptable range according to the pre-determined error criteria (Table 5.2). Though the overall result of the model simulated water levels of the wells are comparable with the measured water levels, the level in some wells were over estimated by the model. This can indicate that the model may have uncertainty in those particular areas (Figure 5.12). In the ideal case, calibration values should be measured at a large number of points which are well distributed over the model domain. Therefore, it is not possible to conclude that the calibration is accurate by only quantifying the errors using ME, MAE and RMSE without considering the distribution of the residuals. From the calibrated model results, the model shows good calibration results with the residual error being distributed for values over the whole range of water levels (high to low) in the model area, but this is not so clear on the remaining part of the model area where no measured data are available to compare with the simulated results. However, in order to check the reliability of the developed model, a sensitivity analysis was made.

5.6. Sensitivity analysis

Sensitivity analysis is the measure of uncertainty in the calibrated model caused by uncertainty in aquifer parameters and boundary conditions. Sensitivity analysis was performed by systematically changing the calibrated values of conditions (Anderson and Woessner, 1992). The main objective of a sensitivity analysis is to understand the influence of various model parameters and hydrological stresses on the aquifer system and to identify the most sensible parameter(s), which will need a special attention in future studies. Running the calibrated model with changes to a parameter by predetermined amounts within a realistic range can be utilized to establish the model's sensitivity to that parameter. Therefore, sensitivity analysis is an essential step in modelling studies.

The response of the calibrated numerical model to changes in model parameters of hydraulic conductivity and recharge was examined. During simulation, when the effect of one parameter was being tested, the other parameters were kept to the steady-state calibrated value and each parameter was changed uniformly over the whole model domain. The magnitude of changes in heads from the calibrated solution was used as a measure of the sensitivity of the model to that particular parameter.The sensitivity analysis process was associated with stressing and parameterizing the calibrated model differently from the calibrated conditions.

The calibrated hydraulic conductivity and recharge values were increased and decreased by multiplier factors of: 0.4, 0.6, 0.8, 1.2 and 1.4. Those values were used as input in the model and the sensitivity analysis was assessed (Figure 5.14). Only one parameter was varied at a time in order to see the effect of the changes on the solution and any effects were evaluated by the same statistical methods used to evaluate the model calibration such as the RMSE. As is shown in Figure 5.14 the model is sensitive to both recharge and hydraulic conductivity. The model is highly sensitive with decrease of the calibrated recharge and hydraulic conductivities values and relatively less sensitive with increase of the recharge and hydraulic conductivity values which produced lower RMS errors.

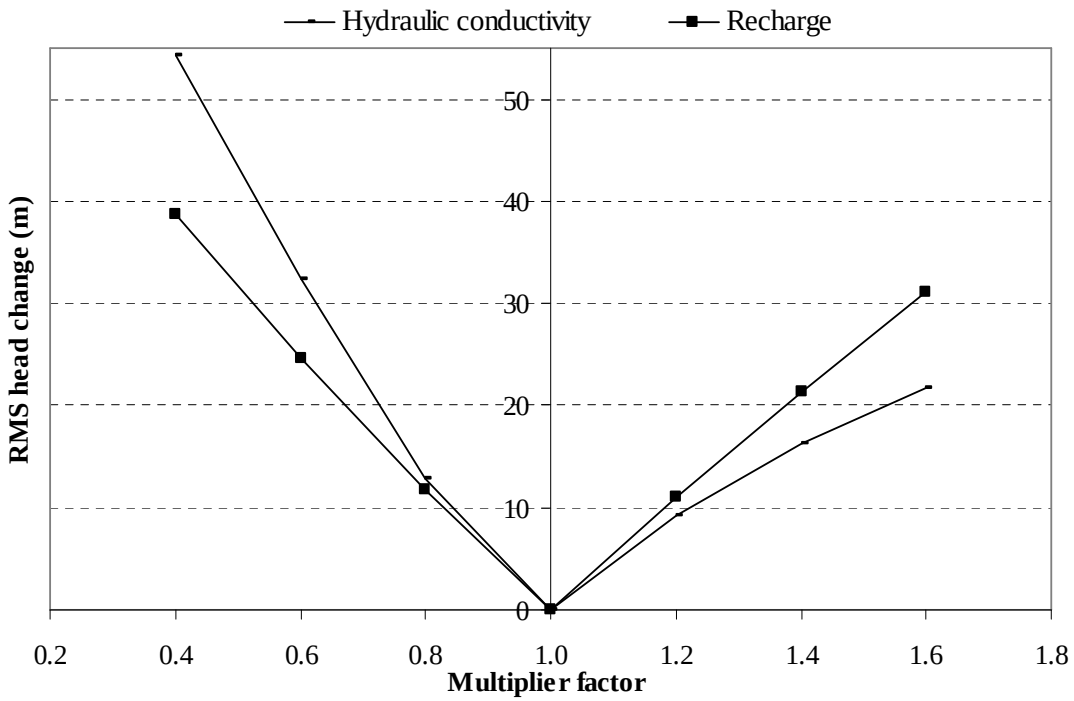

Figure 5.14 Sensitivity analysis of hydraulic conductivity and recharge

6. Pumping scenario analysis

Pumping scenarios were used to test the response of the system under variable groundwater abstraction rates. System response was evaluated by using fluxes and heads of the calibrated model. The system response was compared with resulting changes in water table elevation and groundwater outflow from the model domain. According to WWDSE (2008b), in the Raya Valley there is a large project plan to implement a pressurized irrigation project of about 18,000 hectare using the area's groundwater potential. About 10,000 hectare of irrigation was proposed in the Alamata sub-basin while the remaining 8,000 hectare was proposed in the Mohoni sub-basin (Figure 6.1). Some wells are being used for irrigation at present. However, no data was obtained about the groundwater amount of abstraction and the duration of pumping for the wells. Hence, the actual abstraction rates from the valley are uncertain at this stage.

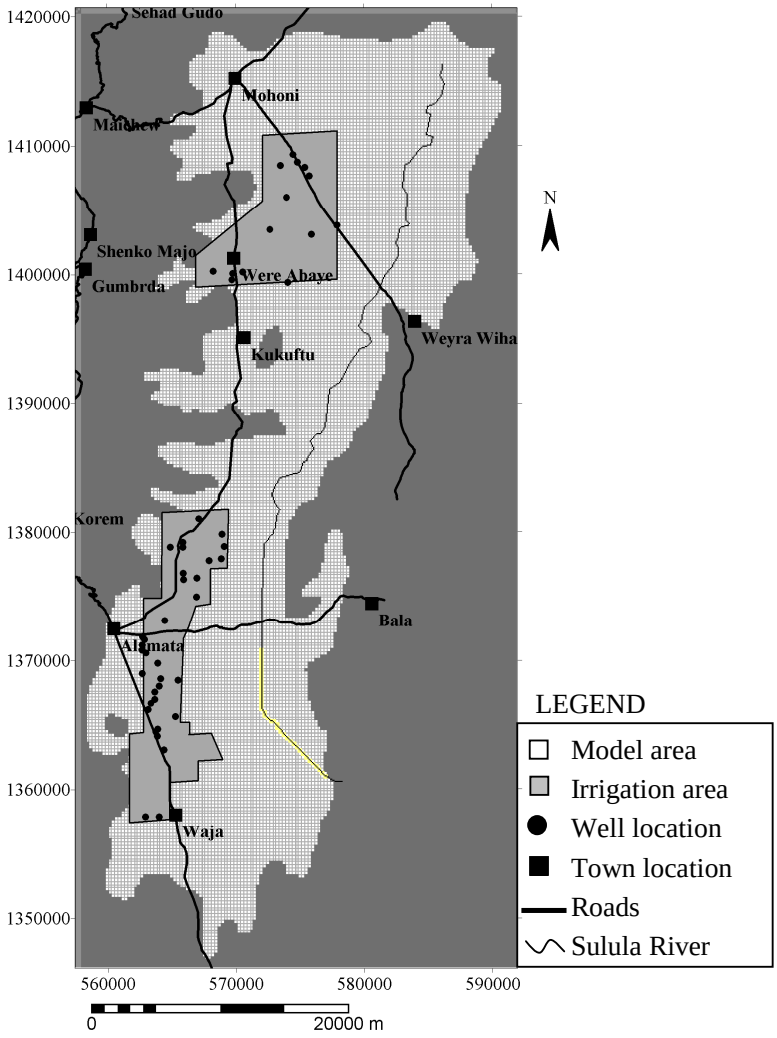

Figure 6.1 Map showing the irrigation area and the well locations

6.1. Irrigation area of the Alamata sub-basin

In this study the 10,000 hectare area in the Alamata sub-basin was selected to analyze the effect of the irrigation on the steady-state calibrated model. Thirty four boreholes in the irrigation area were used as discharging wells to simulate the required crop water demands and to simulate the average head decline. The location of the irrigation area and the wells was shown in Figure 6.1. Accordingly, 100mm and 200mm of water per crop season were taken as scenario-one and scenario-two respectively. Theses amounts were converted to volume considering the irrigation area. For scenario one the total amount of water required was equally divided among the 34 wells. Hence, each well was discharged with about $2451 m^3 d^{-1}$. Whereas, for scenario two, 27 wells were assigned a discharge of $5011 m^3 d^{-1}$, 4 wells (RPW-064-08, RPW-077-08, RPW-097-08, and RPW-098-08) were discharged with $5249 m^3 d^{-1}$, and the remaining 3 wells (WF0/BH1, WF1/V1 and WF1/V10) were discharged with $3456 m^3 d^{-1}$. The discharges of the wells were implemented in the steady-state model through the well package of the MODFLOW program. The model was then run using the pumping scenarios and the result was analysed. In scenario-one a total amount of $8.3 \times 10^{+4}$ $m^3 d^{-1}$ was abstracted which resulted in an average decline of water level by 22m. Whereas, in scenario-two, a total amount of $1.7 \times 10^{+5}$ $m^3 d^{-1}$ which is double the amount of scenario one, was discharged and this resulted in an average decline of the water level by 50m (Table 6.1). These average declines in water level are only for the wells that are found in the irrigation area. The effect of abstraction is mostly in the irrigation area and the influence of the abstraction becomes less away from the area.

Table 6.1 The discharge amount and the average groundwater level decline of the two scenarios

	Number of wells	Discharge ($m^3 d^{-1}$)	Total discharge ($m^3 d^{-1}$)	Average decline in water level
Scenario_1 (100mm per crop season)	34	2451	$8.3 \times 10^{+4}$	22m
Scenario_2 (200mm per crop season)	27	5011	$1.35 \times 10^{+5}$	
	4	5249	$2.1 \times 10^{+4}$	
	3	3456	$1.04 \times 10^{+4}$	
		Total	$1.7 \times 10^{+5}$	50m

The crop water requirements used here are estimated values; they were used here simply to see the effect of abstraction on the model. Moreover, the crop season duration was taken as 120 days or four months. The actual amount and duration would have different values in practice.

The contour map of the simulated head for both pumping scenarios (Figure 6.2) shows that the regional flow direction of the model remains the same, except for local effects around the irrigation area where the contour lines show flow towards the irrigation area. In scenario two the abstraction effect is more pronounced and extends to larger area than scenario one.

In order to increase the abstraction rate with reasonable drawdown, it is recommended to use additional wells from outside the irrigation area, and the abstraction rate of each well should be assigned based on their safe yield from the pumping test data analysis.

According to the pumping test data the wells in the irrigation area were tested with average discharge of 3456m^3d^{-1} during the constant rate test. If all the wells in the irrigation area are to be discharged uniformly with 3456m^3d^{-1}, they can yield about 140mm per the mentioned irrigation area and crop season.

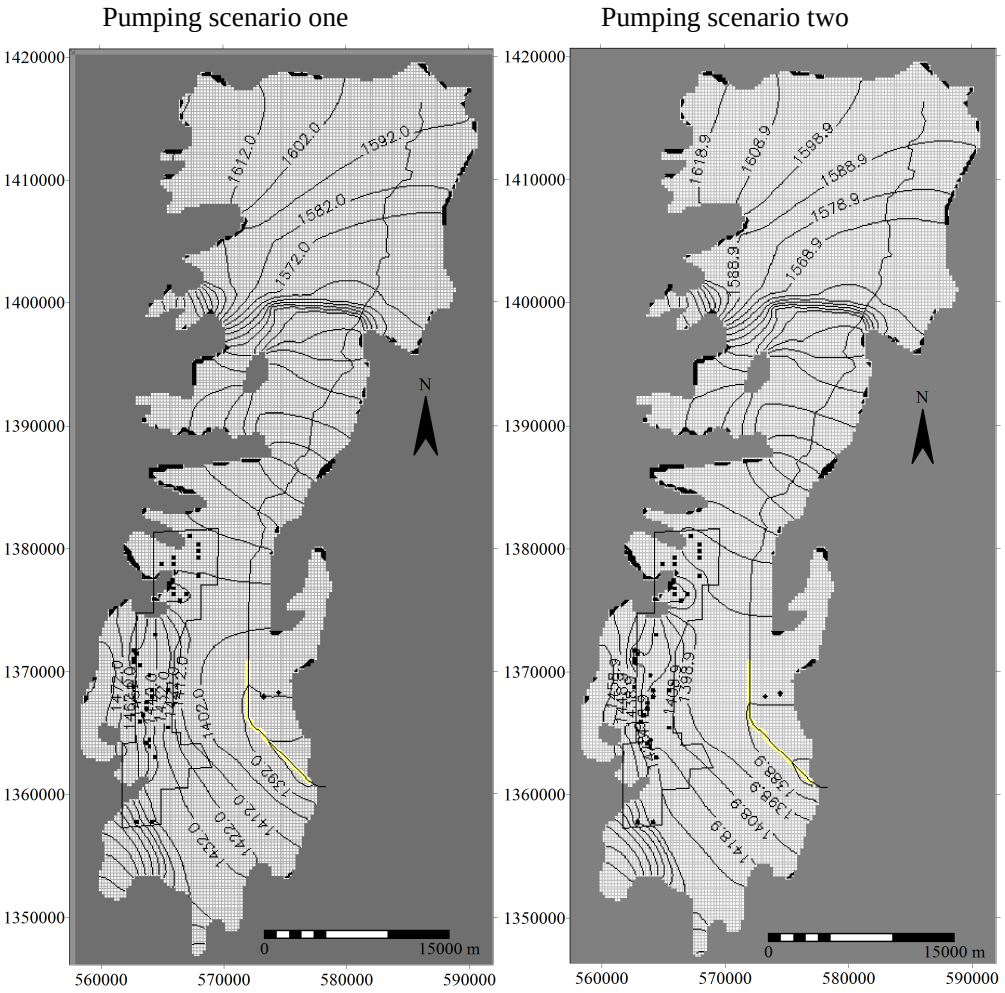

Figure 6.2 Contour map of the model simulated heads for pumping scenario one and two

6.2. Model simulated groundwater budget for the pumping scenarios

The groundwater budget can be quantified on the basis of the model output. The groundwater flow budgets of the Alamata sub-basin calculated by the model for the non-pumping and pumping scenarios were indicated in Table 6.2.

Table 6.2 Model simulated groundwater budget of Alamata sub-basin for different scenarios

Scenario	Flow term	Inflow Mm^3y^{-1}	Outflow Mm^3y^{-1}	Inflow-Outflow Mm^3y^{-1}
Non-pumping	Horizontal exchange	38	0	38
	Drains	0	100	-100
	ET_g	0	24	-24
	Recharge	86	0	86
	Total	124	124	0
Scenario 1 with pumping ($8.3 \times 10^{+4}$ m^3d^{-1})	Horizontal exchange	38	0	38
	Wells	0	30	-30
	Drains	0	70	-70
	ET_g	0	24	-24
	Recharge	86	0	86
	Total	124	124	0
Scenario 2 with pumping ($1.7 \times 10^{+5}$ m^3d^{-1})	Horizontal exchange	38	0	38
	Wells	0	59	-59
	Drains	0	41	-41
	ET_g	0	24	-24
	Recharge	86	0	86
	Total	124	124	0

Figure 6.3 shows the comparison of the hydraulic heads of the non-pumping and the two pumping scenarios, where the heads of the pumping scenarios deviate from the non-pumping heads mostly for the wells which are found in the irrigation area. For the wells outside the irrigation area the influence of pumping became less.

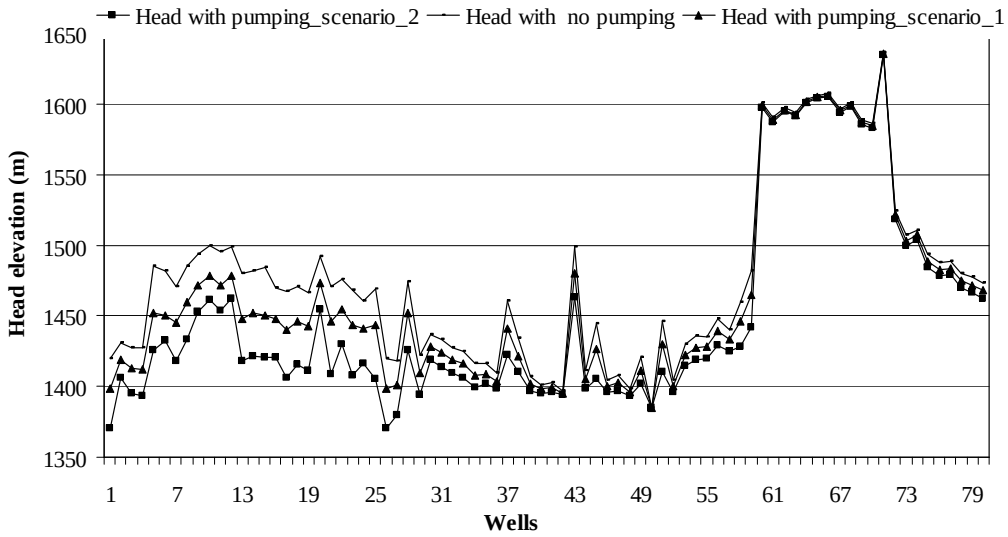

Figure 6.3 Comparison of the observed and simulated heads of the different scenarios

Figure 6.4 shows the scatter plot of the observed hydraulic head versus the heads of the pumping scenarios. There was a groundwater level decline which resulted in a cone of depression in the irrigation area. These scatter plots also confirm that the effect of pumping was largely on the irrigation area where there was extensive abstraction and with less effect away from this area.

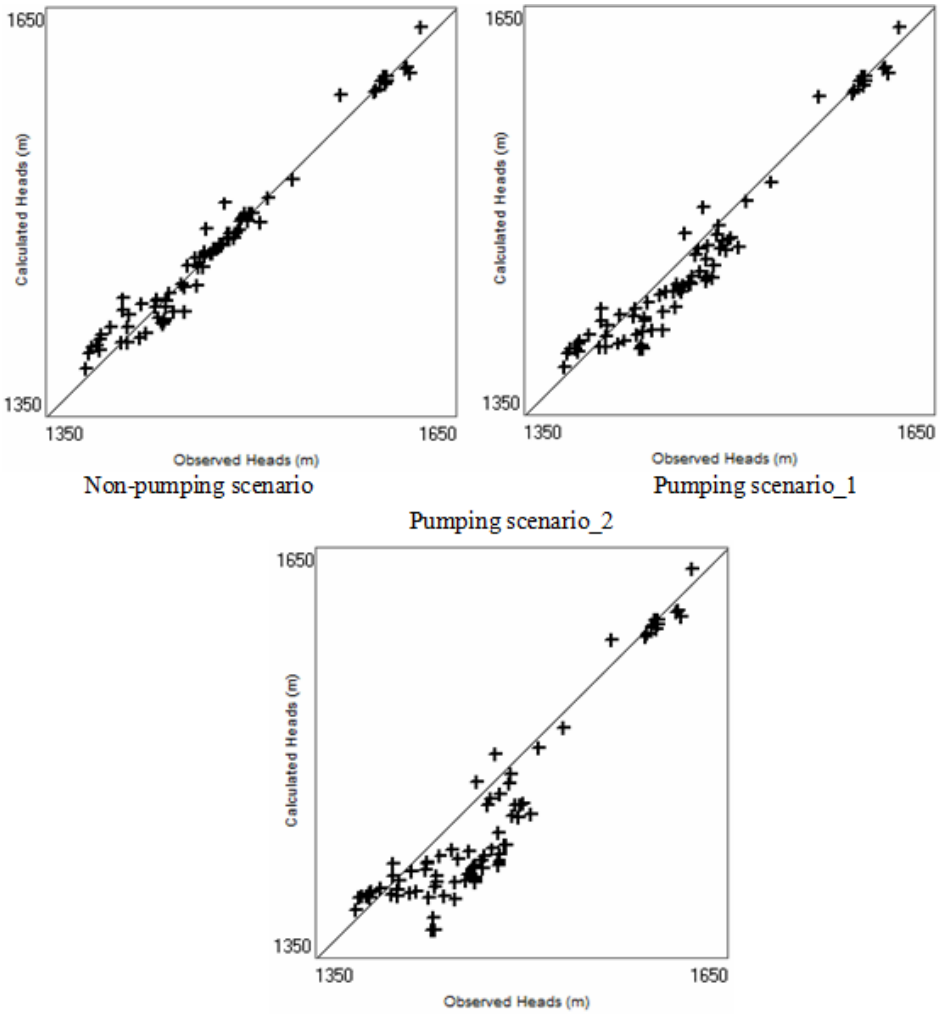

Figure 6.4 Scatter plots of observed and simulated hydraulic heads of the non-pumping and pumping scenarios

Based on this study the annual groundwater recharge of the Mohoni sub-basin using the inverse modeling was estimated as $38Mm^3y^{-1}$ or about $66mmy^{-1}$ and for Alamata sub-basin $86Mm^3y^{-1}$ or about $170mmy^{-1}$. Therefore, for further groundwater resource development plans in the valley, it is important to take into account the balance between the groundwater recharge and the intended abstraction rates both for irrigation and domestic water supply to ensure the sustainability of the resource in the valley.

7. Results and discussions

In this chapter the results of the study will be explained and discussed. The chapter is subdivided in to: hydrochemistry, result of the modelling, groundwater budget, pumping scenario, model limitations and discussion of the model.

7.1. Hydrochemistry

According to the water sample results of the previous study and the current study, the water in the study area is either, Ca- Mg, Mg-Ca, Mg - Na, Na - Ca/Mg or Ca - Na Bicarbonate types. The chemical properties of the groundwater could be associated with the geology of the area and human activities. The conductivity in the area ranges from 412μScm^{-1} in RPW-076-08 to 2800 μScm^{-1} in a hand dug well. Considering only the boreholes, the conductivity ranges from 412μScm^{-1} to 1740 μScm^{-1}. The conductivity increases from the western escarpment towards the valley floor. This is associated with the geology, the ground water flow direction and possible evaporation. Beside this, the SAR of the groundwater which is important for classifying irrigation water showed a value range of between 0.01 and 2.9 therefore the tested samples are safe from sodium danger.

7.2. The result of the groundwater flow modelling

In this study model calibration was achieved through trial and error approach until the hydraulic heads values calculated by the model match the observed values to a satisfactory degree. Model calibration was stopped at the end of the simulation after reasonable matches between the observed and calculated hydraulic head were achieved (Appendix 5). After each run, differences between simulated and observed heads were calculated. The residual between observed and calculated heads was used to calculate the root mean squared error (RMS), the mean error (ME) and the mean absolute error (MAE). The model calibrations indicated a reasonably match between observed and calculated hydraulic heads with RMS error of 10.7m. The calibrated steady-state groundwater flow of this study was able to reasonably simulate the measured heads. Beside this, the contour map of the simulated heads showed a flow direction which is in agreement with the conceptual model flow direction.

7.2.1. Recharge

Although estimating the area's groundwater recharge is one of the objectives of the study, it is the most difficult of all measures in the evaluation of groundwater resources. It requires modelling the interaction between all of the important processes in the hydrological cycle such as infiltration, surface runoff, evapotranspiration and groundwater level variations. For this study, it was even more difficult to estimate the recharge as there were not enough data and no discharge measurements. In this study to estimate the recharge both CMB method and inverse modelling were used. As described in section 4.3, the main sources of recharge to the groundwater are the inflow from the hills and the direct rainfall. Chloride mass balance method was used to estimate the groundwater recharge from

both sources. The average precipitation in the Raya Valley between 1996 and 2005, 724mmy^{-1} was used to estimate the direct recharge. The uncertainties associated with the chloride mass balance method could be related to the uncertainties of the measured chloride content both in rainfall and groundwater, due to errors in measured rainfall amount, the estimation of the inflow amount and its chloride content measurement.

The estimated groundwater recharge from CMB method was used as initial value for the modelling and the model calibrated recharge was then compared with the CMB estimated values (Table 7.1). As streams in the study area were not gauged during the period of the model simulation there was no stream stage data to compare with the calibrated recharge volumes derived from the modelling. The model calibrated recharge rate of the valley was 124Mm^3y^{-1}, while the chloride mass balance method showed that a recharge of 126Mm^3y^{-1}. Hence, the recharge estimated by chloride mass balance method agrees well with the recharge estimated by the model calibration. The groundwater recharges estimated from the model and from the CMB method for the entire Raya Valley and for the two sub-basins were summarized in Table 7.1.

Table 7.1 Summary of the estimated recharge values

	Groudwater recharge (Mm^3y^{-1})	
Area	CMB	Model
Mohoni	46	38
Alamata	80	86
Raya Valley	126	124

As is shown in Table 7.1 the estimated recharge for Mohoni sub-basin using the CMB method was most likely over estimated. This can indicate that the assumption of the inflow from the highlands as 10% of the rain that falls on the source area was over estimated for this sub-basin. However, the overall estimation of the recharge for the Raya Valley using the CMB method and the modeling was almost in agreement. The groundwater recharge was previously estimated as 129Mm^3y^{-1} by Dessie (2003) by applying a water balance method.

7.3. Hydraulic conductivity

The hydraulic conductivity values for the Raya Valley aquifer were obtained from pumping tests data analysis. The tests were performed primarily in order to evaluate well properties rather than aquifer properties, and obtained values may be in accurate. In this study, the limited data set for hydraulic conductivity was certainly a problem when defining this parameter and its variations within the area. In some part of the model area, the hydraulic conductivity has not been investigated, which adds to the uncertainty of the distribution of this parameter.

The horizontal hydraulic conductivity of the model domain was assumed to be higher in the western part and lower towards the centre of the valley. There are some borehole data to ascertain this assumption in the Alamata sub basin, but not over the entire model area. In the calibrated model, the hydraulic conductivity became high along the Sulula River zone and it didn't clearly show the trend of the spatial distribution of the hydraulic conductivity in the entire model domain. This can be due to

the uncertainty, less distributed and limited data of the hydraulic conductivity values. Beside this, as previously discussed, water levels were only measured in some part of the model area. This means that values in hydraulic conductivity outside this area can be changed significantly without affecting the calibration criterion for head values. The hydraulic conductivity obtained from the pumping test data analysis shows high spatial variation. Thus it was tried to optimize the hydraulic properties during the calibration process using the calibration target (hydraulic heads) considering the reasonable range of values from the pumping test data analysis and from literature. The hydraulic conductivity value reported from the well pumping test result ranges from 1 to 39md^{-1}. Whereas the model calibrated hydraulic conductivity ranges from 1 to 47md^{-1}.

Groundwater flow system

Groundwater flow system is a set of flow paths which uses for constructing groundwater flow direction. The flow system indicates the direction of the recharge and discharge areas. Hence, it is essential in the conceptualization of how and where water originates in the groundwater flow system and how and where it leaves the system, which in turn is vital to the development of an accurate model. The head measurements were used to establish initial conditions for the numerical groundwater modelling and for model calibration.

The depth to water below ground level varies between 20 and 60 meters in the Mohoni sub-basin and between 0 and 50 meter in the Alamata sub-basin. On the foot hills of the mountains the depth of water decreases. Figure 5.13 shows the calibrated model-simulated groundwater level contours. It shows that the flow converges from all sides towards the south-east of the model area i.e. towards the outlet. The general hydraulic gradient in the valley area follows the surface topography and the gradient is towards south-east which is in agreement with the flow system defined in the conceptual model of the area. The maps of spatial distribution of the initial hydraulic heads and model simulated hydraulic heads are shown in Figures 7.1.

7.4. Sensitivity analysis

The sensitivity analysis is useful in determining which parameters most influence model results. These parameters should be emphasized in future data collection attempting to improve model accuracy. According to the sensitivity analysis the horizontal hydraulic conductivity and recharge have significant effect on water level, and the model is sensitive to both parameters. The model is highly sensitive with decrease of the calibrated recharge and hydraulic conductivity values and relatively less sensitive with increase of the recharge and hydraulic conductivity values which produced lower RMS errors.

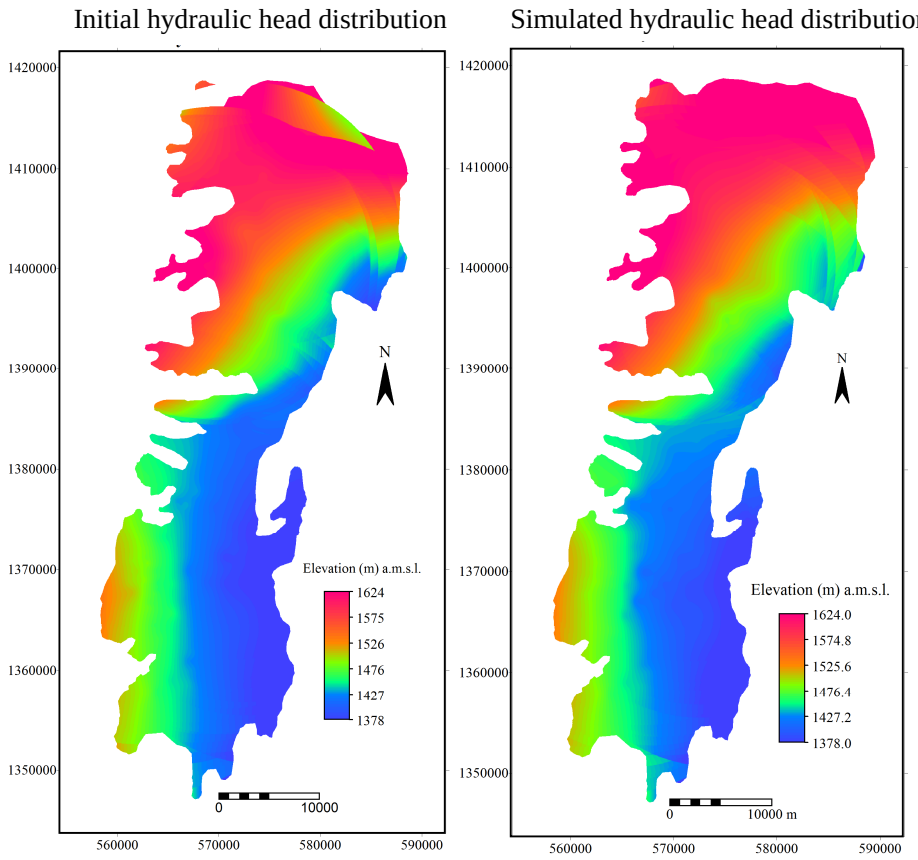

Figure 7.1 Initial and simulated hydraulic head distribution

7.4.1. Water budget of the model domain

Preparation of a water budget involves the identification and quantification of all flows in and out of the groundwater system. The water budget of the model area is one of the ways to quantitatively evaluate the movement of groundwater through an aquifer system. In this study the water balance was established based on the modelling water budget tool in MODFLOW. The summary of the entire domain water budget showed that the model calculated inflow and outflow terms are in balance (Table 5.3). The drain and the groundwater evapotranspiration are the outflow components of the water budget and were estimated by the steady state model as 92mmy^{-1} and 22mmy^{-1} respectively, while the model calibrated recharge rate of the valley was 114mmy^{-1} (Table 5.4). However, groundwater evapotranspiration values in numerical models are usually a rather rough approximation of what actually occurs in nature. As evapotranspiration loss from the saturated zone cannot be measured directly there is no comparison between simulated evapotranspiration losses and measured losses.

7.4.2. Calibrated numerical model

There are indications that the overall result of the calibrated steady-state groundwater flow model developed in this study is realistic.

- The deviation of the simulated heads from the observed heads is within the pre-established calibration target.
- Groundwater flow directions simulated by the model are reasonable and in concordance with the conceptual model.
- The model calculated inflow and outflow terms are balancing.

However, there are limitations and uncertainties in the steady-state groundwater flow model as was described in section 7.6.

7.5. Pumping Scenario

The model was run for pumping scenario and the result was analysed. In scenario-one a total amount of 8.3 x 10^{+4} m^3d^{-1} was abstracted which resulted in an average decline of water level by 22m. Whereas, in scenario-two, a total amount of 1.7 x 10^{+5} m^3d^{-1} was discharged and this also resulted in an average decline of the water level by 50m. These average declines in water level are mostly for the wells that are found in the irrigation area. The influence of the abstraction becomes less away from the area.

The contour map of the simulated head for both pumping scenarios (Figure 6.2) showed that the regional flow direction of the model remains the same, except local effects around the irrigation area where the contour lines show flow towards the irrigation area. In scenario two the abstraction effect is more pronounced and extends to larger area than scenario one.

7.6. Model limitations

Numerical groundwater flow model have limitations in the representation of the real world system, due to simplifications and assumptions which are used during modelling. The data used in this model, both from previous studies and data collected in the field, were subjected to errors, which affects the model to varying extent. The degree of uncertainty in the model was raised due to the lack of data and poor quality of the data that were available. Errors in the observed data used for parameter identification can also contribute to uncertainty in the estimated values of model parameters. Beside this, the steps in the modelling process such as, converting the real world into conceptual model and the conceptual model into numerical model may each introduce errors. All the available measured hydraulic heads were used for calibration. Hence, no independent measured heads were available to validate the model. Therefore, the model was calibrated but not verified. Hence, the results obtained here should not be interpreted as a perfect simulation, rather as a system response within fairly realistic model input parameters. As a result, the model may not be readily used for detail groundwater management purposes due to the mentioned limitations; instead, the results should be interpreted and applied considering all the limitations and drawbacks associated to the input parameters.

7.7. Discussion of the model

The aim of this modelling study was to gain a better understanding of the groundwater circulation in Raya Valley. As is described in the results, there are still uncertainties remaining with regard to the groundwater flow system in this area. These doubts can only be removed through extended data

collection coupled with continued development of the numerical model. There are, however, some aspects of the system that are better understood through the present study. Most importantly, the groundwater circulation in the area is much more complex than was previously assumed. Horizontal heterogeneity has been discovered and vertical heterogeneity is most likely also present in the aquifer area.

Since the objective of the modelling study is the understanding of the groundwater circulation, flow directions have been emphasized rather than the amount of available water. Over the extent of the model area, the groundwater flows from topographic highs towards the valley floor. However, there was no available data during the study to explain the impact of the tectonic structures in the area and the role of the Hashange Lake which is found on top of the western highlands, which has about 1000m elevation difference with the model area. Moreover, the source of the hot springs in the southeastern part of the area near to the outlet can be linked to the tectonic activities because the area is near to the Afar rift valley system. Its relation to the ground water flow patterns has to be studied further.

The model can be used for analysis of contaminant transport in the future. Given that groundwater flow directions are a crucial aspect of the numerical model, it is clear that more data collection is needed to expand the knowledge relating to boundary conditions of the model domain. Particle tracking programs use the hydraulic heads obtained by a flow model to calculate the velocity of the moving particles, and thus errors in the flow model will affect the accuracy of the calculated particle path lines. However, particle tracking is even more sensitive to errors than are hydraulic heads (Lipfert et al., 2004). Therefore, a model can give good results for hydraulic head distribution and still show significant errors in calculated particle path lines. From the previous discussion, it can be concluded that the numerical model has been developed in the proper direction but still requires an extensive amount of work to ascertain that the groundwater flow system is satisfactorily represented in the model.

8. Conclusions and Recommendations

8.1. Conclusions

This modelling study was initiated for the purpose of obtaining a better understanding of the groundwater flow system in the Raya Valley. The following conclusions can be made from results obtained in this study:

This study laid better foundation for the aquifer's conceptual model which was transferred to the numeric model that has capability to reproduce the field data with comparatively good accuracy. The field data together with the model output can be used to understand the aquifer system under steady state condition. But, there are still many doubts remaining with regard to the groundwater flow system in this area. These doubts can only be removed through extended data collection allowing the model to be refined in greater detail for the better accuracy. It is also necessary to simulate transient conditions and make a thorough validation prior to use for predictions.

The calibrated steady-state groundwater flow model of this study was able to reasonably simulate the measured heads. Furthermore, the calibrated model-simulated groundwater level contours showed that the general hydraulic gradient in the valley area follows the surface topography and the gradient is towards southeast which is in agreement with the flow system defined in the conceptual model of the area.

The estimation of the groundwater recharge using CMB method and the inverse modeling are in good agreement. The annual average groundwater recharges of the Raya Valley estimated by CMB method and by the inverse modeling are about 116mm and 114mm respectively. Recharge of the area also showed high spatial variation. High recharge zones were identified in the western part of the study area. The model calculated inflow and outflow terms are in balance. The drain and the groundwater evapotranspiration are the outflow components of the water budget and were estimated by the steady state model as $92 mm y^{-1}$ and $22 mm y^{-1}$ respectively.

According to the analysis of field data together with the pumping test data analysis, the aquifer of the valley is not a fully unconfined system. It appears to be locally semi-confined, presumably due to clay horizons. Based on the sensitivity analysis the horizontal hydraulic conductivity and recharge have significant effect on water level, and the model is sensitive to both parameters.

The steady-state model with pumping scenarios showed that groundwater abstraction of $8.3 \times 10^{+4}$ $m^3 d^{-1}$ and $1.7 \times 10^{+5}$ $m^3 d^{-1}$ in the irrigation area of the Alamata sub-basin resulted in a groundwater level decline of up to 22 and 50 meters in the irrigation area respectively. The contour map of the simulated head for both pumping scenarios showed that the regional flow direction of the model remains the same and the effect of the irrigation decreases away from the irrigation area.

The water sample analysis of the previous and current studies showed that the water in the study area is either, Ca- Mg, Mg-Ca, Mg - Na, Na - Ca/Mg or Ca - Na bicarbonate types. The conductivity in the area ranges from 412μScm^{-1} to 2800 μScm^{-1}. Considering only the boreholes, the conductivity ranges from 412μScm^{-1} to 1740 μScm^{-1}. The conductivity increases from the western escarpment towards the valley floor. The SAR values of the groundwater which is important for classifying irrigation water, ranges between 0.01 and 2.9.

The study concludes that the steady-state numerical model together with the spatial and statistical techniques available in GIS and RS can be used to estimate aquifer properties in the area even with a minimum amount of field data and are able to substantially improve our understanding of the groundwater flow system in response to recharge and abstractions.

8.2. Recommendations

This study can be a good start for the regional groundwater flow modelling of the entire Raya Valley. For detailed modelling in the future, further refinement of the model is possible, which is expected to improve the accuracy of the model, if additional data and further extensive field-based observations become available.

The model was calibrated but not verified. Hence, the results obtained here should not be interpreted as a perfect simulation, rather as a system response within fairly realistic model input parameters. As a result, the model should be applied with caution for detailed groundwater management purposes. The results should be interpreted and applied considering all the limitations and drawbacks associated with the input parameters.

This study has laid the foundation for future detailed predictive transient model development. However, achieving a well-calibrated transient groundwater flow model requires filling the data gaps and collecting temporal data. It is essential to determine distributed multi-temporal recharge for transient model by accounting for all influencing hydro-climatic factors.

Evaluation of hydraulic conductivity and survey of aquifer thickness should be extended to represent the entire area. The Hydraulic conductivity to which the model is highly sensitive requires better characterization. To estimate the hydraulic characteristics of the valley a number of pumping wells and observation wells are required. Group testing of the pumping wells and observation wells should be performed simultaneously and the response of the aquifer should be recorded and analyzed, so as to provide data for transient simulation such as specific yield, storage coefficient, etc. Recharge, as the most sensitive parameter of the model, should also be estimated in a more precise way, because when converting to transient conditions it is necessary to have knowledge on spatial and temporal distribution of recharge.

To improve calibration values, groundwater level and abstraction rates should be monitored at a set of monitoring wells that are properly distributed in the area. Once an improved steady-state model is obtained and the necessary data are obtained, a transient model for the pumping scenario should be

made for better predictions of pumping effect and for better recharge modelling, as recharge and groundwater outflow are strongly time dependent.

When an improved numerical model is obtained, particle tracking should be added and capture zones for selected wells within the model domain should be delineated. This requires further field work and pumping tests at each well selected for delineation of capture zones.

Stream flow along the outlet (Sulula River) and at other main streams should be gauged, as it is useful to establish the basin water balance and identify where, and how much, the rivers gain from and lose to groundwater and the hydraulic conductivity of the streambeds in the area should be determined in order to determine drain conductance and its variations over the model area.

For further groundwater resource development plans in the valley, it is important to take into account the balance between the groundwater recharge and the intended abstraction rates both for irrigation and domestic water supply to ensure the sustainability of the resource in the valley.

In order to increase the abstraction rate with reasonable drawdown in the irrigation area, it is recommended to use additional wells from outside the irrigation area, and the abstraction rate of each well should be determined based on their safe yield from the pumping test data analysis.

Regarding the water quality, as it is shown in the hydrochemistry analysis of this study there are some indications that the groundwater is being contaminated. Beside this, as the Raya Valley is being developed for large scale irrigation project, care should be taken related to the groundwater contamination. Because, many fertilizers contain nitrogen, which, if misused, can enter the groundwater and can cause health problems. Over fertilizing and over-irrigation can cause nitrogen to leach, through the soil to the groundwater. Pesticides can also enter groundwater supplies in the same way. Therefore, it is better to make sure that the fertilizers and pesticides to be applied are appropriate for the situation. Proper disposal of fertilizers and pesticides is critical for maintaining good water quality. It is better to use non-toxic approaches to pest control whenever possible.

Human and animal wastes contain bacteria and nutrients and can contaminate nearby water supplies. Animal lots that are not properly constructed and maintained, have poor drainage, or are located where the water table is close to the surface can cause groundwater contamination. Allowing animals to graze in or directly next to a water body can also have serious impacts on water quality. Allowing animal access to drinking water well can result in waste getting into well. Hence, it is better keeping livestock away from drinking shallow water wells.

References

Allen, G.R., Pereira, L.S., Raes, D. and Smith, M., 1998 Crop Evapotranspiration-Guidelines for computing crop water requirements. FAO Irrigation and Drainage Paper 56.FAO, Rome, Italy, pp. 300.

Anderson, M.P. and Woessner, W.W., 1992. Applied groundwater modeling : simulation of flow and advective transport. Academic Press, San Diego etc., 381 pp.

Bear, J., 1979. Analysis of flow against dispersion in porous media -- Comments. Journal of Hydrology, 40(3-4): 381-385.

Cashman, P.M. and Preene, M., 2001. Groundwater lowering in construction, a practical guide. Spon Press, 476 pp.

Chiang, W.H. and Kinzelbach, W., 2001. Processing MODFLOW (version 5.3), A simulation system for modeling groundwater flow and pollution.

Chiang, W.H., Kinzelbach, W. and Rauch, R., 1998. Aquifer Simulation Model for WINdows ASMWIN 6.0 : groundwater flow and transport modeling, an integrated program. Gebruder Borntraeger Berlin etc., 137 pp.

Dessie, N.H., 2003. Aquifer characterization and hydrochemical investigation in Raya Valley, Northern Ethiopia, PhD Thesis, Institute of Applied Geology, Universität für Bodenkultur Wien.

Eriksson, E., 1985. Principles and applications of hydrochemistry. Chapman & Hall. London, pp. 187.

Fetter, C.W., 2001. Applied hydrogeology + Visual Modflow, Flownet and Aqtesolv student version software on CD - ROM. Prentice Hall, Upper Saddle River, 597 pp.

Foster, S., 1998. Groundwater: assessing vulnerability and promoting protection of a threatened resource. Proceedings of the 8th Stockholm Water Symposium, 10–13 August, Sweden, pp. 79–90.

Freeze, R.A. and Cherry, J.A., 1979. Groundwater. Prentice-Hall, Englewood Cliffs, 604 pp.

Gamachu, D., 1977. Aspects of climate and water budget in Ethiopia. Addis Ababa University Press, Addis Ababa.

Gebrerufael Hailu, K., 2008. Groundwater resource assessment through distributed steady - state flow modeling, Aynalem Wellfield, Mekele, Ethiopia, ITC, Enschede, 106 pp.

Gieske, A.S.M., 1992. "Dynamic of groundwater recharge" case study in Semi arid, Botswana, PhD thesis. Free University of Amsterdam, Amsterdam, The Netherlands, pp. 245.

Halefom Shiferaw, B., 2006. Groundwater Resources Potential Assessment in Alamata Sub-basin, Northern Ethiopia. MSc. thesis, UNESCO-IHE Institute, Delft, 105 pp.

Halford, K.J., Weight, W.D. and Schreiber, R.P., 2006. Interpretation of Transmissivity Estimates from Single-Well Pumping Aquifer Tests, Montana Tech of The University of Montana. 44: 467-471.

Hounslow, A.W., 1995. Water quality data : analysis and interpretation. Boca Raton etc.: CRC Lewis.

Jha, M., Chowdhury, A., Chowdary, V. and Peiffer, S., 2007. Groundwater management and development by integrated remote sensing and geographic information systems: prospects and constraints. Water Resources Management, 21(2): 427-467.

Jyrkama, M.I. and Sykes, J.F., 2007. The impact of climate change on spatially varying groundwater recharge in the grand river watershed (Ontario). Journal of Hydrology, 338(3-4): 237-250.

Kazmin, V., 1975. Explanation of geological map of Ethiopia. Geological Survey of Ethiopia, Addis Ababa.

Kruseman, G.P. and de Ridder, N.A., 1992. Analysis and evaluation of pumping test data. International Institute for Land Reclamation and Improvement /ILRI, Netherlands, 377 pp.

Lakshmi Prasad, K. and Rastogi, A.K., 2001. Estimating net aquifer recharge and zonal hydraulic conductivity values for Mahi Right Bank Canal project area, India by genetic algorithm. Journal of Hydrology, 243(3-4): 149-161.

Lerner, D.N., Issar, A.S. and Simmers, I., 1990. Groundwater recharge : a guide to understanding and estimating natural recharge : International Association of Hydrogeologists. International Contributions to Hydrogeology : IAH International Association of Hydrogeologists;8. Heise, Hannover, 345 pp.

Lipfert, G., Tolman, A.L. and Loiselle, M.C., 2004. Methodology of delineating wellhead protection zones in crystalline bedrock in maine. Journal of the American Water Resources Association, 40(4): 999-1010.

McDonald, M.G. and Harbaugh, A.W., 1988. A Modular Three-dimentional finite-difference groundwater flow model. . Techniques of water Res. Invests. of the U.S. Geol. Survey, Book 6, Ch. A1:, 586 pp.

Mengesha, T., Tadios, C., and and Workneh, H., 1996. Explanation of the geological map of Ethiopia, Ethiopian Geological Survey, Addis Ababa.

REST, 1996. Raya valley development study project, phase I (reconnaissance phase report). Relief Society of Tigray, Tigray National Regional Government. .

RVDP, 1997. Raya Valley hydrogeological study phase II feasibility draft report. Raya Valley Development study Project Tigray National Regional Government.

Sharda, V.N., Kurothe, R.S., Sena, D.R., Pande, V.C. and Tiwari, S.P., 2006. Estimation of groundwater recharge from water storage structures in a semi-arid climate of India. Journal of Hydrology, 329(1-2): 224-243.

Simmers, I., 1988. Estimation of natural groundwater recharge. NATO ASI Series C: Mathematical and Physical Sciences;222. D. Reidel, Dordrecht etc., 510 pp.

Simmers, I., Hendrickx, J.M.H., Kruseman, G.P. and Rushton, K.R., 1997. Recharge of phreatic aquifers in semi - arid areas. International Contributions to Hydrogeology : IAH International Association of Hydrogeologists;19. Balkema, Rotterdam etc., 277 pp.

Todd, D.K., 2005. Groundwater hydrology. Wiley, Hoboken, NJ, 636 pp.

WWDSE, 2008a. Analysis And Evaluation of Aquifer Tests and Safe Yield Estimation of Production Wells In Raya Valley Plain, Raya Valley Pressurized Irrigation Project Final Report, Water Works Design and Supervision Enterprise in association with Concert Engineering & Consulting P.L.C. The Federal Democratic Republic of Ethiopia, Ministry of Water Resources, Addis Ababa, Ethiopia

WWDSE, 2008b. Raya pressurized irrigation project feasibility study final Volume. Water Works Design and Supervision Enterprise in association with Concert Engineering & Consulting P.L.C Federal Democratic Republic of Ethiopia, Ministry of Water Resources, Addis Ababa, Ethiopia.

Yeh, H.-F., Lee, C.-H., Chen, J.-F. and Chen, W.-P., 2007. Estimation of groundwater recharge using water balance model. Water Resources, 34(2): 153-162.

Yongxin, X. and Beekman, H.E., 2003. Groundwater recharge estimation in southern Africa. United Nations Educational Scientific and Cultural Organization (UNESCO), Paris, 207 pp.

Appendices

Appendix 1 Meteorological data

Appendix1.1. Monthly rainfall data

Monthly rainfall (mm) at Alamata station

Year	Jan	Feb	Mar	Apr	May	Jun	Jul	Aug	Sep	Oct	Nov	Dec	Annual
1996	133	0	69	123	115	25	77	250	36	8	58	0	895
1997	46	0	125	27	29	22	87	54	72	192	139	0	792
1998	179	23	26	35	20	0	348	272	64	18	0	0	984
1999	44	0	21	9	7	1	211	432	67	55	0	0	847
2000	0	0	10	44	74	0	246	450	68	15	83	73	1063
2001	0	0	158	13	30	17	225	244	25	10	10	3	733
2002	98	0	18	112	8	4	73	214	46	14	0	90	675
2003	76	70	42	94	25	13	112	234	23	0	0	67	754
2004	33	16	40	168	14	50	117	243	41	8	21	20	770
2005	21	1	110	132	66	24	142	167	33	6	0	0	702
Mean	63	11	62	76	39	15	164	256	47	32	31	25	821

Monthly rainfall (mm) at Waja station

Year	Jan	Feb	Mar	Apr	May	Jun	Jul	Aug	Sep	Oct	Nov	Dec	Annual
1996	20	0	83	121	166	26	94	195	54	15	48	5	827
1997	10	0	90	20	27	4	60	55	7	230	79	0	581
1998	76	31	47	27	38	0	311	345	92	8	0	0	975
1999	41	0	71	36	4	40	92	324	47	0	1	43	699
2000	74	0	0	56	19	7	154	259	7	37	30	8	651
2001	0	0	60	20	26	23	150	197	37	10	0	0	523
2002	63	0	22	64	0	7	65	158	55	0	0	82	516
2003		61	42	93	0	8	113	329	51	0	1	43	740
2004	32	44	31	88	6	22	50	113	25	4	43	8	465
2005	0	8	17	134	88	7	148	169	21	1	0	0	593
Mean	35	14	46	66	37	14	124	214	40	30	20	19	657

Monthly rainfall (mm) at Kobo station

Year	Jan	Feb	Mar	Apr	May	Jun	Jul	Aug	Sep	Oct	Nov	Dec	Annual
1996	79	0	31	75	133	53	147	205	67	18	64	0	872
1997	0	0	43	58	48	52	111	94	37	169	49	0	660
1998	54	32	24	39	12	4	326	312	51	6	0	0	860
1999	316	226	2	12	48	34	0	20	107	25	0	0	790
2000	1	0	2	76	42	5	227	268	49	88	24	83	865
2001	0	0	71	19	16	2	231	220	98	8	4	2	671
2002	5	0	0	0	13	3	100	296	117	16	0	67	616
2003	41	33	35	66	33	11	138	248	42	0	0	43	689
2004	30	0	28	88	3	26	116	162	9	74	36	10	583
2005	8	0	34	158	126	3	125	191	23	9	65	0	742
Mean	53	29	27	59	47	19	152	202	60	41	24	21	735

Monthly rainfall (mm) at Korem station

Year	Jan	Feb	Mar	Apr	May	Jun	Jul	Aug	Sep	Oct	Nov	Dec	Annual
1996	36	1	98	242	165	68	137	281	63	11	73	0	1175
1997	10	2	98	51	93	64	172	56	59	323	164	1	1091
1998	160	39	27	28	80	12	397	356	212	46	0	0	1356
1999	66	0	3	50	13	32	235	350	112	45	2	0	908
2000	0	0	4	48	76	9	318	321	91	133	66	94	1159
2001	2	3	130	22	36	51	283	380	62	13	2	13	998
2002	65	1	34	107	16	3	137	229	90	8	0	93	782
2003	13	24	74	75	24	20	168	381	78	2	4	30	892
2004	14	6	41	55	2	54	144	249	66	35	22	10	697
2005	8	0	106	223	163	28	253	298	41	37	0	0	1157
Mean	37	8	61	90	67	34	224	290	87	65	33	24	1022

Monthly rainfall (mm) at Chercher station

Year	Jan	Feb	Mar	Apr	May	Jun	Jul	Aug	Sep	Oct	Nov	Dec	Annual
1996	143	14	48	25	93	370	91	116	46	7	67	0	1020
1997	6		111	67	32	5	112	50	23	198	79	0	684
1998	21	55	4	37	62	265	91	207	53	3	0	1	799
1999	22	180	0	63	42	1	105	511	74	13	0	1	1012
2000	1	10	7	26	96	0	116	329	57	71	36	2	751
2001	0	67	40	99	26	2	114	315	112	4	8	1	788
2002	11	1	14	34	20	0	114	98	63	25	0	8	388
2003	45	7	21	29	46	100	128	199	42	0	0	2	619
2004	50	1	44	13	28	60	100	95	24	18	17	2	452
Mean	33	42	32	44	49	89	108	213	55	38	23	2	724

Monthly rainfall (mm) at Maichew station

Year	Jan	Feb	Mar	Apr	May	Jun	Jul	Aug	Sep	Oct	Nov	Dec	Annual
1996	9	1	123	146	141	66	117	246	42	4	57	0	952
1997	16	0	52	59	38	83	166	64	64	206	80	0	828
1998	65	33	35	39	116			214	223	11	0	0	737
1999	45	0	11	22	16	12	176	253	78	109	0	2	725
2000	0	0	6	18	65	12	195	194	126	151	61	75	903
2001	0	2	93	9	35	26	212	283	84	25	0	11	780
2002	84	0	34	68	41	21	67	188	93	19	0	34	649
2003	24	38	93	194	13	14	107	325	32	5	2	18	864
2004	13	5	20	128	1	60	141	247	27	38	3	0	683
2005	6	3	51	61	98	18	120	219	23	22	20	20	660
Mean	26	8	52	74	56	35	145	223	79	59	22	16	778

Monthly rainfall (mm) at Zoble station

Year	Jan	Feb	Mar	Apr	May	Jun	Jul	Aug	Sep	Oct	Nov	Dec	Annual
1998							260	395	44	46	0	0	
1999	45	0	55	52	19	22	162	337	122	83	0	2	897
2000	12	0	7	107	74	11		359	48	168	78		863
2001	35	2	63	7	112	22	217				10	3	470
2002	131	8	23	147	46	6	286	286	933				
2003	38	72	122	38	9		234	387	71				971
2004	1	34	24	220	0	31	106	235	46	100	69	5	871
2005			80	109	84	1	172	137	42				626
Mean	44	19	53	97	49	16	205	305	187	99	31	2	783

Monthly rainfall (mm) at Mohoni station

Year	Jan	Feb	Mar	Apr	May	Jun	Jul	Aug	Sep	Oct	Nov	Dec	Annual
1996	13	0	8	152	45	12	0	90	27	1	87	0	435
1997	162	0	44	9	28	64	189	99	0	66	56	0	717
1998	1	17	20	15	33	1	7	229	25	0	0	6	354
1999	32	0	107	3	36	1	36	237	22	22	0	0	496
2000	0	0	29	32	30	16	271	283	4	0	176	23	864
2001	30	0	27	1	4	65	152	126	27	0	25	1	458
2002	1	0	16	41	8	1	12	150	14	0	0	2	245
2003	48	36	35	51	15	0	22	150	100	0	0	0	457
2004	18	1	91	188	0	33	0	139	92	95	3	5	665
Mean	34	6	42	55	22	21	77	167	35	20	39	4	521

Monthly rainfall (mm) at Muja station

Year	Jan	Feb	Mar	Apr	May	Jun	Jul	Aug	Sep	Oct	Nov	Dec	Annual
1996	17	5	124	99	98	46	206	275	68	2	52	9	1001
1997	7	12	94	41	39	96	164	163	21	41	61	13	751
1998	13	0	14	22	68	0	371	273	14	5	0	13	793
1999	15	0	0	31	5	4	313	267	50	26	0	5	715
2000	0	0	9	82	4		213	272	36	17	45	21	699
2001	0	0	12	77	24		285	310	5	0	0	3	715
2002	37	23	63	15	4	3	196	158	12	0	0	37	548
2003	0	21	38	24	0	80	194	247	31	0	14	0	648
2004	0	20	20	44	0		160	208	0	18	0	3	473
2005	0	0	44	56	123		257	191	34	0	0	0	704
Mean	9	8	42	49	36	38	236	236	27	11	17	10	705

Appendix1.2. Monthly maximum temperature

Monthly T_{max} (^{o}C) at Alamata station

Year	Jan	Feb	Mar	Apr	May	Jun	Jul	Aug	Sep	Oct	Nov	Dec	Annual
1996		29.5	30.9	30.8	30.8	32.6	32.4	31.2	31.6	31.2	29.0	28.4	30.8
1997	27.4	29.9	28.9	30.3	34.4	34.5	33.1	33.9	33.3	29.8	28.6	28.7	31.4
1998	27.0	27.7	30.5	34.5	34.5	36.1	31.8	28.8	30.7	30.8	30.4	29.8	31.4
1999	28.8	32.4	31.0	34.1	35.8		30.9	30.1	30.1	30.1	30.0	29.2	31.4
2000	29.7	31.6	32.8	34.2	35.2	36.8	33.2	30.5	30.5	29.3	29.0	26.8	31.8
2001	27.5	30.4	30.5	31.7	34.1	33.8	31.2	28.9	29.6	30.0	27.9	27.5	30.5
2002	24.7	28.0	29.8	30.4	33.7	34.3	33.6	30.6	29.4	30.7	28.8	26.3	30.5
2003	25.8	28.5	29.0	30.1	33.2	34.2	31.4	29.4	30.1	29.9	28.4	26.0	30.0
2004	27.1	27.1	29.5	28.6	33.4	32.8	31.9	29.6	29.5	29.1	28.4	26.3	29.7
2005	25.9	29.4	29.6	29.8	30.3	33.4	31.0	29.9	30.0	29.3	28.4	27.2	29.9
Mean	27.1	29.4	30.3	31.5	33.5	34.3	32.1	30.3	30.5	30.0	28.9	27.6	30.7

Monthly T_{max} (^{o}C) at Waja station

Year	Jan	Feb	Mar	Apr	May	Jun	Jul	Aug	Sep	Oct	Nov	Dec	Annual
1996	27.4	30.9	30.3	30.6	30.6	33.0	32.0	31.4	32.0	31.4	29.0	28.1	30.6
1997	27.6	29.5	29.7	30.6	33.7	33.9	33.1	33.6	34.6	30.3	28.6	29.0	31.2
1998	27.9	29.2	29.8	31.4	33.6	37.4	31.5	29.4	30.3	30.2	29.3	29.1	30.8
1999	27.6	30.5	29.2	32.7	34.3								
2000		27.0	27.7	26.8	28.5	29.6	26.5	24.7	24.7	23.3	23.4		26.2
2001	20.9	23.0	23.4	24.6	27.1						29.0	29.4	
2002	29.8	29.8	31.7	34.0	35.2		35.3	30.6	33.1	31.3	29.7	28.7	31.7
2003		29.9	30.5	31.8	33.9	36.4	34.0	30.8	31.6	31.5	30.0	27.9	31.7
2004	29.2	28.9	30.0	30.1	34.2	34.1	33.3	31.7	31.6	29.9	29.7	26.8	30.8
2005	28.0	31.1	31.1	32.0	31.6	35.9	32.3	31.1	32.2	30.4	29.4	27.9	31.1
Mean	27.3	29.0	29.3	30.5	32.3	34.3	32.2	30.4	31.3	29.8	28.7	28.4	30.0

Monthly T_{max} (^{o}C) at Kobo station

Year	Jan	Feb	Mar	Apr	May	Jun	Jul	Aug	Sep	Oct	Nov	Dec	Annual
1996				30.4	30.1	32.1	31.7	30.2	30.4	29.7	27.1	26.1	29.8
1997	25.4	28.0	29.3	30.3	33.1	33.4	31.9	31.7	32.4	27.9	27.1	27.2	29.8
1998	25.4	26.7	29.1	32.4	33.5	36.0	30.9	28.7	29.8	29.3	28.3	27.6	29.8
1999	26.9	30.4	29.0	32.1	34.2	35.3	30.5	29.7					31.0
2000		29.2	30.4	31.2	33.0	34.7	32.1	30.3	30.5	28.6	27.4	26.1	30.3
2001	25.5	28.1	28.7										27.4
2002					34.3	35.0	34.0	30.9	29.9	30.1	29.5	26.3	31.3
2003	25.9	29.0	30.2	30.9	34.0	34.6	32.1	30.0	30.8	30.3	29.2	26.8	30.3
2004	27.6	28.0	30.2	30.8	34.6	34.2	32.7	31.5	31.9	30.0	29.7	27.1	30.7
2005	26.9	30.2	31.3	31.6	31.7	35.0	32.7	32.2	30.7	30.8	29.4	28.3	30.9
Mean	26.2	28.7	29.8	31.2	33.2	34.5	32.1	30.6	30.8	29.6	28.5	26.9	30.1

Monthly T_{max} (^{o}C) at Korem station

Year	Jan	Feb	Mar	Apr	May	Jun	Jul	Aug	Sep	Oct	Nov	Dec	Annual
1996	19.0	22.1	22.4	22.3	22.4	23.7	22.8	23.5	24.5	23.9	21.2	19.9	22.3
1997	19.8	21.6	22.3	22.4	24.9	24.7	23.3	24.1	24.9	21.4	21.0	21.1	22.6
1998	19.7	20.8	22.1	24.0	24.4	26.1	22.5	21.9	23.3	21.5	20.1	19.9	22.2
1999	19.3	22.3	21.7	24.2	25.9	27.3	22.0	22.7	24.3	25.1	24.6	21.5	23.4
2000	21.6	22.4	23.0	23.5	25.3	27.2	22.9	21.6	22.2	22.1	20.0	18.7	22.5
2001	18.0	20.3	20.3	22.5	24.4	24.5	22.7	21.6	22.1	21.3	19.6	19.9	21.4
2002	17.9	20.5	21.6	22.5	25.6	26.2	25.2	22.4	21.8	22.1	21.7	20.1	22.3
2003	20.3	22.4	22.4	22.6	24.6	25.5	22.4	21.7	22.3	21.4	20.9	19.4	22.2
2004	21.1	20.8	22.2	22.8	26.1	25.1	23.5	22.6	23.0	21.4	20.9	19.5	22.4
2005	19.9	22.9	22.7	22.8	23.0	25.3	22.8	23.2	23.2	22.1	21.1	20.3	22.4
Mean	19.7	21.6	22.1	23.0	24.7	25.6	23.0	22.5	23.2	22.2	21.1	20.0	22.4

Monthly T_{max} (^{o}C) at Maichew station

Year	Jan	Feb	Mar	Apr	May	Jun	Jul	Aug	Sep	Oct	Nov	Dec	Annual
1996	19.0	21.4	21.8	22.1	22.2	23.1	22.4	22.4	23.2	21.7	19.5	18.4	21.4
1997	19.1	21.1	22.2	23.4	24.4	24.9	22.5	22.4	24.2	20.3	19.1		22.1
1998	19.9	19.6	22.1	24.4	21.4	22.4	21.2	20.7	20.2				21.3
1999	19.2	22.8	22.0	24.3	25.8	26.9	20.8	21.4	22.0	20.1	20.8	19.2	22.1
2000	20.5	21.8	23.0	22.9	25.1	26.4	22.8	21.9	22.1	20.3	19.4	18.5	22.1
2001	18.5	21.1	20.7	22.9									
2002	24.1	23.6	25.8	25.4	25.2	23.0	21.8	21.8	21.1	19.3			23.1
2003	20.3	22.4	22.3	23.0	24.8	25.5	23.1	22.3	23.0	21.5	20.8	19.2	22.4
2004	21.2	21.1	22.4	22.1	25.8	24.9			23.0	21.3	21.1	20.0	22.3
2005	19.9	23.1	22.8	23.3	23.4	25.9	22.7	23.2	23.5	21.6	20.6	20.3	22.5
Mean	20.2	21.8	22.5	23.4	24.2	24.8	22.2	22.0	22.5	20.8	20.2	19.3	22.0

Monthly T_{max} (^{o}C) at Zoble station

Year	Jan	Feb	Mar	Apr	May	Jun	Jul	Aug	Sep	Oct	Nov	Dec	Annual
1998	28.0	26.0	27.0	26.0	25.0	24.0							26.0
1999	23.0	27.0	25.0	28.0	10.0	31.0	27.0	26.0	26.0	24.0	24.0	23.0	24.5
2000	23.0	25.0	27.0	28.0	29.0	31.0	27.0	27.0	25.0	23.0			26.5
2001	20.0	23.0	24.0	28.0	29.0	30.0	29.0	23.0	23.0				25.4
2002	21.0	23.0	27.0	28.0	30.0	32.0	28.0						27.0
2003	21.0	25.0	30.0	27.0	28.0								26.2
2004	27.0	27.0	27.0	29.0	30.0	31.0	29.0	28.0	28.0	26.0	25.0	22.0	27.4
2005	25.0	27.0	27.0	30.0	29.0	28.0	28.0	25.0	24.0				27.0
Mean	23.5	25.4	26.8	28.0	26.3	29.6	28.0	25.8	25.2	24.3	24.5	22.5	26.3

Monthly T_{max} (^{o}C) at Mohoni station

Year	Jan	Feb	Mar	Apr	May	Jun	Jul	Aug	Sep	Oct	Nov	Dec	Annual
1996	27.0	30.0	30.0	28.0	30.0	30.0	32.0	27.0	28.0	27.0	26.0	22.0	28.1
1997	28.0	31.0	29.0	27.0	29.0	30.0	30.0	27.0	28.0	26.0	25.0	29.0	28.3
1998	27.0	27.0	24.0	30.0	29.0	30.0	31.0	27.0	28.0	27.0	26.0	27.0	27.8
1999	27.0	31.0	29.0	27.0	28.0	30.0	30.0	26.0	28.0	27.0	26.0	30.0	28.3
2000	28.0	28.0	28.0	27.0	28.0	29.0	32.0	26.0	27.0	27.0	26.0	28.0	27.8
2001	29.0	27.0	25.0	27.0	29.0	30.0	31.0	27.0	27.0	27.0	26.0	19.0	27.0
2002	25.0	27.0	27.0	28.0	28.0	30.0	30.0	27.0	28.0	28.0	28.0	29.0	27.9
2003	26.0	28.0	29.0	28.0	29.0	30.0	30.0	26.0	27.0	26.0	23.0	30.0	27.7
2004	27.0	30.0	30.0	39.0	28.0	29.0	31.0	27.0	27.0	28.0	28.0	30.0	29.5
Mean	27.1	28.8	27.9	29.0	28.7	29.8	30.8	26.7	27.6	27.0	26.0	27.1	28.0

Appendix1.3. Monthly minimum temperature

Monthly T_{min} at Alamata station

Year	Jan	Feb	Mar	Apr	May	Jun	Jul	Aug	Sep	Oct	Nov	Dec	Annual
1996		12.9	16.0	16.4	16.1	16.1	16.7	16.3	15.5	13.9	12.7	11.5	14.9
1997	12.9	12.9	15.8	16.2	17.6	18.6	17.6	17.5	17.0	15.9	16.2	12.8	15.9
1998	14.9	15.0	16.6	17.9	18.1	19.9							17.1
1999	12.4	11.9	13.3	17.3	20.2		18.8	16.7	10.2	5.7	3.9	1.90	12.0
2000	2.3	5.3	6.6	7.9	10.1	11.4	11.6	9.2	8.7	7.9	6.5	6.3	7.8
2001	3.9	6.1	8.3	10.1	12.2	13.9	11.8	10.7	10.4	10.8	7.8	6.9	9.4
2002	9.5	14.4	17.0	17.7	18.6	20.0	19.7	16.7	16.7	15.9	15.4	16.0	16.5
2003	14.3	15.7	17.4	18.0	20.3	20.0	19.4	17.0	17.4	15.9	15.0	12.9	16.9
2004	14.6	8.8	10.1	16.1	18.0	19.5	18.7	17.8	17.1	15.4	15.2	15.1	15.5
2005	14.4	15.3	17.2	17.7	17.9	19.1	18.9	16.3	16.6	15.6	12.0	12.1	16.1
Mean	11.0	11.8	13.8	15.5	16.9	17.6	17.0	15.4	14.4	13.0	11.6	10.6	14.2

Monthly T_{min} at Waja station

Year	Jan	Feb	Mar	Apr	May	Jun	Jul	Aug	Sep	Oct	Nov	Dec	Annual
1996	14.4	12.4	16.2	16.2	15.7	16.6	17.8	17.2	15.2	11.2	10.9	9.0	14.4
1997	12.8	11.6	15.4	15.6	15.7	17.0	17.0	17.5	16.0	16.1	15.6	12.1	15.2
1998	15.2	14.2	16.7	15.3	15.1	17.7	18.4	17.0	15.7	13.8	9.5	6.3	14.6
1999	10.7	9.1	14.4	14.4	16.1								12.9
2000		8.5	11.8	15.5	15.5	16.9	17.5	16.2	15.1	13.1	13.6		14.3
2001	10.4	11.0	11.7	12.2	12.3						9.0	8.4	10.7
2002	11.7	10.4	12.9	17.3	16.6		16.2	15.4	12.1	10.2	9.1	8.1	12.7
2003		10.1	9.9	9.7		16.3	19.3	17.3	15.8	11.3	11.2	10.5	13.1
2004	14.0	12.6	13.2	16.6	13.8	17.1	18.5	20.7	20.6	18.0	15.6	11.6	16.0
2005	13.4	12.4	16.3	14.8	17.0	17.2	17.7	17.0	14.9	10.9	15.5	6.0	14.4
Mean	12.8	11.2	13.8	14.8	15.3	17.0	17.8	17.3	15.7	13.1	12.2	9.0	13.8

Monthly T_{min} at Kobo station

Year	Jan	Feb	Mar	Apr	May	Jun	Jul	Aug	Sep	Oct	Nov	Dec	Annual
1996				17.2	16.5	17.4	18.2	17.5	15.7	12.0	11.7	10.2	15.1
1997	13.2	12.3	15.9	16.2	17.7	18.7	18.5	17.8	16.3	15.5	15.6	11.9	15.8
1998	15.4	15.3	17.2	18.1	17.9	20.7	17.9	17.3	16.1	14.5	10.1	8.4	15.7
1999	11.6	11.1	15.5	16.0	17.5	18.2	17.3	16.2					15.4
2000		10.6	14.1	16.5	16.1	15.9	14.9	11.8	7.1	9.4	7.7	7.2	11.9
2001	7.1	7.4	11.6										8.7
2002					16.9	19.6	19.6	17.6	16.9	13.0	12.1	15.2	16.4
2003	13.5	15.0	16.4	17.0	17.6	19.3	19.9	17.3	16.9	12.6	12.5	11.2	15.8
2004	14.7	13.5	14.4	16.8	16.5	18.3	18.1	17.5	15.5	13.2	12.7	13.9	15.4
2005	13.9	14.1	17.1	17.2	18.1	18.7	18.7	17.8	17.2	13.5	12.5	9.6	15.7
Mean	12.8	12.4	15.3	16.9	17.2	18.5	18.1	16.8	15.2	13.0	11.9	10.9	14.60

Monthly T_{min} at Korem station

Year	Jan	Feb	Mar	Apr	May	Jun	Jul	Aug	Sep	Oct	Nov	Dec	Annual
1996	7.9	5.7	9.9	10.2	7.6	8.5	11.8	12.0	9.2	4.1	4.5	3.2	7.9
1997	5.7	5.7	9.2	8.7	8.7	11.3	12.4	11.4	7.1	8.7	10.0	4.2	8.6
1998	8.5	7.5	9.6	9.3	10.2	9.8	11.9	11.8	10.2	7.0	1.1	-0.6	8.0
1999	3.4	1.7	6.5	7.4	8.6	9.7	11.6	10.6	8.4	6.9	0.4	2.3	6.5
2000	2.5	1.8	5.6	9.5	8.9	10.8	12.3	11.5	8.5	6.8	5.3	4.4	7.3
2001	3.3	3.3	8.5	7.2	9.2	11.8	12.3	11.9	8.2	6.8	2.5	2.0	7.3
2002	6.3	4.5	8.3	8.6	7.1	11.0	11.7	11.1	8.3	4.5	3.0	7.2	7.6
2003	4.3	2.2	3.8	10.1	9.8	11.2	13.1	12.1	9.9	4.1	4.5	2.8	7.3
2004	6.7	5.8	7.4	10.6	7.8	11.3	12.5	12.1	8.0	6.0	5.0	6.2	8.3
2005	6.7	5.8	7.4	10.6	7.8	11.3	12.5	12.1	8.0	6.0	5.0	6.2	8.3
Maen	5.5	4.4	7.6	9.2	8.6	10.7	12.2	11.7	8.6	6.1	4.1	3.8	7.7

Monthly T_{min} at Maichew station

Year	Jan	Feb	Mar	Apr	May	Jun	Jul	Aug	Sep	Oct	Nov	Dec	Annual
1996	8.5	8.4	11	11	11	13	12	13	10	7.7	7.4	6.3	9.94
1997	8	6.9	11	11	12	13	13	12	11	10	10	7	10.41
1998	9.7	9.2	11	12	13	7.3	5.2						9.63
1999	6.5	6.9	9.1	9.9	12	13	10	11	10	9.3	5.3	5.9	9.08
2000	6.1	6.3	8.1	11	12	14	14	12	10	8.6	7.7	6.8	9.72
2001	5.7	6.1	10	9.9	12	13	13	14	12	9.1	5.8	6	9.72
2002	8.1	7.7	10	11	11	14	15	13	9.5	8.1	7.3	9	10.31
2003	7.8	9.2	10.4	11.5	11.7	13.4	13.4	12.7	11.6	7.6	7.1	6.3	10.2
2004	8.9	7.8	9.0	11.7	11.9	13.6	13.6	13.1	10.2	8.1	7.4	7.9	10.3
2005	7.9	8.6	10.7	11.6	12.4	13.8	13.7	13.1	11.6	7.8	4.7	4.7	10.1
Mean	7.7	7.7	10.0	11.1	11.9	12.8	12.3	12.7	10.7	8.5	7.0	6.7	9.9

Monthly T_{min} at Zoble station

Year	Jan	Feb	Mar	Apr	May	Jun	Jul	Aug	Sep	Oct	Nov	Dec	Annual
1996													
1997													
1998	14	13	13	10	4	2							9.33
1999	2	1	4	3	5	5	9	7	6	4	4	2	4.33
2000	1												1.00
2001	8	8	13	11	14	16	16	16	18				13.33
2002	14	15											14.50
2003	10	9.5	8.3										9.27
2004	17	14	16	20	23	21	12	12	8.9	2.3	9.9		14.19
2005	12	13	14.7	14	16	15	13	6.8	4.1				12.07
Mean	9.8	10.5	11.5	11.6	12.4	11.8	12.5	10.5	9.3	3.2	7.0	2.0	9.8

Monthly T_{min} at Mohoni station

Year	Jan	Feb	Mar	Apr	May	Jun	Jul	Aug	Sep	Oct	Nov	Dec	Annual
1996	3	12	13	14	14	15	15	7	15	15	14	12	12.42
1997	17	13	13	14	14	16	15	12	16	13	15	17	14.58
1998	3	12	14	15	16	16	17	13	13	16	12	11	13.17
1999	8	12	12	14	15	16	16	14	16	13	13	14	13.58
2000	3	13	13	14	14	15	18	16	12	13	13	14	13.17
2001	12	13	13	14	14	13	12	15	13	16	14	13	13.50
2002	1	12	12	14	14	16	17	14	14	16	15	16	13.42
2003	1	12	11	14	15	16	16	14	15	14	15	15	13.17
2004	13	13	12	14	14	13	15	15	12	15	15	14	13.75
Mean	6.8	12.4	12.6	14.1	14.4	15.1	15.7	13.3	14.0	14.6	14.0	14.0	13.4

Appendix1.4. Monthly relative humidity (RH) (%)

Monthly relative humidity (%) at Kobo station at 1800

Year	Jan	Feb	Mar	Apr	May	Jun	Jul	Aug	Sep	Oct	Nov	Dec	Annual
1996				46.9	56.3	49.1	53.3	56.8	52.3	43.0	48.4	45.8	50.2
1997	64.5	34.4	43.3										47.4
1998				35.4	30.7	27.0	52.4	63.8	58.9	47.2	33.3	42.9	43.5
1999	56.2	56.9											56.5
2000													
2001													
2002						20.8	32.9	50.0	55.1	38.4	32.8	58.7	41.2
2003													
2004	56.0	42.3	32.9	48.9	21.9	24.2	44.0	55.1	45.5	42.7	36.7	50.6	41.7
2005	53.6	36.6	45.6	38.8	47.4	28.7	46.6	42.3	51.1	37.8	39.2	33.0	41.7
Mean	57.6	42.5	40.6	42.5	39.1	30.0	45.8	53.6	52.6	41.8	38.1	46.2	46.0

Monthly relative humidity (%) at Kobo station at 1200

Year	Jan	Feb	Mar	Apr	May	Jun	Jul	Aug	Sep	Oct	Nov	Dec	Annual
1996		44.0		47.2	56.5	48.6	44.7	50.4	43.8	35.8	35.0	47.0	45.3
1997	58.1	44.0	37.6										46.6
1998		44.0		39.5	33.6	24.3	51.5	60.3	49.7	39.5	35.0	47.0	42.4
1999	56.6	44.0									35.0	47.0	45.6
2000													
2001													
2002		44.0				21.1	29.5	42.6	51.1	30.8	35.0	47.0	36.7
2003													
2004	49.8	44.0	32.6	42.9	22.2	26.4	32.8	44.2	40.8	36.4	35.0	47.0	37.8
2005	51.1	37.3	43.0	39.4	44.3	25.8	41.2	43.6	42.1	36.6	39.0	32.5	39.7
Mean	53.9	43.0	37.7	42.3	39.1	29.2	39.9	48.2	45.5	35.8	35.7	44.6	42.0

Monthly relative humidity (%) at Kobo station at 0600

Year	Jan	Feb	Mar	Apr	May	Jun	Jul	Aug	Sep	Oct	Nov	Dec	Annual
1996	87.0			75.0	86.1	53.0	72.2	84.8	89.1	82.5	79.2	81.2	79.0
1997	88.0	74.1	83.4	75.0		53.0							74.7
1998	87.0			75.0	60.0	53.0	77.0	90.0	93.1	83.3	72.4	76.7	76.7
1999	87.0	83.1		75.0		53.0							74.5
2000													
2001													
2002	87.0			75.0		53.0	66.2	82.4	89.5	78.3	72.0	87.1	75.4
2003													
2004	87.0	82.6	66.8	75.0	50.7	53.0	66.1	79.4	81.8	80.5	75.9	84.0	73.6
2005	84.8	70.3	78.4	72.7	84.7	59.0	71.6	80.8	83.7	77.1	75.2	74.1	76.0
Mean	86.8	77.5	76.2	74.7	70.4	53.9	70.6	83.5	87.5	80.3	75.0	80.6	75.7

Monthly relative humidity (%) at Maichew station

Year	Jan	Feb	Mar	Apr	May	Jun	Jul	Aug	Sep	Oct	Nov	Dec	Annual
1995	53.7	67.3	66.7	73.0	72.3	37.3	65.3	71.3	62.7	55.0	54.7	69.0	62.4
1996	74.7	57.0	70.3	66.0	65.0	51.0	61.0	63.7	55.3	54.3	59.7	58.3	61.4
1997	68.3	52.3	66.3	60.3	51.3	51.0	63.0	58.3	53.7	68.3	76.7	66.0	61.3
1998	80.0	72.3	68.0	54.0	62.0	39.0	71.0	65.7	63.3	52.3	44.0		61.1
1999	59.3	37.3	56.0	44.0	38.0	31.7	66.0	67.3	66.3	72.0	55.3	61.0	54.5
2000	51.3	39.3	43.7	45.3	43.0	35.7	64.3	70.7	64.0	74.0	70.0	68.7	55.8
2001	67.7	53.3	67.7	55.0	52.3	50.0	67.3	72.7	67.0	64.3	59.7	56.7	61.1
2002	76.0	56.3	63.0	56.0	41.0	39.3	50.7	62.3	63.7	57.3	55.0	76.0	58.1
2003	67.0	72.0	58.0	47.0	40.0	38.0	61.0	68.0	64.0	60.0	56.0	70.0	58.4
2004	65.0	56.0	50.0	69.0	34.0	42.0	56.0	66.0	58.0	60.0	60.0	66.0	56.8
Mean	66.3	56.3	61.0	57.0	49.9	41.5	62.6	66.6	61.8	61.8	59.1	65.7	59.1

Monthly relative humidity (%) at Mohoni station

Year	Jan	Feb	Mar	Apr	May	Jun	Jul	Aug	Sep	Oct	Nov	Dec	Annual
1996	53.0	52.0	55.0	51.0	51.0	56.0	79.0	59.0	58.0	47.0	57.0	56.0	56.2
1997	61.0	58.0	51.0	52.0	43.0	31.0	57.0	63.0	74.0	59.0	54.0	55.0	54.8
1998	49.0	56.0	54.0	55.0	52.0	49.0	72.0	53.0	44.0	41.0	56.0	55.0	53.0
1999	58.0	56.0	52.0	57.0	59.0	76.0	79.0	64.0	65.0	58.0	54.0	51.0	60.8
2000	60.0	56.0	52.0	52.0	51.0	69.0	84.0	63.0	58.0	63.0	54.0	54.0	59.7
2001	52.0	57.0	54.0	57.0	50.0	35.0	66.0	97.0	65.0	57.0	50.0	52.0	57.7
2002	51.0	54.0	51.0	53.0	66.0	61.0	52.0	53.0	40.0	42.0	58.0	55.0	53.0
2003	49.0	56.0	53.0	49.0	39.0	55.0	75.0	54.0	61.0	54.0	57.0	56.0	54.8
2004	55.0	56.0	52.0	53.0	56.0	53.0	68.0	57.0	53.0	50.0	59.0	56.0	55.7
Mean	54.2	55.7	52.7	53.2	51.9	53.9	70.2	62.6	57.6	52.3	55.4	54.4	56.2

Appendix1.5. Mean monthly sunshine hours

Mean monthly sunshine hours at Kobo station

Year	Jan	Feb	Mar	Apr	May	Jun	Jul	Aug	Sep	Oct	Nov	Dec	Annual
1996	6.8	5.3	7.9	9.6	9.9	8.5	4.0	5.1	6.8	9.6	9.9	8.8	7.7
1997	8.0	7.3	9.3	6.9	9.4	6.2	3.1	5.1	7.3	9.5	9.7	8.1	7.5
1998	6.3	7.5	8.9	9.5	9.2	6.8	6.7	7.4	6.0	7.1	9.0	7.0	7.6
1999	6.9	4.4	8.7	6.6	9.1	6.3	6.1	6.5	7.0	9.6	10.1	9.3	7.6
2000	9.3	7.2	6.1	7.6	9.1	5.1	5.2	5.1	5.1	8.2	9.3	8.7	7.2
2001	8.0	7.4	8.9	7.9	9.8	8.3	3.4	6.6	7.1	7.9	8.1	7.9	7.6
2002	7.8	8.6	8.7	9.7	6.5	5.7	4.0	5.8	7.7	8.9	9.1	8.5	7.6
2003	8.7	10.2	8.1	9.0	6.8	6.4	8.3	7.1	6.7	7.3	8.6	9.0	8.0
2004	8.1	8.7	9.0	6.8	7.2	6.1	7.3	5.6	6.2	8.1	9.9	9.4	7.7
Mean	7.8	7.4	8.4	8.2	8.6	6.6	5.3	6.0	6.7	8.5	9.3	8.5	7.6

Mean monthly sunshine hours at Maichew station

Year	Jan	Feb	Mar	Apr	May	Jun	Jul	Aug	Sep	Oct	Nov	Dec	Annual
1996	7.4	7.5	6.4	7.7	7.8	7.6	5.8	5.7	7.2	6.6	7.1	7.4	7.0
1997	7.9	8.8	5.5	7.2	8.2	6.2	5.5	6.2	6.7	6.2	6.6	8.4	7.0
1998	5.2	6.3	7.4	8.7	8.7	6.9	4.2	4.3	7.3	8.5	9.0	9.3	7.2
1999	7.4	9.8	7.2	10.2	9.7	7.3	3.9	4.9	7.0	6.0	8.9	7.7	7.5
2000	9.0	9.8	9.7	7.3	9.2	6.3	5.2	5.5	5.9	7.1	7.8	6.3	7.4
2001	4.4	7.9	4.4	6.2	7.2	12.1	4.6	5.0	7.0	7.9	6.9	8.3	6.8
2002	8.2	8.2	7.6	9.4	9.3	6.3	6.1	6.3	6.7	7.8	7.7	6.7	7.5
2003	6.4	8.0	6.3	9.9	9.0	6.0	4.7	4.4	7.3	9.4	8.0	7.9	7.3
2004	6.9	8.0	8.6	7.6	10.5	5.9	5.2	5.4	6.3	8.0	8.3	7.4	7.3
Mean	7.0	8.3	7.0	8.2	8.8	7.2	5.0	5.3	6.8	7.5	7.8	7.7	7.2

Appendix1.6. Mean monthly wind speed (ms^{-1}) at 2m height

Mean monthly wind speed (ms^{-1}) at Kobo station

Year	Jan	Feb	Mar	Apr	May	Jun	Jul	Aug	Sep	Oct	Nov	Dec	Annual
1996	2.6	2.0	2.1	2.0	1.6	1.8	2.1	1.7	1.2	1.3	1.5	1.6	1.8
1997	1.8	2.0	2.1	2.0	2.2	1.9	2.0	1.7	1.6	1.4	1.3	1.4	1.8
1998	1.6	1.7	2.0	2.2	2.0	2.5	2.2	1.6	1.1	1.3	1.4	1.5	1.8
1999	1.6	1.8	2.2	2.1	2.1	2.3	2.0	1.5	0.0	0.0	0.0	0.0	1.3
2000	1.6	1.8	2.2	1.8	1.7	2.2	2.2	2.0	1.5	0.0	0.0	0.0	1.4
2001	1.5	1.7	1.7	1.4	1.2	1.4	0.5	0.8	0.2	1.6	1.7	1.8	1.3
2002	1.8	1.8	1.9	1.8	1.4	2.3	2.1	1.8	0.9	1.0	1.3	1.5	1.6
2003	1.6	1.7	2.0	1.9	1.5	2.0	2.0	1.4	1.0	1.1	1.3	1.3	1.6
2004	1.7	1.9	2.0	2.0	1.8	2.1	2.2	1.5	1.5	1.2	1.3	1.6	1.7
2005	2.0	2.1	2.2	2.0	1.6	1.9	2.0	1.8	1.2	1.2	1.3	1.5	1.7
Mean	1.8	1.9	2.0	1.9	1.7	2.0	1.9	1.6	1.0	1.0	1.1	1.2	1.6

Mean monthly wind speed (ms^{-1}) at Maichew station

Year	Jan	Feb	Mar	Apr	May	Jun	Jul	Aug	Sep	Oct	Nov	Dec	Annual
1996	1.1	1.3	1.3	1.3	1.3	2.9	3.8	2.7	1.2	1.2	1.2	1.2	1.7
1997	1.1	1.3	1.3	1.3	1.5	1.9	3.1	2.0	1.3	1.2	1.0	1.0	1.5
1998	0.9	1.0	1.2	1.4	1.4	1.9	3.6	2.6	1.2	1.2	1.3	1.3	1.6
1999	1.2	1.4	1.4	1.5	1.6	2.0	3.3	2.2	1.1	0.9	1.1	1.1	1.6
2000	1.2	1.3	1.3	1.4	1.4	2.2	3.4	2.8	1.1	0.9	0.9	1.0	1.6
2001	1.2	1.3	1.3	1.0	1.2	2.4	3.2	2.5	1.1	1.2	1.1	1.1	1.6
2002	0.9	1.2	1.2	1.3	1.3	2.4	2.5	2.5	1.1	1.2	1.2	1.1	1.5
2003	1.1	1.3	1.3	1.3	1.3	1.8	3.4	2.7	1.4	1.2	1.2	1.1	1.6
2004	1.2	1.3	1.3	1.2	1.6	1.9	3.2	2.3	1.2	1.2	1.2	1.2	1.6
2005	1.1	1.2	1.3	1.4	1.3	3.0	3.0	2.7	1.2	1.2	0.9	1.0	1.6
Mean	1.1	1.3	1.3	1.3	1.4	2.2	3.3	2.5	1.2	1.1	1.1	1.1	1.6

Appendix 2 Hydrochemistry data

Appendix 2.1 Summary of the water sample results

Sample index	UTM_X	UTM_Y	PH	EC	TDS	Ca	Mg	Na	K	HCO_3	NO_3	SO_4	Cl	NH_3	Water_Type	SAR
	(m)	(m)		(μScm^{-1})	(mgl^{-1})	(mgl^{-1})	(mgl^{-1})	(mgl^{-1})	(mgl^{-1})	(mgl^{-1})	(mgl^{-1})	(mgl^{-1})	(mgl^{-1})	(mgl^{-1})		
RPW-030-08	573856	1396696	7.32	539.00	354.00	62.16	18.36	44.00	1.00	335.60	0.20	9.99	15.45	0.38	Ca-Na-Mg-HCO3	1.26
RPW-032-08	576189	1395698	7.15	539.00	352.00	68.04	17.85	39.00	1.40	350.99	1.96	0.29	11.33	0.19	Ca-Na-Mg-HCO3	1.09
RPW-033-08	575022	1395075	7.42	509.00	332.00	74.76	11.22	40.00	1.00	320.20	6.03	5.30	11.33	0.11	Ca-Na-HCO3	1.14
RPW-034-08	576332	1394432	7.10	512.00	334.00	60.48	12.24	43.00	1.80	297.20	3.10	2.86	13.40	0.18	Ca-Na-HCO3	1.32
RPW-036-08	574094	1392035	7.30	604.00	396.00	75.60	11.22	55.00	1.20	350.99	3.23	7.81	21.60	0.11	Ca-Na-HCO3	1.56
RPW-038-08	574039	1389891	7.54	505.00	330.00	53.76	10.70	63.00	1.20	289.50	6.20	11.65	21.60	0.04	Na-Ca-HCO3	2.05
RPW-064-08	564467	1373141	6.75	664.00	434.00	85.68	31.62	20.00	0.90	379.18	3.71	12.95	30.90	0.31	Ca-Mg-HCO3	0.47
RPW-066-08	566444	1372391	7.20	789.00	514.00	83.16	43.86	34.00	1.10	435.50	12.12	23.99	31.93	0.27	Ca-Mg-HCO3	0.75
RPW-067-08	571726	1373354	7.48	645.00	422.00	47.04	12.24	85.00	3.60	307.40	0.30	99.86	18.54	0.14	Na-Ca-HCO3-SO4	2.85
RPW-068-08	572613	1371922	7.28	617.00	410.00	40.32	24.99	81.00	2.70	345.90	0.38	46.08	20.96	0.21	Na-Mg-Ca-HCO3	2.47
RPW-070-08	570481	1371229	7.09	744.00	486.00	58.80	31.62	74.00	1.90	471.40	0.29	53.69	18.54	0.27	Na-Ca-Mg-HCO3	1.93
RPW-072-08	572671	1370616	7.38	640.00	422.00	42.00	21.50	74.00	3.10	379.18	0.20	49.12	20.60	0.15	Na-Ca-Mg-HCO3	2.32
RPW-075-08	561215	1368924	7.65	648.00	422.00	58.80	30.60	58.00	2.00	397.10	9.38	5.90	16.48	0.28	Ca-Na-Mg-HCO3	1.53
RPW-076-08	567162	1369865	7.26	627.00	412.00	50.40	31.62	47.00	1.90	335.62	4.68	23.51	29.87	0.80	Mg-Ca-Na-HCO3	1.28
RPW-077-08	565483	1368490	6.91	1084.00	710.00	103.30	70.09	38.00	1.70	525.20	29.80	70.73	44.30	0.85	Mg-Ca-HCO3	0.71
RPW-078-08	569076	1366877	7.10	809.00	528.00	58.80	35.70	87.00	2.40	476.53	2.28	69.30	18.54	0.16	Na-Mg-Ca-HCO3	2.21
RPW-080-08	570393	1368715	7.12	681.00	446.00	52.08	24.99	86.00	2.60	374.05	0.48	66.26	21.63	0.21	Na-Ca-Mg-HCO3	2.45
RPW-081-08	566566	1367059	7.38	703.00	460.00	49.56	27.03	86.00	1.70	374.05	10.30	26.94	31.93	0.24	Na-Ca-Mg-HCO3	2.44
RPW-082-08	574045	1365777	7.52	538.00	352.00	57.10	24.50	32.00	4.30	312.60	11.20	5.71	11.33	0.19	Ca-Mg-Na-HCO3	0.89
RPW-083-08	565271	1365661	7.36	590.00	380.00	46.17	30.09	0.51	2.70	363.80	3.48	40.56	16.48	0.23	Mg-Ca-HCO3	0.01
RPW-087-08	567591	1361714	7.45	925.00	604.00	77.28	41.82	81.00	2.70	479.10	3.20	64.55	43.26	0.45	Ca-Na-Mg-HCO3	1.84
RPW-088-08	567019	1360930	7.38	1740.00	1134.00	151.20	90.78	164.00	3.00	589.30	43.14	281.79	150.96	0.62	Ca-Mg-Na-HCO3-SO4	2.60
RPW-093-08	567588	1359766	7.56	657.00	430.00	47.04	25.20	80.00	3.20	420.16	2.45	11.18	16.48	0.33	Na-Ca-Mg-HCO3	2.34
RPW-095-08	565153	1359042	7.27	636.00	416.00	77.30	29.07	28.00	0.80	343.30	13.16	18.18	22.66	0.27	Ca-Mg-HCO3	0.69
RPW-096-08	566902	1358605	7.11	783.00	512.00	53.76	53.55	57.00	2.20	507.28	7.18	6.85	19.57	0.47	Mg-Ca-Na-HCO3	1.32
RPW-097-08	564016	1357876	7.40	484.00	318.00	48.72	19.38	31.00	7.20	302.30	6.86	1.33	8.24	0.15	Ca-Mg-Na-HCO3	0.95
RPW-098-08	562933	1357904	7.37	646.00	420.00	67.20	31.62	46.00	1.00	381.70	6.60	12.95	21.60	0.26	Ca-Mg-Na-HCO3	1.16
ART01	575919	1334560	7.88	429.00	288.00	24.00	12.20	68.00	1.50	245.90	0.80	30.37	13.23	0.08	Na-Ca-HCO3	2.82
ART02	568925	1374980	7.73	494.00	330.00	74.00	9.76	30.00	0.90	333.10	12.62	7.99	15.00	0.18	Ca-Na-HCO3	0.87
SPO_01	577655	1360770	7.56	1694.00	1120.00	100.00	170.80	54.00	8.40	320.30	44.01	429.83	113.40	2.73	Mg-Ca-SO4-HCO3	0.76
GUL_01	567477	1333862	8.45	412.00	268.00	60.00	18.30	17.50	1.40	227.40	5.00	7.80	11.34	0.41	Ca-Mg-HCO3	0.51
BHA_08	566682	1372196	7.34	1238.00	804.00	144.00	61.00	68.00	0.20	543.20	75.70	95.20	81.30	0.81	Ca-Mg-HCO3	1.20
BHA_12	573007	1373083	7.79	1260.00	882.00	100.00	67.10	122.00	3.30	374.00	0.89	364.62	36.80	0.94	Mg-Na-Ca-SO4-HCO3	2.31
		Maximum	**8.5**	**1740.0**	**1134.0**	**151.2**	**170.8**	**164.0**	**8.4**	**589.3**	**75.7**	**429.8**	**151.0**	**2.7**		**2.9**
		Minimum	**6.75**	**412.00**	**268.00**	**24.00**	**9.76**	**0.51**	**0.20**	**227.40**	**0.20**	**0.29**	**8.24**	**0.04**		**0.01**
		Mean	**7.38**	**738.94**	**485.52**	**68.26**	**34.93**	**58.58**	**2.30**	**378.46**	**10.03**	**59.55**	**29.71**	**0.39**		**1.52**

Appendix 2.2 Stiff pattern of the water samples in the Raya Valley

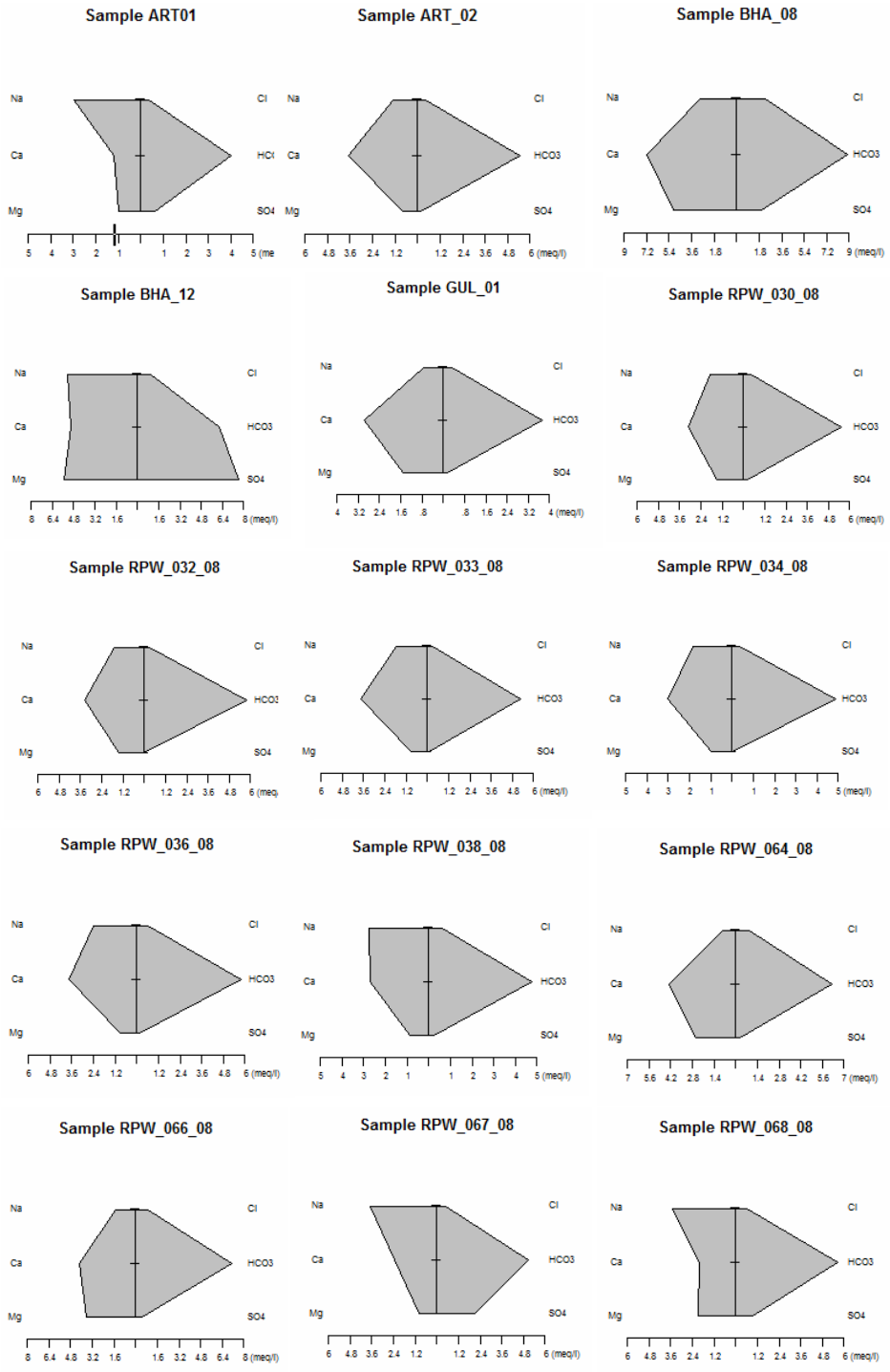

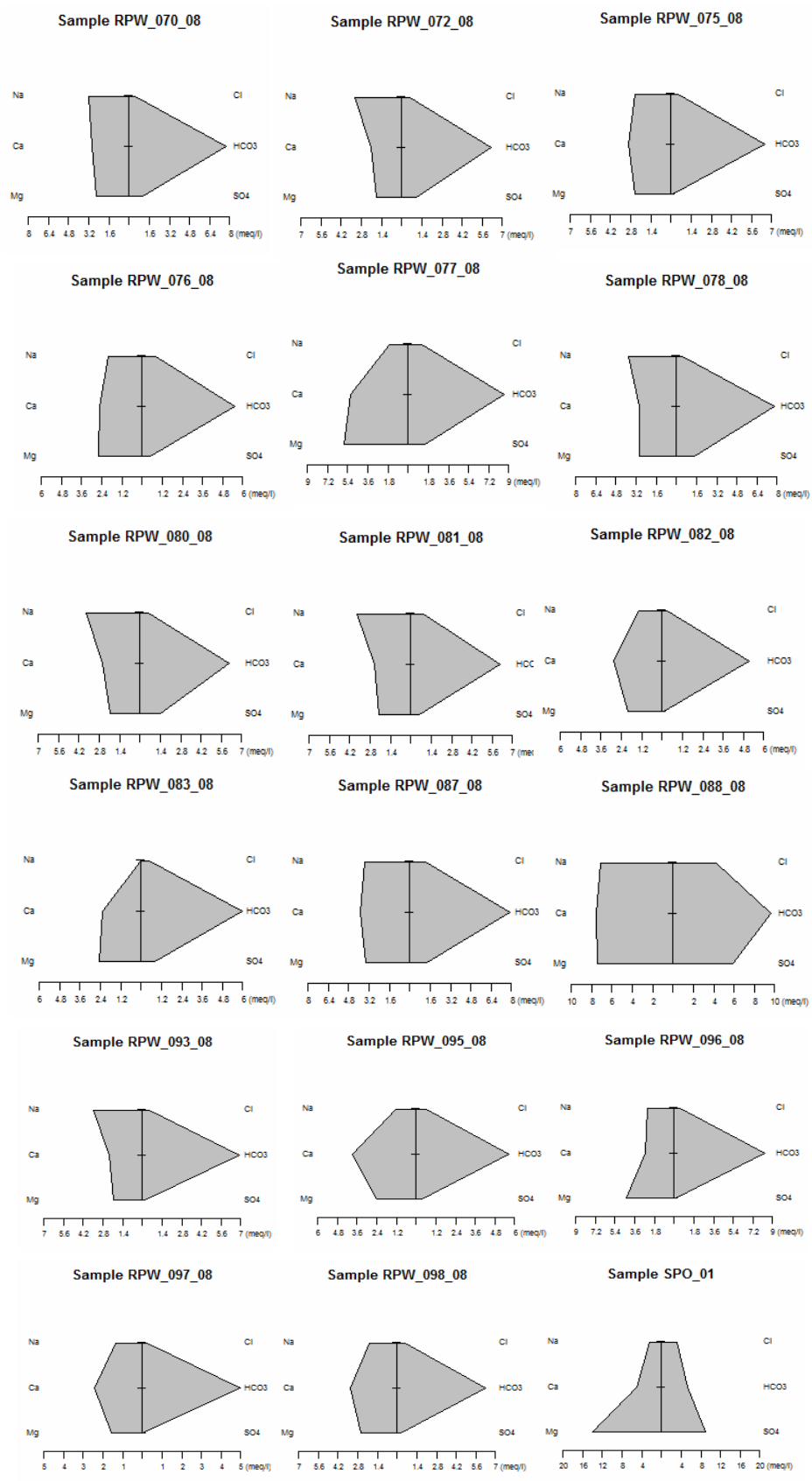
Sample RPW_070_08
Sample RPW_072_08
Sample RPW_075_08
Sample RPW_076_08
Sample RPW_077_08
Sample RPW_078_08
Sample RPW_080_08
Sample RPW_081_08
Sample RPW_082_08
Sample RPW_083_08
Sample RPW_087_08
Sample RPW_088_08
Sample RPW_093_08
Sample RPW_095_08
Sample RPW_096_08
Sample RPW_097_08
Sample RPW_098_08
Sample SPO_01
Na
Ca
Mg
Cl
HCO3
SO4

Appendix 3 Well data

Appendix 3.1 Summary of the borehole data

No	Well	Easting (m)	Northing (m)	surface elevation (m)	SWL (m)	Water level (m)	Depth (m)	Bed rock depth (m)	Aquifer thickness (m)	Q (ls^{-1})	DD (m)
1	WF2/V9	565921	1376322	1438	2.3	1436	78			44	6.2
2	WF4/BH1	567110	1381023	1478	40.7	1437	172	172	131	40	7.1
3	WF4/BH2	565885	1378789	1463	19.7	1443	139	139	119	50	3.4
4	WF4/BH3	564899	1378795	1495	44.2	1451	132	132	88	43	6.3
5	WF0/BH1	562709	1370793	1502	17.8	1484	98	98	80	35	5.1
6	WF0/BH2	563000	1370600	1497	10.4	1487	88	88	78	40	3.2
7	WF0/BH3	563923	1369802	1477	12.2	1465	80	80	68	40	16.0
8	WF0/BH4	562697	1368978	1498	10.3	1488	106	106	96	40	14.5
9	WF0/BH5	561903	1369790	1512	15.0	1497	136	136	121	40	5.3
10	WF0/BH6	561399	1370777	1525	30.2	1495	93	93	63	40	4.8
11	WF0/BH7	561796	1370780	1514	20.8	1493	102	102	81	44	1.8
12	WF0/BH8	561409	1369799	1526	28.5	1498	132	132	104	44	6.0
13	WF1/V1	562872	1371640	1499	17.0	1482	78	78	61	35	16.4
14	WF1/V9	562713	1371855	1501	17.7	1483	73	73	55	35	3.1
15	WF1/V10	562681	1371183	1500	17.2	1483	102	102	85	35	4.6
16	WF5/BH1	563690	1366993	1486	15.9	1470	96	84	68	30	14.6
17	WF5/BH2	564103	1368593	1484	24.8	1459	108	108	83	35	6.1
18	WF5/BH3	563673	1367565	1490	18.8	1471	84	84	65	35	6.2
19	WF5/BH4	564000	1368000	1483	20.5	1462	101	101	80	25	16.2
20	WF5/BH5	561648	1367762	1529	23.5	1506	78	78	55	44	3.9
21	WF6/BH1	563749	1364487	1497	31.9	1465	126	126	94	30	12.3
22	WF6/BH3	563156	1366192	1502	24.5	1478	96	96	72	30	7.6
23	WF6/BH4	563912	1364685	1494	27.5	1466	122	122	94	40	3.0
24	WF7/BH1	564378	1363098	1492	27.8	1464	137	137	109	44	1.7
25	WF7/BH2	563863	1364133	1496	30.5	1466	162	162	132	38	2.5
26	WF3/BH1	565904	1376796	1439	5.0	1434	114	114	109	35	
27	WF3/BH2	566954	1376426	1438	2.7	1435	97	97	94	34	
28	WF6/BH2	563355	1366693	1495	23.0	1472	96				
29	WF3/BH3	567905	1377793	1434	2.0	1432	168	168	166		
30	RPW-043-08	572369	1384905	1458	51.0	1407	192	184	133	30	29.0
31	RPW-045-08	572436	1382113	1435	29.3	1406	178	170	141	30	28.1
32	RPW-046-08	569905	1381800	1448	28.6	1419	180	174	145	38	21.0
33	RPW-050-08	571429	1379689	1424	18.2	1406	166	160	142	44	10.6
34	RPW-052-08	570263	1378912	1420	9.9	1410	136	134	124	35	39.0
35	RPW-057-08	569431	1376222	1418	9.4	1409	201	196	187	31	19.9
36	RPW-058-08	571642	1376249	1409	13.0	1396	186	180	167	65	
37	RPW-063-08	571462	1374198	1405	14.8	1390	224	216	201	34	11.4
38	RPW-064-08	564467	1373141	1475	21.7	1453	112	88	66	35	8.4
39	RPW-066-08	566444	1372391	1446	9.3	1437	146	140	131	39	9.6
40	RPW-067-08	571726	1373354	1401	13.4	1388	218	212	199	32	15.5
41	RPW-068-08	572613	1371922	1399	15.5	1383	264	256	240	36	10.6
42	RPW-070-08	570481	1371229	1409	23.5	1386	144	138	115	20	42.6
43	RPW-072-08	572671	1370616	1397	17.3	1380	262	254	237	32	15.6
44	RPW-075-08	561215	1368924	1529	28.4	1501	130	125	97	48	7.6

No	Well	Easting (m)	Northing (m)	surface elevation (m)	SWL (m)	Water level (m)	Depth (m)	Bed rock depth (m)	Aquifer thickness (m)	Q (ls^{-1})	DD (m)
45	RPW-076-08	567162	1369865	1437	14.5	1423	232	228	214	39	7.9
46	RPW-077-08	565483	1368490	1466	15.4	1451	137	128	113	31	4.4
47	RPW-078-08	569076	1366877	1430	20.6	1409	96	90	69	30	15.1
48	RPW-079-08	568008	1367866	1438	20.5	1418	210	204	184	40	6.1
49	RPW-080-08	570393	1368715	1413	25.5	1388	138	134	109	13	2.7
50	RPW-081-08	566566	1367059	1453	17.0	1436	190	184	167	40	22.7
51	RPW-082-08	574045	1365777	1388	9.5	1378	276	270	260	42	13.6
52	RPW-083-08	565271	1365661	1471	11.4	1460	170	164	153	50	8.7
53	RPW-084-08	568850	1368728	1427	22.6	1404	146	140	117	30	26.2
54	RPW-087-08	567591	1361714	1435	6.4	1429	170	162	156	41	6.3
55	RPW-088-08	567019	1360930	1437	7.0	1430	176	170	163	49	11.8
56	RPW-092-08	571968	1384297	1450	42.9	1407	194	190	147	34	4.9
57	RPW-093-08	567588	1359766	1436	5.9	1430	288	282	276	46	15.7
58	RPW-095-08	565153	1359042	1455	5.6	1449	196	188	182	53	17.3
59	RPW-096-08	566902	1358605	1454	14.4	1440	186	180	166	46	12.2
60	RPW-097-08	564016	1357876	1475	13.8	1461	144	140	126	51	16.9
61	RPW-098-08	562933	1357904	1488	5.6	1482	154	146	140	48	8.5
62	WF13/BH1	574502	1409298	1649	51.7	1597	138	130	78	34	2.6
63	WF13/BH2	575754	1407602	1621	30.3	1591	168	158	128	38	4.3
64	WF13/BH4	574837	1408721	1643	43.9	1599	144	140	96	32	3.8
65	WF13/BH5	575406	1408290	1634	36.2	1598	132	132	96	44	2.4
66	WF9/BH1	569813	1400983	1646	30.4	1616	151	146	116	44	5.1
67	WF9/BH2	569708	1399528	1636	22.9	1613	150			35	13.0
68	WF9/BH3	569798	1400023	1635	20.7	1614	128			30	13.7
69	WF9/BH4	570553	1400160	1622	27.1	1595	150	150	123	44	3.4
70	WF13/BH3	573500	1408434	1655	56.0	1599	128	128	72	0	
71	WF11/BH1	573994	1405945	1636	46.5	1590	130	129	83	27	
72	RPW-013-08	572677	1403437	1614	58.6	1565	116	98	39	17	12.2
73	RPW-023-08	568247	1400186	1658	34.0	1624	110	80	46	13	35.4
74	RPW-024-08	574055	1399330	1568	38.3	1530	140	128	90	28	4.1
75	RPW-028-08	578718	1398109	1514	33.6	1480	226	220	186	25	5.0
76	RPW-030-08	573856	1396696	1559	47.5	1512	174	164	117	25	5.3
77	RPW-032-08	576189	1395698	1523	31.3	1492	182	178	147	32	17.9
78	RPW-033-08	575022	1395075	1529	39.0	1490	162	154	115	30	20.8
79	RPW-034-08	576332	1394432	1514	47.0	1467	226	220	173	25	12.0
80	RPW-036-08	574094	1392035	1524	39.6	1484	160	134	94	30	3.4
81	RPW-037-08	574690	1390976	1511	33.5	1477	160	154	120	31	
82	RPW-038-08	574039	1389891	1514	39.0	1475	182	178	139	25	20.0

Appendix 3.2 Chloride concentration of groundwater and rain water

No	Sample index	UTM_X (m)	UTM_Y (m)	Cl_{gw} (mgl^{-1})	P (mmy^{-1})	Cl_p (mgl^{-1})
1	RPW-030-08	573856	1396696	15.45	724	0.8
2	RPW-032-08	576189	1395698	11.33	724	0.8
3	RPW-033-08	575022	1395075	11.33	724	0.8
4	RPW-034-08	576332	1394432	13.4	724	0.8
5	RPW-036-08	574094	1392035	21.6	724	0.8
6	RPW-038-08	574039	1389891	21.6	724	0.8
7	RPW-064-08	564467	1373141	30.9	724	0.8
8	RPW-066-08	566444	1372391	31.93	724	0.8
9	RPW-067-08	571726	1373354	18.54	724	0.8
10	RPW-068-08	572613	1371922	20.96	724	0.8
11	RPW-070-08	570481	1371229	18.54	724	0.8
12	RPW-072-08	572671	1370616	20.6	724	0.8
13	RPW-075-08	561215	1368924	16.48	724	0.8
14	RPW-076-08	567162	1369865	29.87	724	0.8
15	RPW-077-08	565483	1368490	44.3	724	0.8
16	RPW-078-08	569076	1366877	18.54	724	0.8
17	RPW-080-08	570393	1368715	21.63	724	0.8
18	RPW-081-08	566566	1367059	31.93	724	0.8
19	RPW-082-08	574045	1365777	11.33	724	0.8
20	RPW-083-08	565271	1365661	16.48	724	0.8
21	RPW-087-08	567591	1361714	43.26	724	0.8
22	RPW-088-08	567019	1360930	150.96	724	0.8
23	RPW-093-08	567588	1359766	16.48	724	0.8
24	RPW-095-08	565153	1359042	22.66	724	0.8
25	RPW-096-08	566902	1358605	19.57	724	0.8
26	RPW-097-08	564016	1357876	8.24	724	0.8
27	RPW-098-08	562933	1357904	21.6	724	0.8
28	ART01	575919	1334560	13.23	724	0.8
29	ART02	566925	1374980	15	724	0.8
30	SPO_01	577655	1360770	113.4	724	0.8
31	GUL_01	567477	1333862	11.34	724	0.8
32	BHA_08	566682	1372196	81.3	724	0.8
33	BHA_12	573007	1373083	36.8	724	0.8
34	S02	558873	1418657	31.9	From spring arround Maichew	
35	GUL_01	567360	1333979	11.3	From Golina River	

Appendix 4 Pumping test analysis curves

Appendix 4.1 Cooper-Jacob straight-line time-drawdown

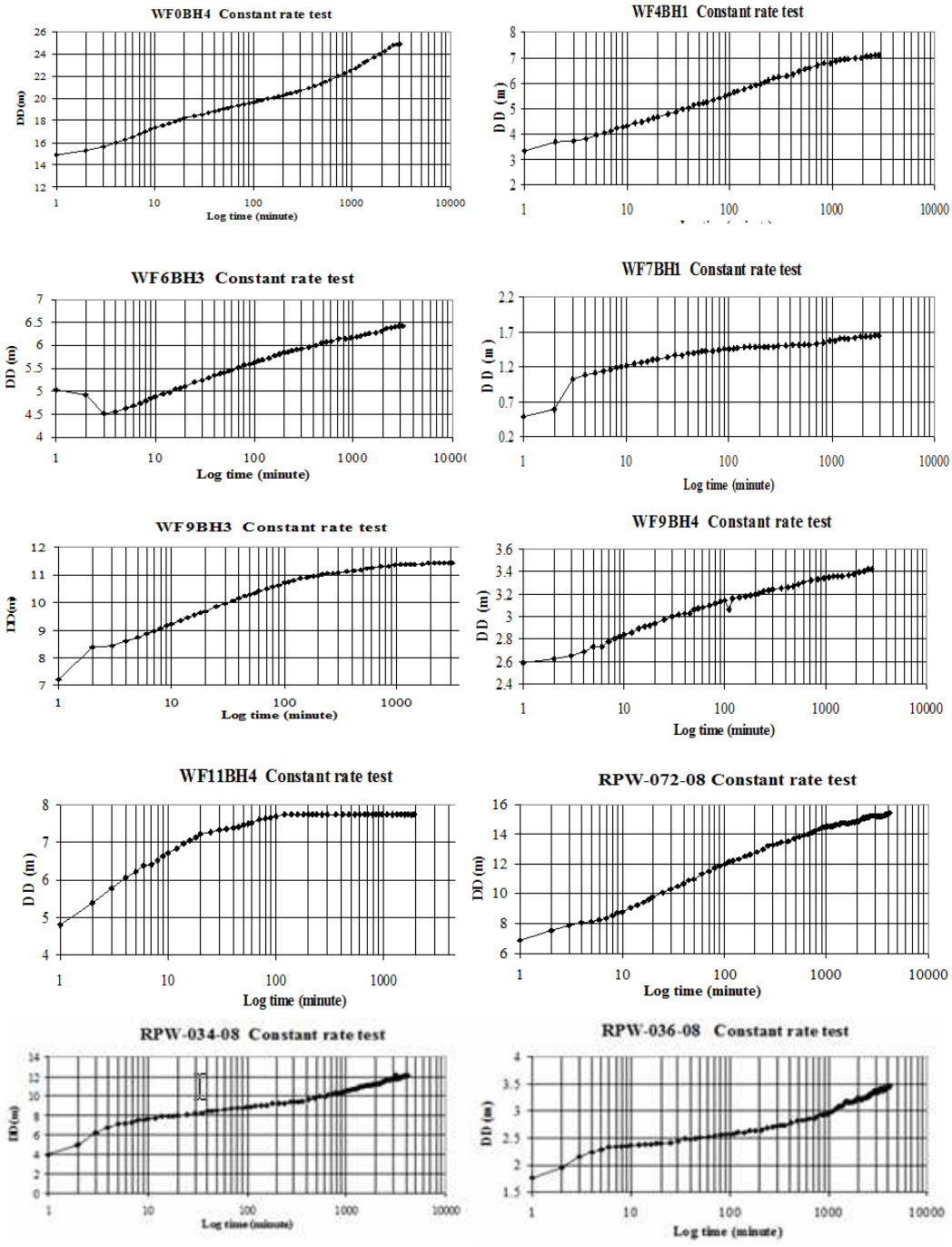

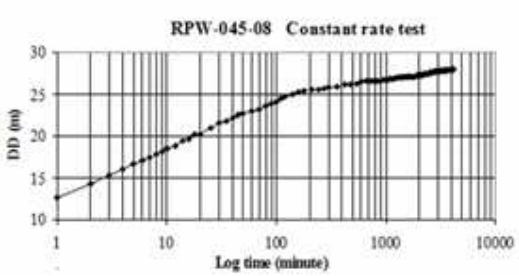

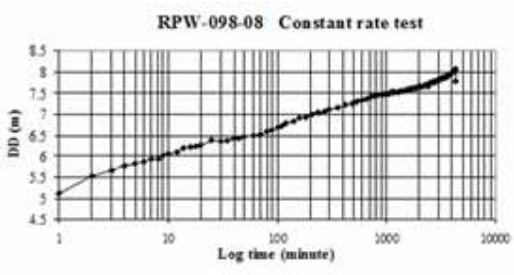

Appendix 4.2 Theis recovery graphs

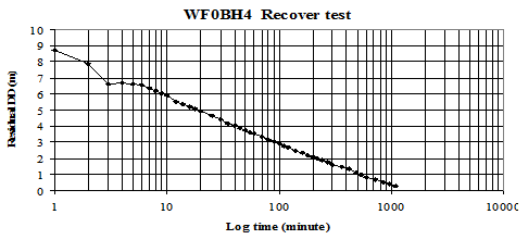

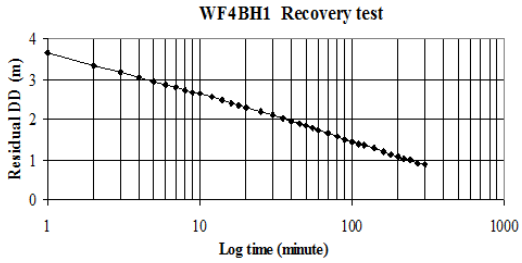

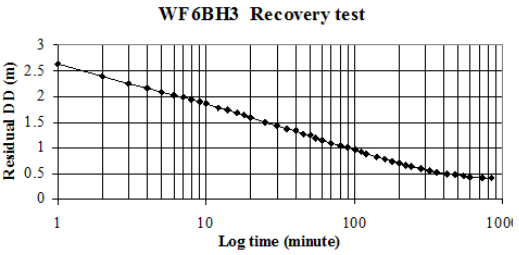

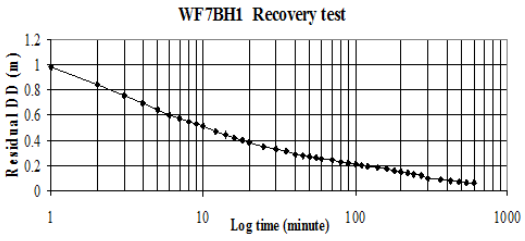

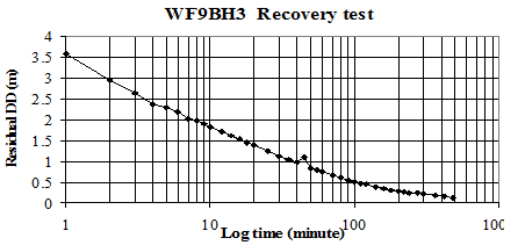

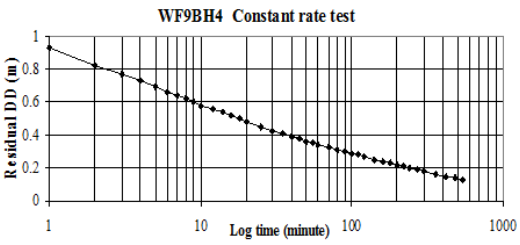

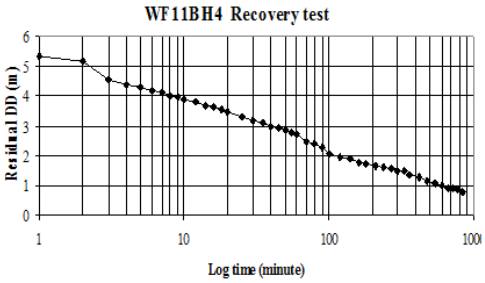

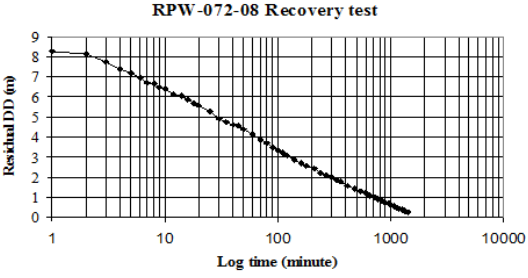

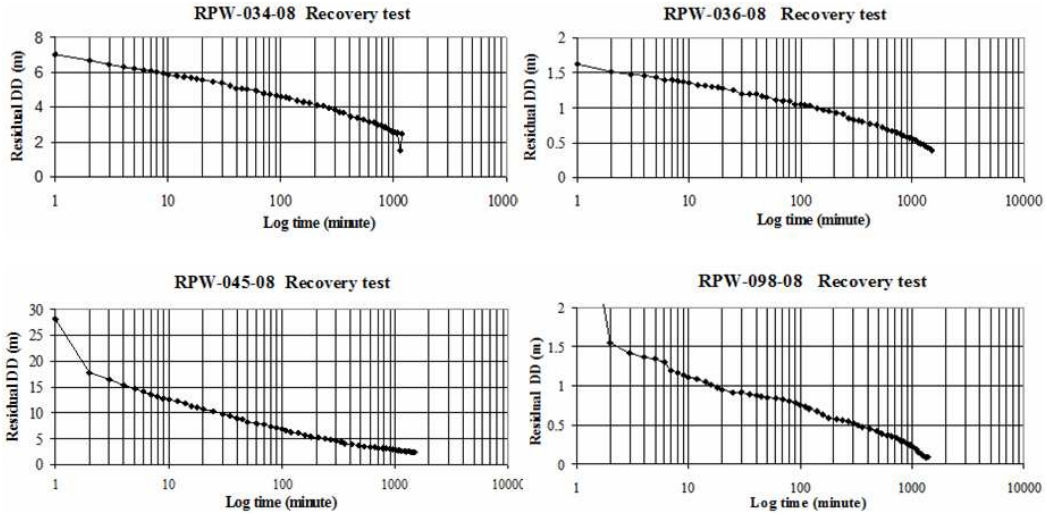
RPW-034-08 Recovery test
Residual DD (m)
Log time (minute)
RPW-036-08 Recovery test
Residual DD (m)
Log time (minute)
RPW-045-08 Recovery test
Residual DD (m)
Log time (minute)
RPW-098-08 Recovery test
Residual DD (m)
Log time (minute)

Appendix 5 Simulated head at the observed head locations

Well name	Easting (m)	Northing (m)	Observed head (m)	Simulated head (m)	Residual (m)
WF2/V9	565921	1376322	1436.0	1419.7	16.3
WF4/BH1	567110	1381023	1437.0	1430.6	6.4
WF4/BH2	565885	1378789	1443.0	1427.2	15.8
WF4/BH3	564899	1378795	1451.0	1427.5	23.5
WF0/BH1	562709	1370793	1484.0	1485.0	-1.0
WF0/BH2	563000	1370600	1487.0	1481.4	5.6
WF0/BH3	563923	1369802	1465.0	1471.0	-6.0
WF0/BH4	562697	1368978	1488.0	1485.3	2.7
WF0/BH5	561903	1369790	1497.0	1493.9	3.1
WF0/BH6	561399	1370777	1495.0	1499.4	-4.4
WF0/BH7	561796	1370780	1493.0	1495.6	-2.6
WF0/BH8	561409	1369799	1498.0	1499.0	-1.0
WF1/V1	562872	1371640	1482.0	1480.2	1.8
WF1/V9	562713	1371855	1483.0	1481.4	1.6
WF1/V10	562681	1371183	1483.0	1484.6	-1.6
WF5/BH1	563690	1366993	1470.0	1469.6	0.4
WF5/BH2	564103	1368593	1459.0	1467.1	-8.1
WF5/BH3	563673	1367565	1471.0	1470.3	0.7
WF5/BH4	564000	1368000	1462.0	1466.7	-4.7
WF5/BH5	561648	1367762	1506.0	1492.3	13.7
WF6/BH1	563749	1364487	1465.0	1470.6	-5.6
WF6/BH3	563156	1366192	1478.0	1476.2	1.8
WF6/BH4	563912	1364685	1466.0	1468.0	-2.0
WF7/BH1	564378	1363098	1464.0	1460.2	3.8
WF7/BH2	563863	1364133	1466.0	1469.0	-3.0
WF3/BH1	565904	1376796	1434.0	1419.6	14.4
WF3/BH2	566954	1376426	1435.0	1417.9	17.1
WF6/BH2	563355	1366693	1472.0	1473.7	-1.7
WF3/BH3	567905	1377793	1432.0	1422.6	9.4
RPW-045-08	572436	1382113	1406.0	1436.6	-30.6
RPW-046-08	569905	1381800	1419.0	1433.1	-14.1
RPW-050-08	571429	1379689	1406.0	1427.6	-21.6
RPW-052-08	570263	1378912	1410.0	1424.9	-14.9
RPW-057-08	569431	1376222	1409.0	1415.9	-6.9
RPW-058-08	571642	1376249	1396.0	1416.1	-20.1
RPW-063-08	571462	1374198	1390.0	1409.7	-19.7
RPW-064-08	564467	1373141	1453.0	1460.4	-7.4
RPW-066-08	566444	1372391	1437.0	1434.4	2.6
RPW-067-08	571726	1373354	1388.0	1406.8	-18.8
RPW-068-08	572613	1371922	1383.0	1401.1	-18.1
RPW-070-08	570481	1371229	1386.0	1402.4	-16.4
RPW-072-08	572671	1370616	1380.0	1396.6	-16.6
RPW-075-08	561215	1368924	1501.0	1499.1	1.9
RPW-076-08	567162	1369865	1423.0	1411.4	11.6
RPW-077-08	565483	1368490	1451.0	1444.6	6.4

Well name	Easting (m)	Northing (m)	Observed head (m)	Simulated head (m)	Residual (m)
RPW-078-08	569076	1366877	1409.0	1404.8	4.2
RPW-079-08	568008	1367866	1418.0	1408.2	9.8
RPW-080-08	570393	1368715	1388.0	1398.7	-10.7
RPW-081-08	566566	1367059	1436.0	1420.9	15.1
RPW-082-08	574045	1365777	1378.0	1385.2	-7.2
RPW-083-08	565271	1365661	1460.0	1445.8	14.2
RPW-084-08	568850	1368728	1404.0	1404.8	-0.8
RPW-087-08	567591	1361714	1429.0	1430.1	-1.1
RPW-088-08	567019	1360930	1430.0	1435.6	-5.6
RPW-093-08	567588	1359766	1430.0	1435.1	-5.1
RPW-095-08	565153	1359042	1449.0	1447.5	1.5
RPW-096-08	566902	1358605	1440.0	1440.5	-0.5
RPW-097-08	564016	1357876	1461.0	1459.6	1.4
RPW-098-08	562933	1357904	1482.0	1481.6	0.4
WF13/BH1	574502	1409298	1597.0	1600.3	-3.3
WF13/BH2	575754	1407602	1591.0	1590.5	0.5
WF13/BH4	574837	1408721	1599.0	1597.3	1.7
WF13/BH5	575406	1408290	1598.0	1594.0	4.0
WF9/BH1	569813	1400983	1616.0	1602.9	13.1
WF9/BH2	569708	1399528	1613.0	1606.2	6.8
WF9/BH3	569798	1400023	1614.0	1607.2	6.8
WF9/BH4	570553	1400160	1595.0	1596.6	-1.6
WF13/BH3	573500	1408434	1599.0	1600.7	-1.7
WF11/BH1	573994	1405945	1590.0	1588.4	1.6
RPW-013-08	572677	1403437	1565.0	1586.1	-21.1
RPW-023-08	568247	1400186	1624.0	1636.6	-12.6
RPW-024-08	574055	1399330	1530.0	1524.6	5.4
RPW-028-08	578718	1398109	1480.0	1506.8	-26.8
RPW-030-08	573856	1396696	1512.0	1510.8	1.2
RPW-032-08	576189	1395698	1492.0	1493.4	-1.4
RPW-033-08	575022	1395075	1490.0	1487.4	2.6
RPW-034-08	576332	1394432	1467.0	1488.3	-21.3
RPW-036-08	574094	1392035	1484.0	1480.1	3.9
RPW-037-08	574690	1390976	1477.0	1477.2	-0.2
RPW-038-08	574039	1389891	1475.0	1473.6	1.4